

Sediment oxygen consumption

Role in the global marine carbon cycle

Jørgensen, Bo Barker; Wenzhöfer, Frank; Egger, Matthias; Glud, Ronnie Nøhr

Published in:
Earth-Science Reviews

DOI:
[10.1016/j.earscirev.2022.103987](https://doi.org/10.1016/j.earscirev.2022.103987)

Publication date:
2022

Document version:
Final published version

Document license:
CC BY

Citation for published version (APA):
Jørgensen, B. B., Wenzhöfer, F., Egger, M., & Glud, R. N. (2022). Sediment oxygen consumption: Role in the global marine carbon cycle. *Earth-Science Reviews*, 228, Article 103987.
<https://doi.org/10.1016/j.earscirev.2022.103987>

Go to publication entry in University of Southern Denmark's Research Portal

Terms of use

This work is brought to you by the University of Southern Denmark.
Unless otherwise specified it has been shared according to the terms for self-archiving.
If no other license is stated, these terms apply:

- You may download this work for personal use only.
- You may not further distribute the material or use it for any profit-making activity or commercial gain
- You may freely distribute the URL identifying this open access version

If you believe that this document breaches copyright please contact us providing details and we will investigate your claim.
Please direct all enquiries to puresupport@bib.sdu.dk



Invited Review

Sediment oxygen consumption: Role in the global marine carbon cycle

Bo Barker Jørgensen^{a,*}, Frank Wenzhöfer^{b,c,e}, Matthias Egger^d, Ronnie Nøhr Glud^{e,f}^a Section for Microbiology and Center for Electromicrobiology, Aarhus University, Ny Munkegade 114, 8000 Aarhus, C, Denmark^b HGF-MPG Group for Deep-Sea Ecology and Technology, Alfred-Wegener-Institute, Helmholtz-Center for Polar and Marine Research, Am Handelshafen 12, 27570 Bremerhaven, Germany^c Max Planck Institute for Marine Microbiology, Celsiusstrasse 1, 28359 Bremen, Germany^d Egger Research and Consulting, Flurhofstrasse 16, 9000 St. Gallen, Switzerland^e Department of Biology, DIAS, Nordsee and HADAL Centres, University of Southern Denmark, 5230 Odense M, Denmark^f Tokyo University of Marine Science and Technology, 4-5-7 Konan, Minato-ku, Tokyo 108-8477, Japan

ARTICLE INFO

Keywords:

Organic carbon mineralization

Total oxygen uptake

Diffusive oxygen uptake

Benthic fauna

Global budget

Database

ABSTRACT

The seabed plays a key role in the marine carbon cycle as a) the terminal location of aerobic oxidation of organic matter, b) the greatest anaerobic bioreactor, and c) the greatest repository for reactive organic carbon on Earth. We compiled data on the oxygen uptake of marine sediments with the objective to understand the constraints on mineralization rates of deposited organic matter and their relation to key environmental parameters. The compiled database includes nearly 4000 O₂ uptake data and is available as supplementary material. It includes also information on bottom water O₂ concentration, O₂ penetration depth, geographic position, water depth, and full information on the data sources. We present the different *in situ* and *ex situ* approaches to measure the total oxygen uptake (TOU) and the diffusive oxygen uptake (DOU) of sediments and discuss their robustness towards methodological errors and statistical uncertainty. We discuss O₂ transport through the benthic and diffusive boundary layers, the diffusion- and fauna-mediated O₂ uptake, and the coupling of aerobic respiration to anaerobic processes. Five regional examples are presented to illustrate the diversity of the seabed: Eutrophic seas, oxygen minimum zones, abyssal plains, mid-oceanic gyres, and hadal trenches. A multiple correlation analysis shows that seabed O₂ uptake is primarily controlled by ocean depth and sea surface primary productivity. The O₂ penetration depth scales with the DOU according to a power law that breaks down under the abyssal ocean gyres. The developed multiple correlation model was used to draw a global map of seabed O₂ uptake rates. Respiratory coefficients, differentiated for depth regions of the ocean, were used to convert the global O₂ uptake to organic carbon oxidation. The resulting global budget shows an oxidation of 212 Tmol C yr⁻¹ in marine sediments with a 5-95% confidence interval of 175-260 Tmol C yr⁻¹. A comparison with the global flux of particulate organic carbon (POC) from photic surface waters to the deep sea, determined from multiple sediment trap studies, suggests a deficit in the sedimentation flux at 2000 m water depth of about 70% relative to the carbon turnover in the underlying seabed. At the ocean margins, the flux of organic carbon from rivers and from vegetated coastal ecosystems contributes greatly to the budget and may even exceed the phytoplankton production on the inner continental shelf.

1. Introduction

The seabed is the largest reservoir of organic matter on Earth and is a long-term sink for biomass produced in the ocean or supplied from rivers. A fourth of the particulate organic carbon (POC) exported from the photic zone of the global ocean reaches the seafloor (Dunne et al., 2007). Along the continents, there is also an important lateral transport

of POC from terrestrial and coastal ecosystems to the sea (Regnier et al., 2013). Less than a tenth of the globally deposited POC is buried and stored in the seabed over thousands to millions of years (Wallmann et al., 2012). By far the most is mineralized back to CO₂ and inorganic nutrients that are subsequently released from the sediments into the water column.

CO₂ from the atmosphere equilibrates with the surface ocean and is

* Corresponding author.

E-mail addresses: bo.barker@bio.au.dk (B.B. Jørgensen), frank.wenzhoefer@awi.de (F. Wenzhöfer), info@eggermatthias.com (M. Egger), rnglud@biology.sdu.dk (R.N. Glud).<https://doi.org/10.1016/j.earscirev.2022.103987>

Received 31 May 2021; Received in revised form 27 February 2022; Accepted 5 March 2022

Available online 12 March 2022

0012-8252/© 2022 The Authors. Published by Elsevier B.V. This is an open access article under the CC BY license (<http://creativecommons.org/licenses/by/4.0/>).

assimilated by phytoplankton. A fraction of this fixed, particulate organic carbon sinks out of the photic zone and down into the dark ocean. This generates a biological pump by which carbon is sequestered in the deep ocean and in the seabed. By the net burial of organic carbon, the seabed provides an important long-term sink in the global CO₂ balance. It also affects the global O₂ balance in the atmosphere, which, due to the 500-fold larger concentration of O₂ than of CO₂, is regulated on a much longer time scale of many thousands of years.

Our current understanding of the deposition and mineralization of organic matter in the seabed is based on many types of data and analyses, ranging from remote sensing of the chlorophyll distribution and experimental productivity studies in the photic zone to sediment trap studies, measurements of the sediment community oxygen consumption, and modeling. There are several well-established approaches to determine the Total Oxygen Uptake (TOU) or the Diffusive Oxygen Uptake (DOU) of marine sediments, including a) the enclosure of sediment to measure the rate of oxygen depletion in the overlying seawater, b) the measurement of oxygen penetration into the sediment and calculation of the diffusion flux, and c) the measurement of oxygen and turbulence of water flow at a point above the sediment and calculation of the oxygen flux by eddy covariance technique. The measurements by a) and b) may be done either directly on the seafloor using flux chambers and profiling instruments or shipboard in retrieved sediment cores.

In order to understand the role of seabed respiration in the global marine carbon cycle, we established a comprehensive database of sediment O₂ uptake rates and accompanying environmental information from the literature and from public databases. From these data we developed algorithms for a multiple correlation of TOU or DOU to key parameters. The algorithms are used to map the global distribution of oxygen uptake of the seafloor and determine the environmental controls on benthic oxygen uptake and organic carbon turnover. A main objective was thereby to establish a global budget for the oxygen and carbon cycles of the seabed, including analyses of their robustness towards methodological errors and statistical uncertainty.

1.1. What is in this review

Our data compilation and analysis includes only marine sediments. Our objective is to relate pelagic marine primary productivity to export from the photic zone, deposition on the seafloor, and seabed mineralization processes. The sediments receive POC both from the overlying water column and from lateral transport by ocean currents and from land. The sediments also receive material that moves along the seabed through resuspension-resettling cycles or through down-slope mass wasting. In shallow, coastal regions there is a large organic production directly on the seafloor in the form of microbenthic photosynthesis and growth of seagrasses that contribute to the organic source. In our analysis, we do not include vegetated coastal ecosystems, such as salt marshes, mangroves, macroalgae or seagrass beds. Due to their great heterogeneity, intertidal mud flats or rocky bottoms are also not included in the dataset.

We start this review with a presentation of the TOU and DOU database and our rationale for selecting only *in situ* data for the depth range 10–6500 m by the global modeling. This is followed by an overview of the mechanisms of seabed oxygen uptake, the role of diffusion and faunal activity, and the coupling to anaerobic processes in the sediment. We then discuss five examples of sediment environments that demonstrate the great diversity of the seabed. The global distribution of *in situ* sediment oxygen uptake is mapped, using a multivariate correlation analysis of the database, and the controls on seabed oxygen uptake are discussed. This provides the basis for a global budget of seabed oxygen uptake and a new perspective on its role in the marine organic carbon cycle. The constraints on the budget are discussed in relation to other available information on organic carbon fluxes to the seafloor and the mineralization or burial of organic matter.

2. Quantification of seabed O₂ uptake

2.1. Different approaches

There are generally three basic approaches to quantify the benthic O₂ consumption rates: by sediment incubations, by flux calculations from oxygen profiles, and by eddy covariance technique. Below we will briefly describe these approaches and the extent to which they provide accurate data for the *in situ* O₂ consumption or possibly interfere with the solute exchange of the seabed.

2.1.1. Total O₂ uptake by sediment incubations

The most widely used approach for quantifying the benthic O₂ consumption rate is to enclose a sediment area and monitor the O₂ decline in the well-mixed overlying water phase (e.g., [Pamatmat and Fenton, 1968](#)). This can be achieved by incubating sediment cores in the laboratory (*ex situ*) or by placing benthic chambers directly on the seafloor (*in situ*). When knowing the enclosed sediment area and water volume, the O₂ decline can be converted into a total oxygen uptake rate of the sediment. A commonly used unit, which will also be applied here, is mmol O₂ m⁻² day⁻¹. In order to determine the O₂ consumption rate of the undisturbed seabed, it is important not to change critical environmental parameters. Numerous designs of benthic chambers and sediment core incubation systems have been developed and applied over the years (reviewed by [Tengberg et al., 1995](#)), but given that the incubation approach is invasive, it is difficult not to affect the benthic system. It should always be considered how best to ensure that temperature, O₂ concentration, flow velocity and faunal activity during the incubation remain as close to natural conditions as possible.

Temperature affects metabolic rates and the solubility and transport of O₂. It is therefore critical to incubate sediments at *in situ* temperature. If the sediment has been transiently heated during recovery, sufficient time should be given for the system to revert to the earlier steady state O₂ distribution before starting measurements. It can be more challenging to ensure unaltered O₂ availability, especially in environments with low O₂ concentration. By laboratory incubations, the correct initial O₂ concentration of the overlying water can be established using a manual or digital gas-mixer ([Rasmussen and Jørgensen, 1992](#)). Given that O₂ is gradually consumed during incubation, the decreasing O₂ concentration of the overlying water will ultimately affect the O₂ uptake rate ([Hall et al., 1989](#); [Kononets et al., 2021](#)), and the initial, linear O₂ decline should therefore be determined ([Bender et al., 1989](#); [Glud, 2008](#)).

The flow velocity of seawater affects the benthic O₂ uptake, both in permeable sand and in non-permeable sediments with high O₂ consumption rates where the thickness of the Diffusive Boundary Layer (DBL) affects the O₂ exchange ([Jørgensen and Revsbech, 1985](#); [Boudreau, 2001](#); [Glud et al., 2007](#); Chapter 3.2). Stirred benthic chambers or laboratory core incubation systems have been designed to establish a rather uniform flow velocity and DBL thickness across most of the sediment surface ([Berelson and Hammond, 1986](#); [Buchholtz-ten Brink et al., 1989](#); [Glud et al., 1995a](#); [Khalili et al., 2008](#)). In permeable sediments, advective porewater transport is induced by wave action, near-bed flow gradients, and bioirrigation ([Huettel et al., 2014](#); [Jahnke et al., 2000](#); [Reimers et al., 2004](#)). The near-bed hydrodynamics are critical for the solute exchange but are difficult to establish during enclosure. The strategy has therefore been to establish well-defined pressure gradients over the sediment and impose known rates and patterns of porewater advection to assess the TOU under reproducible and realistic conditions ([Huettel and Gust, 1992b](#); [Janssen et al., 2005](#)).

Fauna respiration and bioirrigation contribute to the benthic O₂ uptake ([Aller and Aller, 1998](#); [Kristensen et al., 2012](#); [Snelgrove et al., 2018](#)), yet it is difficult to assess whether an enclosure maintains the natural activity of the fauna. The best representation of the natural benthic community is to apply relatively large chambers ([Tengberg et al., 1995](#)), which increase the probability that also the larger fauna is

included and that no, or only few, animals are damaged during insertion of the chamber (Glud and Blackburn, 2002). However, sampling instruments designed to recover sediment cores with an intact surface generally use rather small core liners of ≤ 10 cm diameter (Barnett et al., 1984). They tend to exclude larger fauna and to affect faunal behavior. The TOU of laboratory incubations therefore generally underestimate the *in situ* TOU measured by larger benthic chambers (Archer and Devol, 1992; Glud et al., 1998, 2003; Ferrón et al., 2008). Changes in light conditions, flow velocities, or concentrations of suspended material can also lead to alterations of faunal behavior. This affects the bioirrigation and ventilation of anoxic sediment layers. Passive flushing of relict burrows in the seabed also depends on flow conditions (Munksby et al., 2002).

2.1.2. Small-scale benthic heterogeneity and diffusive O_2 uptake

The fine-scale O_2 distribution across the sediment-water interface can be resolved by Clark-type microelectrodes (Revsbech et al., 1980; Revsbech, 1989) or by microoptodes (Klimant et al., 1995). These enable the quantification of the Diffusive Oxygen Uptake (DOU) of the sediment. The DOU can be determined in different ways, but the simplest and most widely used approach is to apply Fick's first law of diffusion. If O_2 is measured in the DBL, the flux is simply the product of the molecular diffusion coefficient and the O_2 gradient (Jørgensen and Revsbech, 1985). If the O_2 gradient is measured just beneath the sediment surface, also the sediment porosity and the tortuosity must be taken into account (e.g., Andrews and Bennett, 1981; Ullman and Aller, 1982; Glud et al., 1995; Revsbech et al., 1998; Chapter 3.1 and 3.2). Finally, the DOU can be derived from the whole porewater O_2 profile by modeling the volume-specific O_2 consumption rate, which also requires knowledge of porosity and the tortuosity in the sediment (Berg et al., 1998). Oxygen microprofiles provide detailed insight into the distribution and turnover of O_2 at a given position in the sediment. However, sediments are often characterized by small-scale heterogeneity, and a number of O_2 microprofiles may be required to reach a representative value for the DOU of a seafloor area (Jørgensen et al., 2005; Glud et al., 2009a).

In continental shelf and slope sediments, the Oxygen Penetration Depth (OPD) can be determined directly from measured O_2 profiles, which are usually restricted to <10 cm depth. In the oligotrophic deep sea, oxygen penetration often exceeds the measurement depth achieved by vertically inserted microsensors. An oxygen penetration depth of several meters, as found in mid-oceanic gyre sediments, can then be measured by retrieving whole sediment cores and inserting microsensors into the side through small holes in the core liner (Røy et al., 2012; Fischer et al., 2009). It is necessary to use microsensors for such measurements as these cause minimal disturbance and have minimal oxygen consumption (micro-optodes do not consume O_2).

The difference between TOU and DOU measured concurrently in non-permeable sediments reflects the faunal contribution to the benthic O_2 uptake (Rasmussen and Jørgensen, 1992; Glud et al., 2003). The difference includes the faunal respiration and the O_2 uptake along burrow walls surrounded by otherwise anoxic sediment. More detailed insights into the spatial benthic O_2 distribution can be obtained by planar optodes fixed to the wall of a benthic enclosure or to an "inverted periscope" (Glud et al., 1996, 2001). The O_2 distribution in the sediment can thereby be imaged over an area of several cm^2 in real time and provide important information on the spatio-temporal O_2 dynamics around burrow structures or seagrass roots (Wenzhöfer and Glud, 2004; Volkenborn et al., 2012; Santner et al., 2015). The approach is invasive, however, and conditions along the wall may not correctly represent conditions of the undisturbed seabed (Polerecky et al., 2006; Meysman et al., 2010).

2.1.3. *In situ* versus *ex situ* measurements of DOU and TOU

Both DOU and TOU can be measured *ex situ* in recovered sediment cores or *in situ* directly on the seabed, either by divers in shallow water

or by benthic landers in deeper waters (Fig. 1).

In situ technologies for measuring benthic fluxes have been developed for a wide depth range, from shallow waters to the deep sea, usually with 6000 m as the maximal depth rating (e.g., Pamatmat and Fenton, 1968; Smith Jr. et al., 1976; Reimers, 1987; Tengberg et al., 1995; Reimers and Glud, 2000; Reimers et al., 2001). Recently, lander systems have been developed that cover the depth range down to the bottom of the deepest hadal trenches (11,000 m) (Glud et al., 2013; Luo et al., 2018).

Parallel *in situ* and *ex situ* O_2 microprofile measurements in deep sea sediments have revealed that core recovery can induce significant alterations in the consumption and distribution of O_2 in the sediment (Glud et al., 1994). The difference between *ex situ* and *in situ* data increases with increasing water depth because sample retrieval alters chemical, physical and biological properties. Oxygen microprofiles measured on board a ship generally exhibit shallower O_2 penetration depths and higher O_2 consumption rates than measured *in situ* (Fig. 2). This difference increases with increasing water depth (Chapter 5.2.5). The effect is ascribed to strong decompression and transient heating during core recovery, both of which may cause damage and cell lysis to sensitive organism and induce enhanced metabolic activity of resilient microbes that benefit from released, labile organic compounds (Glud et al., 1999). This effect is reflected in elevated concentrations of dissolved organic matter and ammonium in the surface sediment of cores recovered from the deep sea (Hall et al., 2007). When incubating the recovered sediment cores at *in situ* temperature, the O_2 microprofile may gradually revert to the original shape. Yet, given that O_2 diffusion is a slow process, this may take days to months if the O_2 penetrates several cm or dm into the sediment. Therefore, *ex situ* measurements tend to overestimate the benthic O_2 consumption rate and underestimate the O_2 penetration depth in the deep sea (Glud, 2008).

Much of our knowledge about O_2 exchange and carbon mineralization at the vast ocean floor originates from single point ("snapshot") measurements by stationary lander systems. However, marine sediments often exhibit strong heterogeneity and lateral variability at different scales. At the small scale, this can be visualized by multiple O_2 microsensor measurements in recovered sediment cores (Jørgensen et al., 2005) or directly *in situ* (Glud et al., 2009a). Both approaches have demonstrated the existence of mm to cm-scale microbial hotspots with intensified O_2 consumption, presumably associated with local deposition of POC or fauna activity. On an intermediate dm-scale, such a mapping of DOU and OPD requires a moving, transecting microprofiler. Deep sea "crawlers" (Fig. 1D; Sherman and Smith Jr., 2009; Wenzhöfer et al., 2016a, Lemburg et al., 2018) can move autonomously over the seabed while repeatedly inserting chambers and microsensors during long-term deployments. This has documented lateral heterogeneity and temporal variability, such as large organic aggregates or abrupt deposition events (Smith Jr. et al., 2008, 2016; von Appen et al., 2021). Future studies should focus on such benthic dynamics by more extensive use of long-term observatories and integrative technologies to quantify benthic carbon mineralization (Smith Jr. et al., 2013; Soltwedel et al., 2016; Toussaint et al., 2014).

2.1.4. Benthic O_2 exchange determined by Eddy Covariance

In recent years, the Aquatic Eddy Covariance (AEC, also called eddy correlation) approach has been increasingly applied to quantify benthic O_2 exchange. The technique was introduced to aquatic applications by Berg et al. (2003). The *in situ* benthic O_2 exchange rate is determined from concurrent measurement of fluctuations in the vertical flow component (w') and the O_2 concentration (C') in the same minute water volume within the turbulent boundary layer. Provided that w' and C' are measured continuously over tens of minutes, and the water flow is parallel to the seabed, the vertical O_2 flux can be calculated from the time-integrated product of w' and C' (Berg et al., 2003). The two parameters are typically recorded at 64 or 32 Hz by an Acoustic Doppler Velocimeter (ADV) and a fast O_2 microsensor, respectively.

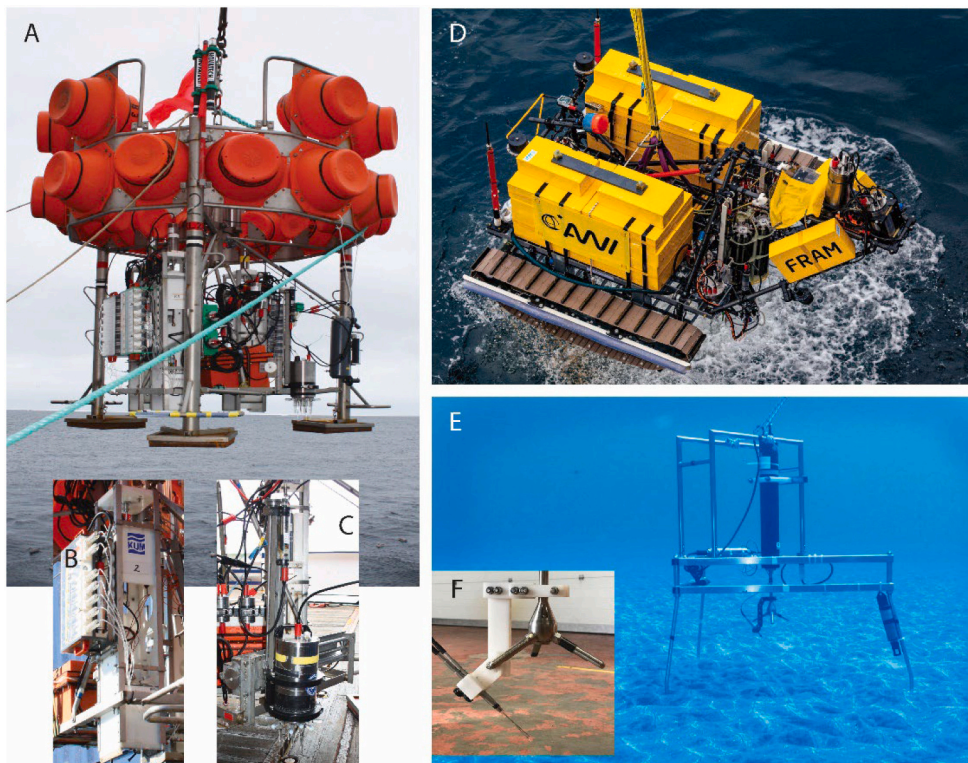


Fig. 1. Instruments for measuring oxygen uptake rates *in situ*, directly on the seabed. A) Free-falling autonomous benthic lander system carrying three incubation chambers (inset B) and an array of microsensors (inset C) on a transecting micro-profiler. D) Deep-sea crawler with two benthic chambers and three multiple sensor profiling units for long-term studies. E) Eddy covariance system deployed at 28 m water depth to measure the benthic O₂ flux from 20 cm above seafloor (photo by Lucas Zañartu). F) Acoustic Doppler velocimeter (ADV) and fast O₂ microsensors used on the eddy covariance instrument (photo by Karl Attard).

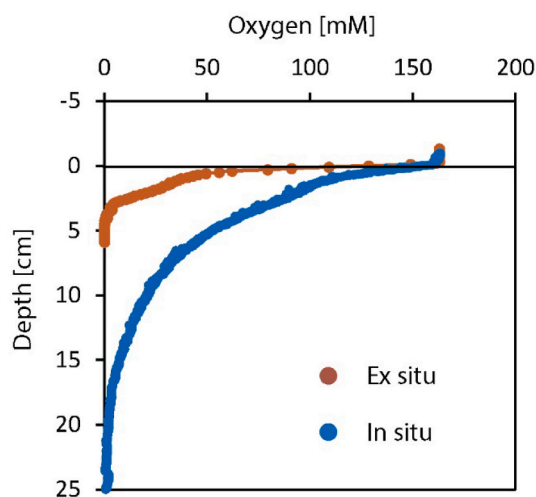


Fig. 2. Effect of core retrieval on sediment oxygen uptake. Two oxygen profiles measured *ex situ* and *in situ*, respectively, at the same temperature on the same station at 5500 m water depth in the Atacama Trench off Chile (data from Glud et al., 2021).

Measurements are done 10–20 cm above the seabed (Fig. 1), the height depending on the topography and rugosity of the sediment surface (Berg et al., 2007).

The eddy covariance measures the benthic O₂ exchange rates of a 10–100 m² large ellipsoid footprint upstream from the measuring point (Berg et al., 2007). The technique can, thus, provide non-invasive measurements of the benthic O₂ exchange rate across a relatively large sediment area without affecting the *in situ* conditions (Berg and Huettel, 2008). In this respect it is superior to chamber incubations or O₂ profile measurements for assessing benthic O₂ exchange rates. Due to the rather advanced technology required and the complex data handling

procedures, the approach is still only used by relatively few research groups. This situation will change as standardized instruments, software packages, and data treatment procedures are developed (McGinnis et al., 2011; Long, 2021; Berg et al., 2022). Currently, the number of AEC-derived O₂ uptake data is rapidly increasing. The approach has particularly been applied in complex settings such as seagrass beds, permeable sands, and coral reefs (Long et al., 2013; Rheuban et al., 2014; McGinnis et al., 2014; Reimers et al., 2016). The approach also has great potential in deep sea settings (Berg et al., 2009; Donis et al., 2016).

2.2. Data analysis

Benthic oxygen fluxes compiled in our database were derived from previously published data compilations (Wenzhöfer and Glud, 2002; Glud, 2008; Stratmann et al., 2019), supplemented by data from other databases or sources. We searched the literature using combinations of relevant search terms (such as benthic, sediment, O₂, oxygen, flux, consumption, respiration, and uptake). The benthic oxygen consumption rates were measured using different techniques, including core or chamber incubations, O₂ profile modeling, and eddy covariance. Data are reported accordingly in the database as total or diffusive oxygen uptake. Since our goal was to establish a database on seafloor respiration for the modeling of global organic matter mineralization, a few quality criteria were needed to select the published data:

- 1) *Ex situ* data from >1000 m water depth are expectedly compromised and were not included in the database (see discussion in Chapter 2.1; Fig. 2).
- 2) Shallow coastal sites are influenced by benthic photosynthesis, which produces O₂ within the sediment and adds fresh, labile organic matter at the seafloor. By shallow water oxygen uptake rates, we therefore used only those data that were clearly measured under dark conditions.
- 3) Low O₂ concentrations affect the efficiency of aerobic respiration, including the re-oxidation of products from anaerobic mineralization, especially in dynamic settings (Middelburg and Levin, 2009;

Levin et al., 2009a). We therefore excluded data from locations with $<25 \mu\text{M O}_2$ in the bottom water in our global modeling. Sediments underlying such oxygen minimum zones constitute only 4% of the outer shelf and upper slope and play no significant role in the global sediment O_2 uptake budget (Chapter 4.2).

- 4) Extreme environments, such as fish farms or sites affected by sewage outlets or other local, anthropogenic influence, do not represent natural marine sediments, as benthic communities are modified and benthic consumption rates are enhanced (Sweetman et al., 2014). Data from such sites were therefore excluded.

Using the above criteria, we identified a total of 3904 data on benthic O_2 uptake rates, of which 1780 were measured *in situ* within the full ocean depth range of 0–11,000 m and 2124 were measured *ex situ* at <1000 m water depth.

These data on TOU and DOU are compiled in an Excel file and are available as supplementary material (Supplementary Table S1). Data are presented in the unit $\text{mmol O}_2 \text{ m}^{-2} \text{ d}^{-1}$. If originally published in another unit, fluxes have been recalculated to this unit. If multiple measurements were done at the same site, these were averaged before use for our correlation analysis. Such multiple measurements are indicated by “0”, while single measurements are indicated by “1” and the mean values of multiple measurements are indicated by “2” in Suppl. Table S1. If available for DOU data, we also included the Oxygen Penetration Depth (OPD). Additionally, we included the station number (if available), bottom water O_2 concentration (in μM or % saturation), geographic position, water depth, and full reference to the data source. We labeled the data according to depth region: Inner shelf 0–10 m, Inner shelf 10–50 m, Outer shelf 50–200 m, Slope 200–1000 m, Slope 1000–2000 m, Rise 2000–4000 m, Abyss 4000–6500 m, and Hadal (>6500 m). Data were also categorized according to ocean (Arctic, Atlantic, Indian, Pacific and Southern Ocean) and according to region (e.g., Black Sea).

We used a multiple correlation analysis to model the trends of our data relative to the controlling environmental parameters and to calculate the global distribution of oxygen uptake in the seabed (Chapter 5). For this purpose, we made a critical quality control of all data in order to ensure that the data included in our analysis fulfilled certain criteria. All data selected for our model analysis are supplied with the identifier “1” or “2” in Suppl. Table S1. The selection criteria for data used for our multiple regression analysis and model were the following:

A) We used only measurements done *in situ* directly on the seafloor for the depth range 10–6500 m in our global regression analysis, for reasons explained above. Oxygen uptake rates at water depths of 0–10 m are treated separately in our assessment (see Chapter 5.2.1). Given that there are only few *in situ* data from the coastal zone and that recovery artifacts for this depth range are considered minor, also *ex situ* data from 0 to 10 m were included in our assessment. Data from water depths <10 m are supplied with the identifier “3” in Suppl. Table S1.

B) Pore water advection in permeable sediments is an important factor for the benthic O_2 exchange rates (Huettel and Webster, 2001). Pore water advection fluctuates in nature due to varying bottom water currents, wave dynamics and changes in seafloor topography (e.g., by ripple movements). Benthic oxygen consumption measurements in permeable sediments are therefore often strongly biased by these environmental conditions and are consequently excluded.

C) For the multiple regression analysis, we also excluded fluxes from hadal trenches, as these are characterized by enhanced accumulation of organic material and relatively high mineralization rates and cannot be quantitatively assessed by extrapolating findings from deep-sea trends in general (Glud et al., 2021; see Chapter 4.5).

In order to correlate the seafloor O_2 uptake rates to the organic carbon produced in surface waters for the same geographic position, we extracted the net primary production (NPP; $\text{mg C m}^{-2} \text{ d}^{-1}$) from monthly averaged data computed over a 10-year period (1998–2007; available at www.science.oregonstate.edu/ocean.productivity/custom.php). These NPP data are also provided in Suppl. Table S1.

In Chapter 6.5 we discuss the quantitative importance of benthic environments not included in the regression analysis and global extrapolation.

3. Mechanisms of seabed O_2 uptake

3.1. The benthic boundary layer

The benthic boundary layer (BBL) is the lowest part of the water column, in which the flow is distinctly affected by the seabed, and in which shear stress dampens the motion of seawater (Dade et al., 2001). Vertical gradients of solutes that are exchanged between seawater and sediment, such as oxygen and inorganic nutrients, become apparent in the logarithmic layer that comprises the lower meters to decimeters of the BBL (Holtappels et al., 2011; Trowbridge and Lentz, 2018). When such gradients are combined with *in situ* determinations of the turbulent diffusion coefficients, solute fluxes across the sediment-water interface can be calculated (Inoue et al., 2007; Holtappels and Lorke, 2011).

Within a few dm or cm of the seafloor, vertical motion and turbulence fade out and viscous transport of momentum becomes predominant (Boudreau and Jørgensen, 2001). At even smaller scale, in the viscous sublayer within a few cm from the seabed, there is a steep drop in flow velocity towards the stagnant sediment-water interface. In the thin water film adjacent to the sediment surface, with a thickness of a mm or less, water motion is so strongly reduced that the vertical transport of solutes is dominated by molecular diffusion. This is the diffusive boundary layer (DBL). Moving into the sediment, the seawater flow over the topography of coastal sands and other permeable sediments causes pressure gradients that drive a slow advection of pore water within the uppermost centimeters of the sediment. These flow and transport properties of the BBL are critical to consider when performing oxygen uptake measurements because the approaches used may cut off the natural flow and thereby compromise the oxygen flux.

To avoid interference with the benthic boundary layer, the eddy covariance technique was developed for measurements of the oxygen flux to the seabed. A comparison of the eddy covariance data with oxygen flux determinations using benthic chamber incubations or *in situ* O_2 microprofile measurements have shown rough agreement without a clear systematic difference. Thus, somewhat contrary to expectations, the eddy covariance data were statistically not higher than the other techniques for sediments in which the oxygen uptake was dominated by microbial respiration (Reimers et al., 2012; Attard et al., 2014; Donis et al., 2016). In a sediment with abundant fauna, the eddy covariance showed ca. 30% higher oxygen flux than flux chambers, which again showed about 30% higher oxygen flux than calculated from O_2 microprofiles (Berg et al., 2003).

As described, the diffusive boundary layer drapes the sediment surface as a sub-mm thin, unstirred layer through which solute exchange is dominated by molecular diffusion. The role of this DBL for the oxygen flux across the sediment-water interface has been demonstrated by the use of microsensors in laboratory-incubated sediments (Jørgensen and Revsbech, 1985) and directly on the seafloor (e.g., Reimers et al., 1986; Archer et al., 1989; Gundersen and Jørgensen, 1990; Glud et al., 1994). The thickness of the DBL generally varies between a tenth of a mm and a few mm. It is thinner by higher current velocities of the overlying seawater and thicker by increasing roughness of the sediment surface (Dade, 1993; Røy et al., 2002; Han et al., 2018). Fig. 3A shows an O_2 microprofile measured *in situ* in a coastal sediment at 10°C . It illustrates the abrupt shift from the well-mixed water flow above the sediment to the steep gradient in the 0.5-mm thick DBL. Since the O_2 flux is continuous from the mixed layer and into the DBL, the steepness of the vertical gradient above and within the DBL is inversely proportional to the transport coefficient for oxygen and other solutes.

The stability of the DBL depends on currents and turbulence in the overlying seawater and is constantly changing. Dynamic modeling has shown that the benthic O_2 uptake of a coastal sediment may vary by 30%

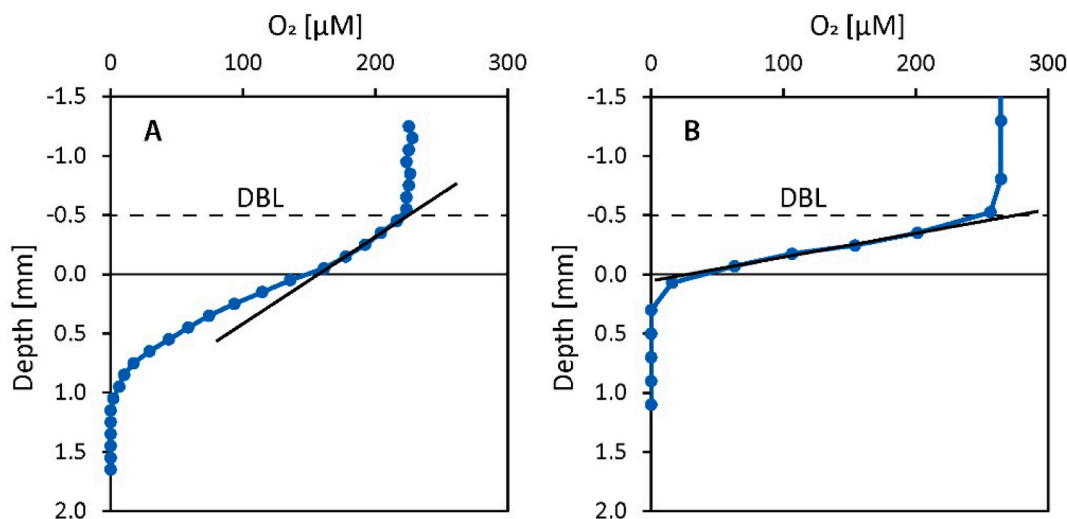


Fig. 3. Two examples of O_2 profiles in marine sediments and in the overlying diffusive boundary layer. A) Coastal sediment from a eutrophic bay. B) Sulfidic sediment with mat of filamentous sulfur bacteria on top. Black lines indicate the gradients used to calculate diffusive fluxes. ((A) from Glud et al., 2003; B) from Jørgensen and Revsbech, 1983).

or more within hours or days because of changes in the DBL thickness (Glud et al., 2007). The DBL may impede the O_2 uptake of sediments that have a high respiration rate (Kelly-Gerrey et al., 2005). However, the impedance is generally small, less than 5-20%, even in sediments of the eutrophic coastal zone (Rasmussen and Jørgensen, 1992; Glud et al., 2007).

High-resolution microsensors measurements of O_2 in the DBL enable calculations of the diffusive oxygen flux to the sediment-water interface. Since diffusion through the stagnant DBL is not impeded by particles, it can be calculated by a simple diffusion equation:

$$\text{DBL Flux} = D \times dC/dz \quad (\text{Eq. 3.1})$$

where D is the molecular diffusion coefficient of O_2 at the relevant temperature and salinity (Schulz and Zabel, 2006), while dC/dz is the vertical O_2 gradient. A similar flux calculation from microsensor-determined O_2 gradients within the sediment must take both porosity and tortuosity into account:

$$\text{Sediment Flux} = \phi \times D_s \times dC/dz \quad (\text{Eq. 3.2})$$

where ϕ is the porosity of the surface sediment and D_s is the whole sediment diffusion coefficient. D_s is equal to the molecular diffusion coefficient corrected for tortuosity, for example using the equation: $D_s = D/(1 + 3(1 - \phi))$ (Rasmussen and Jørgensen, 1992; Iversen and Jørgensen, 1993).

It is apparent that the measurement of O_2 microgradients within the DBL provides a simpler approach to calculate the diffusive O_2 flux to the sediment surface than measurements within the sediment. The latter require high-resolution determinations of either the porosity or the diffusivity or both, e.g. by the use of a diffusivity microsensor (Revsbech et al., 1998). The importance of porosity and tortuosity is evident from the O_2 microgradient shown in Fig. 3A, where the slope of the gradient increases abruptly by 1.65-fold right at the sediment-water interface. Since the O_2 flux must be the same just above and beneath this interface, the ratio $D/(\phi \times D_s)$ is also 1.65. The molecular diffusion coefficient at 10 °C is $1.46 \times 10^{-5} \text{ cm}^2 \text{ s}^{-1}$ (Schulz and Zabel, 2006). The sediment porosity in the top few tenths of a mm is then: $\phi = 0.79$. The diffusive oxygen uptake of the sediment according to Eq. 3.1 is $13 \text{ mmol } O_2 \text{ m}^{-2} \text{ d}^{-1}$, which is within a typical range for a coastal marine sediment.

Some sediments have an extremely high oxygen uptake, and nearly the entire drop in O_2 concentration occurs in the DBL. Fig. 3B shows such an example, where oxenic seawater with $265 \mu\text{M } O_2$ at 20 °C flowed over a highly sulfidic sediment with a 0.5-mm thick DBL. The diffusive

O_2 uptake was $85 \text{ mmol m}^{-2} \text{ d}^{-1}$ (Jørgensen and Revsbech, 1983). This approaches the theoretical maximum, about $100 \text{ mmol } O_2 \text{ m}^{-2} \text{ d}^{-1}$, of diffusive flux of across the sediment-water interface. An even higher diffusive O_2 flux would require a higher flow velocity and, thus, a thinner DBL to enable a steeper O_2 gradient.

The DBL closely follows the topography of the sediment surface, even down to the mm-scale. It is smoothed out over sediment roughness elements smaller than half the thickness of the DBL (Jørgensen and Des Marais, 1990; Røy et al., 2005). Fig. 4 shows the topographic surfaces of the DBL, the sediment surface, and the base of the oxic zone in the sediment. The DBL was 0.6 mm thick and the mean depth of O_2 penetration was 1.2 mm, i.e. rather similar to Fig. 3A. Due to this mini-topography of the DBL, the diffusion of oxygen is not simply a vertical flux but rather a complex, 3-dimensional flux, where the direction of net diffusion is always perpendicular to the DBL and sediment topography.

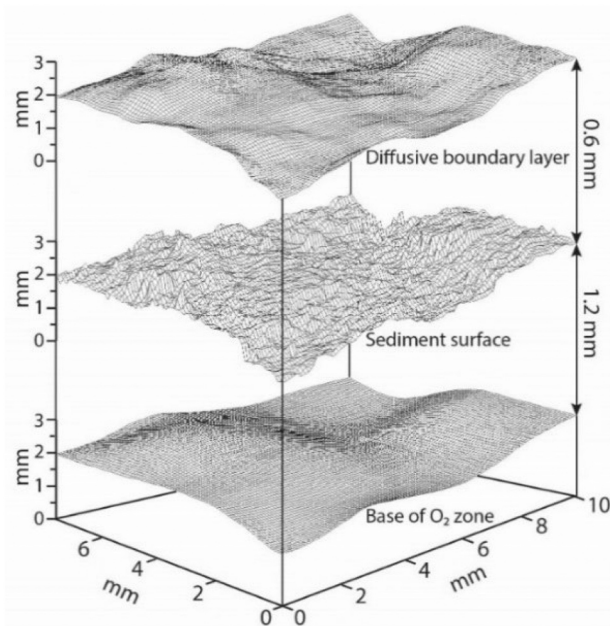


Fig. 4. 3-dimensional view of 0.8 cm^2 of a marine mud flat showing the sediment surface in between the upper extent of the diffusive boundary layer and the lower extent of the oxic sediment zone (from Røy et al., 2005).

This 3-dimensional DBL-flux was found to exceed the vertical DBL-flux by about 10% in estuarine mud of low roughness and up to about 25% in nearshore sand of high roughness (Glud et al., 2003; Røy et al., 2005). None of the diffusive oxygen uptake data in our database have been corrected for this 3-dimensional enhancement and are, therefore, generally too low by a small percentage.

Due to currents and wave action, half of the inner continental shelf (<50 m depth) consists of permeable sands (Hall, 2002), often with distinct bedforms such as ripples and dunes. The water flow across these topographic bedforms generates pressure gradients that drive pore water advection through the upper 2–15 cm. The depth of flow penetration depends on the sediment topography and permeability. The forced advection enhances the solute exchange across the sediment-water interface (Huettel and Gust, 1992a; Huettel et al., 2014). Sandy sediments thereby trap phytoplankton and other fine organic particles from the water column and often have a high oxygen respiration in spite of a low organic carbon content (Huettel and Rusch, 2000; Cook et al., 2007). As the oxygen uptake depends on the overlying seawater flow and internal pore water advection, the proper measurement of oxygen consumption in permeable sediments poses methodological challenges. The eddy covariance technique is the most useful approach for this purpose at moderate current velocities (McCann-Grosvenor et al., 2014). Such measurements at water depths of 30–70 m, e.g. in the North Sea or off the US west coast (McGinnis et al., 2014; Reimers and Fogaren, 2021), indicate that the O₂ consumption is similar to or slightly higher than non-permeable sediments at similar water depths and with similar primary productivity in the overlying water column.

Currents are sometimes so strong that they cause bedform migration and severely complicate even eddy covariance measurements (Ahmerkamp et al., 2015). Strong currents across the seabed combined with a resulting high shear stress drive particle resuspension from the sediment surface into the turbulent benthic boundary layer (e.g., Tengberg et al., 2003). A dynamic balance between active resuspension and resettling of particles thereby establishes a nepheloid layer of elevated particle density in the lowest few m above the seabed. The particles typically have high O₂ respiration and nutrient regeneration rates and constitute a highly mobile, particulate component of the boundary layer. Particle resuspension is a function of current velocity and possible wave action, while the settling velocity is also affected by the degree of particle flocculation. Flocs have been found to be larger and have higher settling velocity close to the seafloor in summer, possibly because the production of transparent extracellular polymers (TEP's) by microorganisms cause particle agglutination during the warm summer period (Fettweis and Baeye, 2014). Very high flocculation may generate a fluid mud layer flowing over the sediment in river estuaries with strong tides (Becker et al., 2013).

3.2. Diffusion-mediated O₂ uptake

The relative contribution of diffusive O₂ uptake to total O₂ uptake was found to increase with depth in the ocean, from half on the eutrophic inner continental shelf with dense benthic communities to being completely dominant in the oligotrophic deep sea with a more sparse benthos (Glud, 2008; Stratmann et al., 2020). It is interesting that, at both the high and the low extremes of oxygen uptake, molecular diffusion becomes the predominant mechanism of oxygen transport. At the high end, microbial biofilms of filamentous sulfur bacteria, *Beggiatoa* spp., have an O₂ penetration depth of only 0.1–0.2 mm, and the entire O₂ pool in the sediment turns over in about one second (Fig. 3B; Jørgensen and Revsbech, 1983). At such a high flux with short diffusion distance and fast turnover, molecular diffusion outruns advection. At the low end, oxygen diffuses tens of meters into sediments of the central ocean gyres, even down to the basaltic crust, and O₂ in this deep oxic zone turns over extremely slowly in tens of thousands of years (Chapter 4.4; D'Hondt et al., 2015).

An example of a sediment O₂ profile with an intermediate

penetration depth of 3 cm is shown in Fig. 5A. The profile was measured at 0.1 mm depth resolution directly on the seafloor in one of the deep oceanic trenches by the autonomous free-fall “Hadal-Profiler Lander”. The 400 data points form a smooth curve that even resolves the O₂ gradient within the 0.5-mm thick DBL. The volume-specific O₂ consumption rates were calculated from the O₂ concentration profile, using the modeling software PROFILE of Berg et al. (1998) (Fig. 5B). The model showed two intervals of high O₂ consumption rates. One was the top 0.5 cm where freshly deposited organic matter was available for aerobic respiration by the microbial community. The other was the bottom of the oxic zone, near the oxic-anoxic interface, driven by the oxidation of reduced inorganic products from anaerobic degradation. Thus, out of the total diffusive oxygen uptake of 1.63 mmol O₂ m⁻² d⁻¹, ca. 15% occurred in the lower peak at 2–3 cm depth. Compared to the extreme examples described above, the total O₂ pool in this sediment had an intermediate turnover time of ca. 1 day. Such a turnover time shows that the O₂ distribution and flux may still be compromised during the time it takes to retrieve sediment cores from the deep sea and perform O₂ analyses on board a ship (Glud et al., 2021).

3.3. Fauna-mediated O₂ uptake

Faunal activity plays an important role for the biogeochemical function of benthic habitats. The benthic fauna ingests and decomposes organic material, reworks sediment and ventilates burrow structures. These latter activities are commonly referred to as bioturbation (Kristensen et al., 2012). The fauna-mediated O₂ uptake encompasses fauna respiration and fauna-stimulated microbial respiration. It also includes enhanced re-oxidation of reduced products from the microbially driven anaerobic respiration, which can contribute significantly to the benthic O₂ uptake (e.g., Aller, 1994; Kristensen and Kostka, 2006; Middelburg, 2018). The way that fauna activity affects diagenetic pathways and enhances the benthic O₂ uptake depends on the type of fauna and its feeding mode.

Filter feeding epifauna, such as mussels, oysters or cold-water corals, acts as bioengineers that form beds and reefs, which effectively entrap suspended material and host a diverse biota. Recent investigations using eddy covariance technique have shown that the benthic O₂ consumption in such beds and reefs exceeds the O₂ uptake of adjacent sediments by 5- to 20-fold and that they act as hotspots for organic carbon mineralization (Rovelli et al., 2015; Attard et al., 2020; Volaric et al., 2020). Deposit-feeding epifauna such as brittle stars, sea stars and sea cucumbers, move along the sediment surface, ingesting detrital material. They are particularly prominent along the deeper margins and in the abyss (Gorska et al., 2020). Their feeding mixes the upper sediment layers and their digestion hydrolyses complex organic material, while their defecation concentrates organic material and forms hot-spots with intensified microbial oxygen consumption (Jørgensen, 1977b; Huffard et al., 2016; Durden et al., 2020; www.youtube.com/watch?v=MZmF8-Wudu4).

Burrowing macrofauna (in-fauna) strongly affects the benthic redox zonation and is particularly important for the biogeochemical processes in coastal sediments (e.g., Aller, 1994; Kristensen et al., 2012). Depending on their feeding mode, burrowing deposit feeders rework and mix the sediment matrix. *Biodiffusers* typically induce a random local mixing over short distances, yet the material transport can be considerable. As an example, it was estimated that a natural population of the sea urchin, *Echinocardium* sp., with 40 individuals per m², translocated a volume of 20 L of sediment per m² per day (Lohrer et al., 2005). Natural coastal populations of biodiffusers typically support a particle biodiffusion coefficient of 1–2 cm² yr⁻¹ (Dupont et al., 2006; Gilbert et al., 2007; Quintana et al., 2007). *Upward and downward conveyors* continuously displace material vertically from deeper layers to the sediment surface or vice versa. A natural population of 50 lugworms, *Arenicola marina*, per m², living head-down in J-shaped burrows, has been estimated to yearly ingest and completely mix the upper 30 cm of

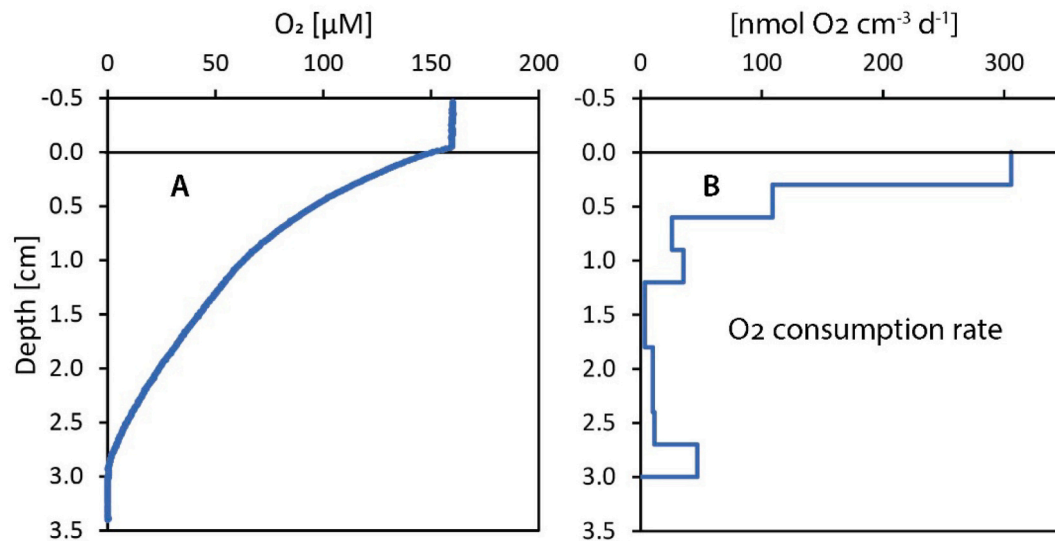


Fig. 5. Depth distribution of A) oxygen concentration and B) volume-specific oxygen consumption rates in a deep-sea sediment. *In situ* O₂ data from Station A10 at 7770 m water depth in the Atacama Trench, East Pacific off northern Chile (data from Glud et al., 2021).

sediment (Riisgård and Banta, 1998). *Regenerators*, such as fiddler crabs, live in permanent burrow systems and infills that are constantly excavated. The material is deposited on the sediment surface, inducing an effective and continuous overturn of the sediment (Huang et al., 2007). Thus, deposit feeding fauna directly contributes to the degradation of organic material via ingestion, while sediment reworking exposes otherwise buried recalcitrant organic material to frequent redox shifts, which stimulates the microbially driven degradation of the material (Aller, 1994, 2004; Kristensen and Holmer, 2001). Overall, sediment reworking enhances the efficiency of the oxidative processes, maintains a high buffer capacity against sulfide release, and enhances the phosphate binding capacity of coastal sediments (Aller, 2004).

Filter feeding and ventilating in-fauna establishes burrow structures and mediates a rapid solute exchange between the oxic bottom water and the subsurface sediment. The irrigated burrows enlarge the oxic-anoxic interface and form a complex, 3-dimensional mosaic of microhabitats with highly heterogeneous redox zonation as compared to non-irrigated sediments (Wenzhöfer and Glud, 2004; Zhu et al., 2006; Volkenborn et al., 2012; Camillini et al., 2019). Bioirrigation significantly enhances the benthic O₂ uptake due to stimulated aerobic microbial respiration and enhanced oxidation of reduced products along the walls of ventilated burrows and galleries (Fig. 6). Furthermore, irrigation facilitates a close coupling between oxic and anoxic microbial processes, such as nitrification and denitrification, or enhanced formation of iron and manganese oxides, thus stimulating microbial metal respiration (Aller, 1990; Pelegri and Blackburn, 1994; Munksby et al., 2002; Webb and Eyre, 2004). The irrigation is typically intermittent, creating highly dynamic oxic environments in the subsurface sediment, and results in small-scale variation in diagenetic processes. These dynamic conditions support a diverse and physiologically versatile microbial community (Papaspyrou et al., 2006; Bertics and Ziebis, 2009; Woulds et al., 2016).

Densities of fauna and empirical allometric relations for fauna respiration have been used to assess that fauna respiration in coastal settings may account for 25 to 40% of the TOU (Piepenburg et al., 1995; Heip et al., 2001; Rodil et al., 2019). The fauna-mediated O₂ uptake generally exceeds the calculated faunal respiration, however, mainly due to fauna-enhanced, microbial respiration and re-oxidation of reduced products from anaerobic respiration (Forster and Graf, 1995; Hansen and Kristensen, 1997; Vopel et al., 2003; Glud et al., 2003).

To correctly assess the *in situ* contribution of fauna, it is essential to maintain the natural behavior and respiration of the communities. This is difficult in small, confined sediment cores or in laboratory enclosures.

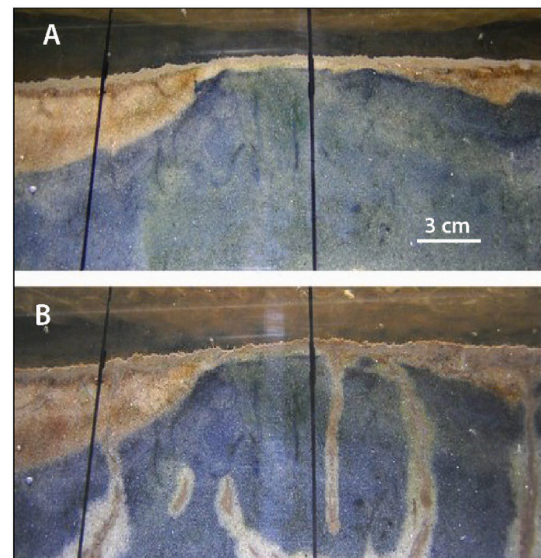


Fig. 6. The effect of bioirrigation. Permeable sediment from the German Wadden Sea was placed in a large flume with a transparent wall. The photographs show the zonation before (A) and one week after (B) the introduction of benthic in-fauna (lugworms and soft-shell clams). The fauna induced subsurface irrigation with oxic water and gradually oxidized the otherwise reduced sediment. Oxidized sediment is brown due to iron oxides, reduced sediment is dark gray due to iron sulfides. (Photos by Ronnie N. Glud).

Natural faunal assemblies consist of numerous species of very different sizes that are difficult to transfer and maintain in the laboratory. Therefore, *in situ* assessments of TOU using large benthic chambers generally provide a more correct representation of the fauna-mediated O₂ uptake, with higher rates than obtained from incubations of smaller, retrieved sediment cores (Glud and Blackburn, 2002; Glud et al., 2003) (Chapter 2.1). Furthermore, the benthos in coastal sediments may respond to changes in light intensity, water flow and food availability, exhibiting diel or tidally induced temporal patterns in activity (Loo et al., 1996; Wenzhöfer and Glud, 2004; Thouzeau et al., 2007). Thus, chamber enclosures might not capture environmentally induced dynamics in oxygen flux or may underestimate the contribution of filter feeding by communities that gage their filtration activity to the

food availability (Riisgård, 1994; Riisgård et al., 2003). Under such circumstances, combined measurements of *in situ* O₂ microprofiles and non-invasive eddy covariance can best reveal the importance of fauna-mediated O₂ uptake (Glud et al., 2016).

Only a limited number of *in situ* studies have quantified the TOU and DOU in parallel. Studies in coastal settings generally show that the fauna-mediated O₂ uptake accounts for about half of the TOU (Archer and Devol, 1992; Forster et al., 1999; Meile and Van Cappellen, 2003; Glud, 2008, and references therein). The fauna-mediated O₂ uptake increases with the faunal abundance (Clough et al., 2005; Norkko et al., 2015; Belley and Snelgrove, 2016). However, in many heterogeneous settings macrofauna biomass correlates poorly with the fauna-mediated O₂ uptake (Moodley et al., 1998; Glud, 2008; Snelgrove et al., 2018). This is presumably due to the variability in feeding modes of the benthos, the behavioral responses of natural communities, and the fact that mass-specific respiration rates are size dependent (Ghedini et al., 2018). Functional traits, and the extent to which a given fauna activity enhances the benthic O₂ demand, are also context dependent. For instance, the enhancement of benthic O₂ uptake by a given irrigation activity depends on the O₂ penetration depth.

Studies of the importance of fauna for benthic solute exchange mostly focus on macrofauna, but in sediments with very shallow O₂ penetration, meiofauna (metazoans of 0.04-1 mm size) can add significantly to benthic solute transport and to O₂ consumption (Aller and Aller, 1992; Rysgaard et al., 2000; Nascimento et al., 2012; Bonaglia et al., 2014). It was recently demonstrated that meiofaunal activity enhanced reoxygenation of surface sediments after hypoxia (Bonaglia et al., 2020). The contribution of meiofauna to the metazoan biomass generally increases with water depth (Stratmann et al., 2020). Allometric trends suggest that meiofauna respiration is responsible for 8-19% of the benthic O₂ consumption at abyssal and hadal water depths in the southwest Pacific (Leduc et al., 2016). Yet, the importance of meiofauna for the biogeochemical function and the oxygen demand of marine sediments is still poorly understood.

3.4. Time scales

Suspended POC in the open ocean originates mainly from primary production in the surface waters according to its young ¹⁴C-age and isotopically light δ¹³C-composition (McNichol and Aluwihare, 2007). The flux of POC from rivers and estuaries to coastal seas, together with the resuspension of sediment from the shelf and upper continental slope, also contribute by a lateral transport of POC from the continental shelf to the deep sea (Bauer and Druffel, 1998; Raymond and Bauer, 2001). The total pool of suspended POC in the ocean has a mean residence time of 5-10 years according to Thorium isotope studies (Bacon and Anderson, 1982). The settling speed of marine snow varies strongly depending on the degree of flocculation and the sediment load of particles, and the settling time from the photic zone to the seafloor at several thousand m depth may vary from days for a flocculating phytoplankton bloom to years for the finest suspended particles (e.g., Smith Jr. et al., 2018).

The rate of POC mineralization drops continuously with its increasing age as it sinks down through the water column, settles on the seafloor, and is gradually buried into the sediment. Middelburg (2019) compiled data on the degradation rate of POC from sediment traps, from laboratory experiments, and from sediment cores. His combined plot shows that the degradation rate constant drops by 9 orders of magnitude as its age increases by 9 orders of magnitude, from less than a day to a million years. The log-log plot in Fig. 7 shows a linear fit, i.e. a power law function, between POC reactivity and POC age, whereby the first-order kinetic coefficient, *k* (in yr⁻¹), is equal to: $0.21 \times t^{-0.985}$, where *t* is the time in years. The exponent is very close to -1, which shows that the POC reactivity drops in inverse proportion to its age. This relationship has important implications for whether the POC is degraded in the water column or in the sediment, and where CO₂ and inorganic nutrients are released. It also has implications for which fraction of the deposited

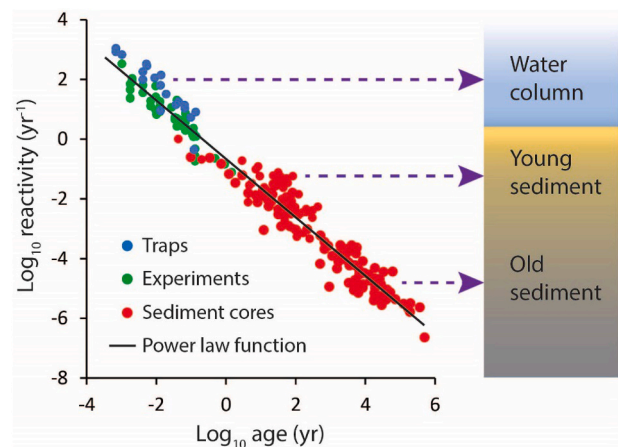


Fig. 7. Degradation rate constants (“reactivity”) of organic matter as a function of its age. Data sources are from sediment trap material, laboratory experiments, and sediment cores. The data plot is double logarithmic and is fitted by a power law function (after Middelburg, 2019; data courtesy of Jack J. Middelburg).

organic matter is buried on a long time scale and is thereby withdrawn from the modern oceanic carbon cycle.

After the POC settles on the seafloor, the aerobic degradation continues. The organic matter is here orders of magnitude more concentrated than in the water column, and a very different community of benthic organisms participate in the degradation. The macrobenthos may drive particle mixing down to 5-15 cm in the sediment (Boudreau, 1998). In ocean margin sediments, this ensures that aerobic mineralization continues to play a role until the organic matter is completely buried beneath the bioturbated zone. The anaerobic microorganisms then take over and continue the mineralization at ever decreasing rates. Direct measurements of oxygen respiration and sulfate reduction rates in a coastal marine sediment show how aerobic and anaerobic degradation follow a power law function with depth and, thus, with age of the

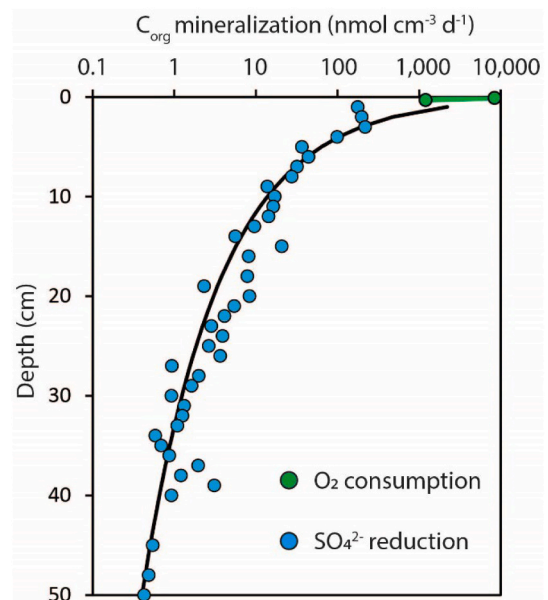


Fig. 8. Organic carbon mineralization rates by oxygen respiration and sulfate reduction in a coastal marine sediment (Aarhus Bay, Denmark). The curve shows a power law fit to the data. Oxygen respiration was confined to the top 0.5 cm and the data show the seasonal range of O₂ respiration rates. (Data from Rasmussen and Jørgensen, 1992, and Petro et al., 2019).

organic matter. An example is presented in Fig. 8 in a semi-log plot in which data at 3-50 cm depth are fitted by the power law function: Mineralization rate = $2200 \cdot z^{-2.2}$ nmol C_{org} cm⁻³ d⁻¹, where z is the depth in cm.

The global distribution and budget of oxygen uptake in the seabed, as discussed in Chapters 5 and 6, represent processes that occur today and have occurred through the later part of the Holocene. However, on a time scale of tens of thousands of years, the ocean productivity and the seafloor respiration have changed greatly. Marine sedimentation on the continental shelves has occurred only since the last 10,000 years, after the shelves became flooded following the last glaciation and sea-level low-stand. Today, the coastal zone and inner shelf region have the highest rates of sediment accumulation and organic matter mineralization. Thus, an estimated 88% of the global accumulation of organic carbon in marine sediments currently occurs within 500 km from the nearest coast or out to 2000 m water depth (Wallmann et al., 2012; Xie et al., 2019). Beyond this ocean margin, the seafloor has much lower sedimentation rates, and the degradation of organic matter in the deep sea is affected by geochemical processes that take place on a much longer time scale. An extreme example of this are the 10- to 100-m deep, oxic sediments of the mid-oceanic gyres where the calculated turnover time of O₂ is 20,000-40,000 years, i.e. much longer than the current interglacial period (D'Hondt et al., 2015).

3.5. Coupling to anaerobic processes

A fraction of the organic matter deposited on the seafloor escapes the uptake and respiration by aerobic organisms and is buried beneath the bioturbated zone. Here, it continues to be attacked by extracellular hydrolytic enzymes from the microbial community and is gradually degraded and fermented to small organic molecules (Fig. 9) (Jørgensen, 2006). These molecules are substrates for bacteria and archaea with an anaerobic respiration. The dominant terminal electron acceptors by this respiration change down through the anoxic sediment, largely in accordance with a decreasing energy yield of the respiratory process: nitrate, manganese oxide, iron oxide, sulfate and carbon dioxide (Froelich et al., 1979).

The anaerobic respiration processes result in a corresponding sequence of reduced products: N₂/NH₄⁺, Mn²⁺, Fe²⁺, H₂S and CH₄. In addition, CO₂, NH₄⁺, HPO₄²⁻ and other inorganic ions are released by the organic matter degradation. The reduced products accumulate in the

sediment where a small fraction is buried. Next to organic matter, pyrite (FeS₂) is the most important sink for reducing power. Most of the dissolved, reduced products diffuses upwards along concentration gradients. As they reach into overlying biogeochemical zones with higher redox potential, they are oxidized through a redox cascade of processes as illustrated in Fig. 9. Very simplified, the CH₄ is thereby oxidized by SO₄²⁻, H₂S is oxidized by Fe(III), Fe²⁺ is oxidized by Mn(IV), etc. In reality, the zonation of processes is not that clear-cut. The different processes overlap, and the sediment is temporally and spatially heterogeneous due to faunal activity and other factors. The ultimate oxidant at the end of the redox cascade is O₂, which is consumed by the chemical or biological oxidation of the inorganic species.

The quantitative role of each electron acceptor differs strongly between sediments, depending on water depth, sedimentation rate, organic carbon content and other parameters. In coastal waters and inner shelf sediments, sulfate reduction is the most important anaerobic process (Jørgensen, 1982; Canfield et al., 2005). Studies of sulfate reduction in these sediments using ³⁵S radiotracer show that about 90% of the produced H₂S is ultimately oxidized back to sulfate (Jørgensen et al., 2019). If the sediment is highly sulfidic, the oxidation may take place near the sediment surface by aerobic or nitrate-reducing sulfide oxidizers, such as filamentous sulfur bacteria or cable bacteria (Jørgensen, 1977a; Pfeffer et al., 2012). If the sediment is less sulfidic, the coupling to oxygen is mostly indirect via iron, which is then the main oxidant for sulfide (Findlay et al., 2020). The resulting Fe²⁺ and iron sulfides may subsequently be oxidized by O₂ as a result of bioturbation and burrow ventilation by benthic invertebrates. The iron oxidation may also be indirect via manganese oxides that oxidize both solid phase and dissolved Fe(II) (Aller and Rude, 1988; Schippers and Jørgensen, 2001).

With increasing water depth and distance from land, iron reduction and manganese reduction take over the role as the main electron acceptors by anaerobic mineralization (Canfield et al., 2005). Abyssal sediments under the ocean gyres constitute the extreme end-members of this trend, with oxygen penetration all the way down to the basaltic crust (D'Hondt et al., 2015). The anaerobic mineralization processes and their contribution to sediment oxygen consumption are, thus, biased towards the ocean margins, even more biased than the oxygen consumption (Bradley et al., 2020). Whereas the coastal zone and continental shelf out to 200 m water depth comprise only 7% of the ocean area, they include about 75% of the global marine sulfate reduction (Canfield et al., 2005) and about 60% of the global sediment oxygen

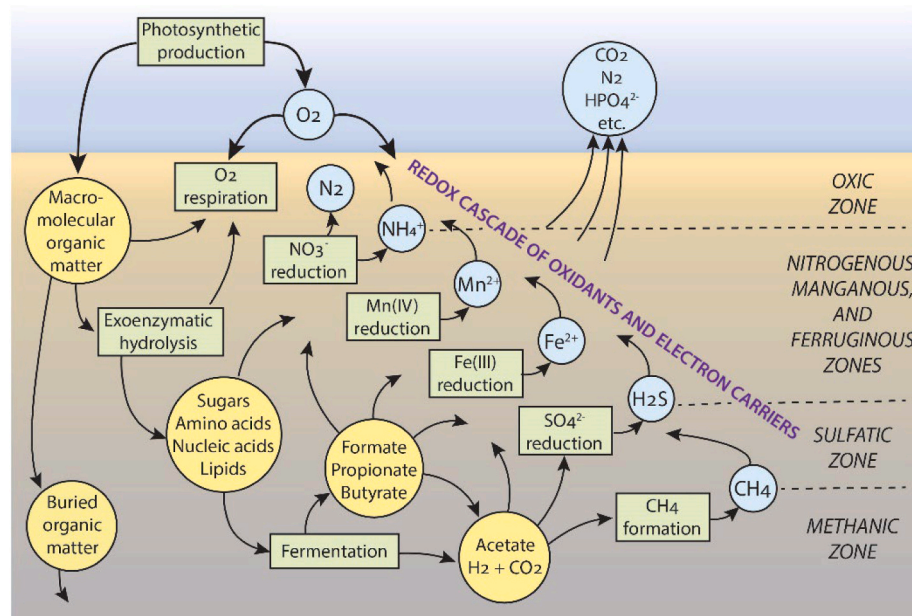


Fig. 9. Organic matter mineralization in marine sediment with a vertical zonation of the main biogeochemical processes and electron acceptors. The scheme emphasizes the degradation pathways via hydrolysis and fermentation that provide substrates for anaerobic respiration with an energetic depth sequence of oxidants. The reduced respiration products diffuse upwards and are re-oxidized through a redox cascade that ultimately transfers most of the reducing power from the anoxic sediment to O₂. (From Jørgensen, 2021).

consumption (Chapter 6.3). Whereas oxygen uptake in the seabed is mostly driven by the respiration of heterotrophic organisms, including benthic macrofauna, meiofauna and microorganisms, oxygen is also consumed by the oxidation of reduced, inorganic products from the redox cascade. In shelf sediments, these products are dominated by sulfide and iron sulfides, and 25-50% of the entire oxygen consumption is used for the re-oxidation of these inorganic species (Jørgensen et al., 2019).

Since about 90% of the produced sulfide is re-oxidized to sulfate by oxygen, either directly or indirectly, most of this anaerobic mineralization is included in the total oxygen uptake (TOU). The TOU measurement thereby includes also most of the organic matter mineralization that takes place beneath the oxic and bioturbated zone. It may not include the deep mineralization to methane and CO₂. However, the methane production and its oxidation at the bottom of the sulfatic zone generally contribute only 1-10% to the total mineralization by sulfate reduction and is thus a small component in the overall organic carbon turnover (Flury et al., 2016; Jørgensen, 2021).

In conclusion, half of the oxygen consumption in inner shelf sediments is involved in the re-oxidation of sulfide and only half of the oxygen consumption is available for the benthic fauna and for aerobic, heterotrophic microorganisms. This oxygen consumption by sulfide oxidation drops with ocean depth to about a tenth in the continental rise and fades out in the abyss (Canfield et al., 2005). The coupling of oxygen uptake to sulfide and iron oxidation in coastal sediments may impose a seasonal delay in the sediment oxygen consumption. During summer and fall the surface sediment builds up a pool of iron sulfides that hold back the sulfide from immediate reaction with oxygen and gradually becomes oxidized during winter. This “iron curtain” can function as a barrier against release of sulfide from the sediment in summer and delay the oxygen debt of the sediment (Seitaj et al., 2015).

An important aspect of the re-oxidation of sulfide and other reduced inorganic species is that the processes are microbially catalyzed and provide energy for a chemoautotrophic growth of microorganisms. This has been studied by dark incubation experiments with marine sediment amended with ¹⁴C-labeled HCO₃⁻. Based on such experiments, Vasquez-Cardenas et al. (2020) calculated the autotrophic growth in coastal marine sediment to be equivalent to 1-11% of the total oxygen uptake with a mean value of 4%. They also made a literature survey of such measurements and found a range of 1-22%, with a mean of 7%. This mean corresponds to the 7% estimated as a maximum value by Jørgensen and Nelson (2004), based on a growth yield by chemoautotrophic sulfide oxidizers of 15% and assuming that half of the oxygen uptake was allocated to sulfide oxidation. The anaerobic oxidation of organic matter has a lower energy yield than the aerobic oxidation, but this is compensated by the oxidation of reduced respiration products through chemoautotrophic microorganisms. Their dark CO₂ fixation and growth generate easily degradable microbial necromass that can be used by aerobic organisms (Middelburg, 2011). Yet, this accounts for only a small fraction relative to the total influx of organic matter and is probably not detectable in budgets of carbon cycling in marine sediments (Bradley et al., 2018).

4. Regional examples

The global map of seabed oxygen uptake rates and their correlation with environmental parameters presented in Chapter 5 are compiled from highly diverse marine systems, ranging from eutrophic seas to oxygen minimum zones, abyssal plains, mid-oceanic gyres, and deep-sea trenches. We here provide examples of the environmental conditions of these systems and discuss how the oxygen and carbon cycles of their sediments are controlled.

4.1. Eutrophic seas: Baltic Sea

The Baltic Sea represents an example of a eutrophic coastal sea with

strong terrestrial influence and a close benthic-pelagic coupling. With an area of about 400,000 km², it is one of the largest brackish water bodies in the world and arguably has one of the largest anthropogenically induced oxygen-deficient bottom waters in the world (Meier et al., 2018). The water column is stratified by a seasonal thermocline and a permanent halocline at 60-80 m depth, between a brackish upper water mass and more saline bottom water originating from the North Sea. The deglaciation of the entire basin some 13,000 years ago, and its transition from freshwater to brackish-marine conditions about 8000 years ago, explains why the relatively young sea still has a low diversity of genuine brackish-water species of animals and plants (Björck, 1995; Hällfors et al., 1981).

Starting in the 1950s, the Baltic Sea has become increasingly eutrophic due to a high nutrient load of nitrogen and phosphorous from the large catchment area of predominantly forestland to the north and farmland to the south. This has accelerated the carbon cycling and oxygen consumption in the Baltic seabed. Jonsson and Carman (1994) estimated a > 1.7-fold increase in organic matter deposition in the northern Baltic Sea proper between the late 1920's and the late 1980's. This trend will continue, enhanced by a predicted increase of up to 20-50% in POC flux from land due to increasing runoff (Omstedt et al., 2012). Reduction in nitrogen and phosphorous loads since the 1980's has led to a gradual alleviation of eutrophication (Andersen et al., 2017) but not yet to an alleviation of hypoxia caused by high oxygen consumption in the lower water column (Meier et al., 2018).

Oxygen concentrations are low in the deep basins, and hypoxia may even occur during the summer months in shallow coastal areas. A third of the central Baltic Sea had <2 mL O₂ L⁻¹ during the past two decades, while a fifth was totally anoxic and sulfidic. Major inflows of saline and oxygenated bottom water occur irregularly and provide a transient oxygen supply to the deep basins. However, this ventilation with saline bottom water also increases the stability of stratification and reduces the vertical mixing of oxygen from above until the stratification slowly weakens again (Conley et al., 2009; Carstensen et al., 2014).

Long periods of extensive hypoxia have occurred in many high-latitude shelf basins during the Holocene due to the combined effect of global sea level rise and local glacio-isostatic rebound. In the central Baltic Sea, such periods in the past are apparent from organic-rich, laminated sediment intervals that have now returned, starting in the 1950's, due to the combined effect of eutrophication and continued warming (Kotilainen et al., 2014; Jilbert et al., 2015). Thus, remote sensing data from 1990 to 2008 suggest an accelerated temperature increase of up to 1 °C per decade, mostly in the northern part of the Baltic Sea (International Council for the Exploration of the Sea, 2018).

The net primary production in the Baltic Sea is about 3.8 Tmol C yr⁻¹ (Leipe et al., 2011), of which a third is exported beneath the photic zone (Heiskanen and Leppänen, 1995). Leipe et al. (2011) estimated a total organic carbon (C_{org}) burial rate in the Baltic Sea of 0.30 ± 0.24 Tmol C yr⁻¹, corresponding to 8% of the net primary production. This C_{org} burial is a relatively high fraction of the deposited POC, in particular in the hypoxic basins where the buried fraction ranges from one to two thirds (Omstedt et al., 2014). A large burial efficiency was suggested to be due to a large contribution of poorly degradable terrestrial POC (Nilsson et al., 2021). Recent estimates by Nilsson et al. (2019) conclude that 1.9 ± 0.7 Tmol C yr⁻¹ is deposited in total on the Baltic seabed, with a mean burial efficiency of 4%, but with a large variability between the different basins (2.5-16%).

Data from sediment trap studies and measurements of the total oxygen uptake of the sediments are rather scattered in the Baltic Sea. Rates of TOU from the muddy seabed at water depths from 15 to 130 m are mostly in the range of 7-15 mmol O₂ m⁻² d⁻¹ (Koop et al., 1990; Rasmussen and Jørgensen, 1992; Conley et al., 1997; Glud et al., 2003). The contribution by benthic macrofauna respiration is high in some areas, up to 50% of the TOU and occasionally even higher (Glud et al., 2003).

Climate change during the 21st century will impact the phytoplankton production in many regional seas (Holt et al., 2016). An

increase of the net primary productivity is predicted for the Baltic Sea, whereby a primary driver is an increased wind-driven ventilation and upwelling in the central Baltic Sea and reduced sea ice cover in the northern Baltic Sea. Massive cyanobacterial blooms are currently observed by satellite nearly every summer. The cyanobacteria provide a positive feed-back on eutrophication by extensive N_2 -fixation. The sedimentation and decay of senescent cyanobacteria stimulate hypoxia in the deep bottom water, which in turn enhances phosphate release from the sediment and thereby supports cyanobacterial blooms (Funkey et al., 2014). The fast, annual deposition of a diatom spring bloom may also cause a peak in sediment O_2 uptake and even create a sulfidic surface sediment (Moelsund et al., 1994).

4.2. Oxygen minimum zones

Oxygen minimum zones (OMZs) along the open ocean margins are mainly driven by strong coastal upwelling and a high export rate of plankton-derived organic matter into the underlying water column. Hypoxia develops when the O_2 consumption during degradation of the sinking detritus exceeds the O_2 renewal by mixing with oxic water masses. There is not a strict definition of hypoxia or of the resulting OMZs in the ocean, but $<0.5 \text{ mL } O_2 \text{ L}^{-1}$ is often used as an upper threshold (e.g., Helly and Levin, 2004; Paulmier and Ruiz-Pino, 2009). This corresponds to $<22 \mu\text{M } O_2$ or $<7\%$ of sea surface air saturation at 5°C . The largest OMZs occur near the eastern ocean margins where predominant wind-systems drive surface water off shore and draws up nutrient-rich deeper water that supports a high primary productivity. The main OMZs occur in the Eastern South Pacific and Eastern Tropical North Pacific plus the Arabian Sea and Bay of Bengal. In some of these OMZs, the O_2 concentration reaches zero ($<2 \text{ nM } O_2$; Revsbech et al., 2009). The anoxic or near-anoxic conditions in the OMZs cause massive losses of combined nitrogen to N_2 in the ocean by supporting the microbial processes of anammox and heterotrophic denitrification (Lam and Kuypers, 2011).

Paulmier and Ruiz-Pino (2009) estimated that the total areal extent of the oceanic OMZs is $30 \times 10^6 \text{ km}^2$, or 8% of the total oceanic area. Over most of this area, the O_2 minimum occurs in midwater of the open ocean at depths of 50–1000 m. Within that depth range, the OMZs impinge on the seafloor mainly on the outer continental shelf and the upper slope. Helly and Levin (2004) estimated that hypoxic OMZ bottom water with $<0.5 \text{ mL } O_2 \text{ L}^{-1}$ covers a global sediment area of $1.15 \times 10^6 \text{ km}^2$, corresponding to 4% of the outer shelf and upper slope together (50–1000 m water depth) and only 3% of the total OMZ area. An estimated $0.76 \times 10^6 \text{ km}^2$ of this seabed has anoxic, or nearly anoxic, bottom water with $<0.2 \text{ mL } O_2 \text{ L}^{-1}$.

The areal extent of benthic hypoxia has expanded over the past half-century and will expectedly continue to expand over the coming decades (Schmidtke et al., 2017; Breitburg et al., 2018). This is primarily due to the diverse effects of ocean warming, which include decreasing O_2 solubility by increasing temperature, reduced ventilation by stronger thermal stratification, stronger winds that drive upwelling, increased nutrient supply, and increased respiration rates of sinking POC in the upper ocean (Levin, 2018). A concurrent shoaling of the upper boundary of OMZs now spreads hypoxic bottom water further onto the continental shelves, which will affect their benthic fauna and microbial processes (Gilly et al., 2013). These trends have similarities to coastal hypoxia in silled basins and fjords, which is also enhanced by global warming but is increasingly affected by anthropogenic processes such as eutrophication (Middelburg and Levin, 2009; Breitburg et al., 2018). The Baltic Sea is an example of periodic hypoxia (Chapter 4.1), while the Black Sea is an example of permanent anoxia beneath a water depth of 50–150 m (e.g., Stanev et al., 2018).

Benthic flux chambers have been used for *in situ* measurements of the O_2 uptake at very low bottom water O_2 concentrations in OMZ regions. They have also been used to detect the out-flux of reduced solutes or DIC produced from anaerobic mineralization in the sediment. Chamber

incubations at low ambient O_2 concentration are challenged by a relatively rapid exhaustion of oxygen in the chamber, which might affect exchange rates of O_2 and other solutes. To ensure reliable benthic exchange rates at low O_2 concentration, sophisticated gill systems have been developed that maintain the O_2 level of the enclosed water by a continuous O_2 supply (Sommer et al., 2008). Yet, to determine the benthic organic carbon mineralization rates in such settings, DIC exchange rates may be a better option than O_2 consumption rates (e.g., Rassmann et al., 2020).

Due to such *in situ* measurements, data are available for the O_2 uptake of ocean margin sediments underlying the major OMZs with different degrees of hypoxia in the bottom water. We extracted the relevant data from our database using the following criteria:

- only data from the open ocean margins were selected, not data from coastal basins, silled fjords and other enclosed systems (such as the Black Sea or the Baltic Sea);
- only data from the outer shelf (50–200 m) and the upper slope (200–1000 m) were selected, i.e. from the ocean depths where OMZs may impinge on the seabed;
- only data with concurrent measurements of TOU and bottom water O_2 concentration were selected.

This selection left 199 data for the outer shelf and 88 data for the upper slope. A plot of TOU vs. bottom water O_2 concentration is shown for the entire dataset in Fig. 10A. In order to better resolve data for the most hypoxic OMZ regions, the same data are shown with expanded bottom water O_2 scale in Fig. 10B.

Fig. 10 shows clearly that the measured *in situ* O_2 uptake rates are strongly reduced under low O_2 concentrations relative to rates under high O_2 for the same ocean depth of 50–1000 m. Thus, TOU rates in OMZ sediments with $<25 \mu\text{M } O_2$ ($<0.5 \text{ mL } O_2 \text{ L}^{-1}$) appear to be an order of magnitude lower than in sediments with much higher bottom water O_2 concentrations (Archer and Devol, 1992). Nearly all these data are from the Pacific margin of South and North America, notably off Peru, Mexico, California and Oregon. By the lowest O_2 concentrations, nitrate may be an important alternative oxidant. For example, on the Pacific shelf off Mexico at 100–200 m depth there was only 0–6 $\mu\text{M } O_2$ in the bottom water but 20–30 $\mu\text{M } NO_3^-$ (Harnett and Devol, 2003). This could explain why the respiratory quotient, RQ, calculated from the DIC release relative to the O_2 uptake was mostly very high, in the range of 2–10 (Berelson et al., 1987, 2019; Jahnke et al., 1990, 1997; Sommer et al., 2016). As discussed in Chapter 6.2, a mean RQ for this depth range of the seabed outside of OMZs is $DIC:O_2 = 0.80\text{--}0.85$. The low O_2 uptake relative to the organic carbon mineralization may be compensated by NO_3^- uptake (see below). This shows that the DIC flux can be a more useful measure of organic matter mineralization than the O_2 flux under low bottom water O_2 in OMZ sediments.

The very low TOU rates occur in the absence of fauna and faunal respiration. They are therefore also related to a shift in O_2 transport across the sediment surface from partly bioirrigation to purely molecular diffusion (cf. Chapter 3). On the other hand, OMZ sediments underlie regions with high primary productivity and, expectedly, have high POC deposition rates with high mineralization potential. Although a relatively large fraction of the deposited POC may be buried in OMZ sediments (Baroni et al., 2020), it is not obvious whether the opposite directed effects of enhanced POC flux and low O_2 concentration will result in higher or lower O_2 flux. Apparently, the balance is a lower O_2 flux.

A large part of the mineralization in OMZ sediments must be anaerobic and lead to reduced products that diffuse to the sediment surface and require an oxidant. Nitrate in the bottom water or iron(III) in the sediment may contribute as oxidants. It should thereby be noted that each TOU data point in Fig. 10 represents only a momentary situation, at the time of measurement, while the long-term data may be more complex. The ability of the sediments to retain sulfide depends on their periodic re-oxidation as the bottom water O_2 and NO_3^- concentrations vary seasonally or occasionally due to mesoscale variability in ocean

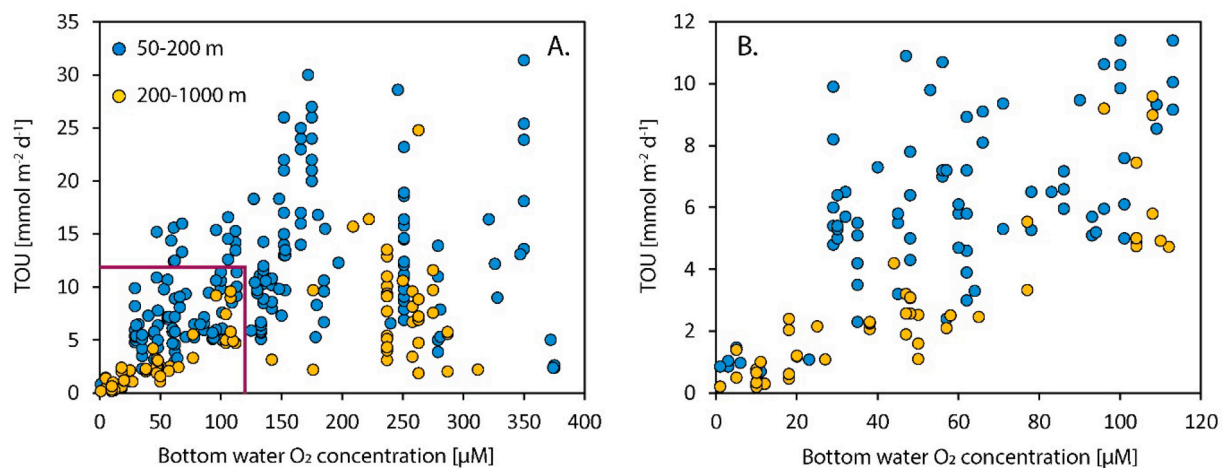


Fig. 10. Total O₂ uptake (TOU) of the seafloor on the outer shelf (50-200 m) and the upper slope (200-1000 m). A) The global dataset includes high-O₂ regions outside of OMZs and low-O₂ regions where the OMZs impinge on the ocean margin. B) Same data with expanded scales.

circulation, intensity of upwelling, and primary productivity (e.g., Vergara et al., 2016). Such a re-oxidation establishes a pool of oxidized iron minerals near the sediment surface that oxidizes and precipitates the diffusive sulfide flux from below (Seitaj et al., 2015).

In some hypoxic shelf regions, such as the shelf off northern Chile and Peru, benthic exchange rates are affected by dense communities of filamentous, sulfide-oxidizing bacteria, *Thioploca* spp. These use their high concentrations of intracellular nitrate for sulfide oxidation and may function as an effective barrier against H₂S release as long as nitrate is available in the anoxic bottom water (Fossing et al., 1995). The bacteria perform a dissimilatory nitrate reduction to ammonium, which results in a high NH₄⁺ flux from the sediment (Sommer et al., 2016). Sediments under hypoxic bottom water are thus important sources of NH₄⁺ to the water column, also in other OMZs, such as off SW and NW Africa (Dale et al., 2014; Kalvelage et al., 2013). The NH₄⁺ is oxidized to NO₂⁻ and NO₃⁻ by nitrifying bacteria in the hypoxic OMZ water, or is combined with NO₂⁻ to produce N₂ by anammox bacteria under anoxic conditions (Lam and Kuypers, 2011). A direct H₂S flux from the sediment was observed by flux chamber measurements to occur only when the bottom water became anoxic and nitrate dropped to <5 μM (Dale et al., 2016).

Extensive release of H₂S from OMZ sediments appears to be an exception, even under fully anoxic bottom water. It has been observed in the most productive upwelling systems, such as on the shelf off Namibia where the oxidation of sulfide to elemental sulfur after H₂S emission into the water column generates large areas of milky-white sulfur turbidity that can even be observed from satellite (Ohde and Dadou, 2018). This emission of H₂S from the diatom ooze on the Namibian shelf is not only due to anoxia but is also driven by eruptions of methane gas that accumulates in the mud (Brüchert et al., 2003).

Organic carbon preservation in the seabed is generally enhanced under hypoxic or anoxic conditions (Canfield, 1994), and burial is therefore more efficient under OMZs compared to more oxic regions of the continental margin (Harnett et al., 1998; Baroni et al., 2020). Yet, the significance of bottom water O₂ on organic carbon burial efficiency is complex and may depend on several confounding factors, such as oxygen exposure time, bioturbation by burrowing macrofauna, sediment deposition rate, and age or degradation state of the deposited POC (e.g., Canfield, 1994; Dale et al., 2015).

There is a strong selectivity in the benthic faunal composition where the OMZs impinge on ocean margin sediments. Hypoxia leads to a reduction in species richness of all benthic faunal groups and in some cases selects for species that are specially adapted to thrive under very low O₂ (Gooday et al., 2010). At the same time, OMZs may enhance regional diversity in some taxa, such as Foraminifera, many of which are particularly tolerant of anoxia and may even respire by dissimilatory

nitrate reduction (Piña-Ochoa et al., 2010; Orsi et al., 2020). There is generally a reduced activity of burrowing macrofauna in OMZ sediments, where bioturbation was observed to fade out and where laminated sediments became predominant at <5 μM O₂ (Levin et al., 2009b).

4.3. Abyssal plains

The abyssal plains cover 85% of the ocean bed and represent the largest marine ecosystem on Earth. The term “plain” might be misleading as the abyssal realm is characterized by an undulating bathymetry with reliefs of 300-1000 m tall formations (Harris et al., 2014). The spatial distribution of benthic fauna and of the O₂ consumption rate at the abyssal seafloor is ultimately controlled by the export of organic material from the photic zone (Rowe, 1973, 2013; Smith et al., 2008). Thus, the benthic activity is generally decreasing with increasing distance to the ocean margins and with increasing water depth (Jahnke et al., 1990; Wenzhöfer and Glud, 2002). However, this pattern may be confounded by the regional or local bathymetric relief focusing material in depressions and troughs of the abyss (Chen et al., 2013).

Beside the increasing awareness of the spatial variation in deposition rates at abyssal depths, there is increasing evidence that the benthic carbon requirement of abyssal communities as inferred from O₂ uptake measurements exceeds the vertical supply of organic carbon calculated from sediment trap studies (Smith Jr. and Kaufmann, 1999; Wiedmann et al., 2020). This is partly attributed to lateral transport of POC from ocean margins or mounts and the vertical transport of larger algal aggregates and carrion that circumvent sediment traps (Jahnke and Jackson, 1992; Smith Jr., 1987). Indeed, large food falls of whales, salps and jellyfish have been identified as locally important sources of organic matter input to the deep seafloor (Smith, 2006; Billett et al., 2006; Treude et al., 2009; Smith Jr. et al., 2014) (Fig. 11).

Aggregation enhances the sinking velocity of POC (Deuser and Ross, 1980; Nowald et al., 2015) and governs the rapid transport of fresh organic matter to the seabed. Large pulses of fresh phytodetrital matter have on several occasions been observed on abyssal sediments (Billett et al., 1983; Smith and Baldwin, 1984; Lampitt, 1985). One striking example was the observation of large algal aggregates released from melting sea ice settling at the seafloor at 4500 m water depth in the central Arctic Ocean (Fig. 11). The settling aggregates locally increased the benthic oxygen uptake by more than ten-fold (Boetius et al., 2013). The deposition in deep sea sediments is thus very dynamic, and sedimentation events that are quantitatively important for the pelagic-benthic coupling may not be recorded. To our knowledge, there are today only three long-term observatories that monitor the seasonal variation of carbon export, benthic community structure and benthic

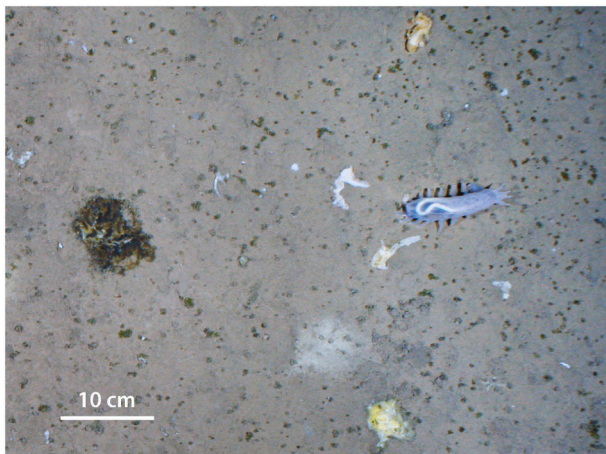


Fig. 11. Small and large, dark algal deposits, up to 10 cm in diameter, and remains of plankton organisms on the seafloor at 4355 m water depth in the central Arctic Ocean. In the middle is a holothurian (*Kolga hyalina*). The image was taken during RV Polarstern expedition ARK-XXVII/3 in 2012 at station IceArc 6 (N 85° 06.11' E 122° 14.72') using the Ocean Floor Observing System (OFOS). (Boetius et al., 2013; Photo: AWI-OFOS-team).

oxygen consumption in abyssal settings. These are the North-East Pacific Station M (Smith Jr. et al., 2018), the North Atlantic PAP (Lampitt et al., 2010), and the Arctic HAUSGARTEN (Soltwedel et al., 2016).

The most comprehensive data set of seasonal variations in carbon export and benthic oxygen consumption in the deep sea has been realized by Station M in the deep sea off central California (Fig. 12) (Smith Jr. et al., 2001, 2013, 2016). The time series has revealed distinct seasonal pulses of elevated export fluxes during or shortly after surface blooms that transiently enhanced the supply of labile organic material at the seabed (Smith Jr. et al., 2016). Similar observations have been made for PAP and HAUSGARTEN (Lampitt et al., 2010; Bauerfeind et al., 2009; Lalande et al., 2013). These deposition events fuel the benthic ecosystem and trigger a strong growth response by the benthic community (Witte et al., 2003). Deposition events also enhance the sediment oxygen consumption rate, at Station M by a factor of two to three (Fig. 12; Smith Jr. et al., 2016) and at HAUSGARTEN by a factor of two (von Appen et al., 2021). Such events can easily be missed by single lander deployments during deep sea expeditions. The available database does not reflect the dynamics of the deep sea and may therefore also not correctly represent the average carbon mineralization rates. More high-

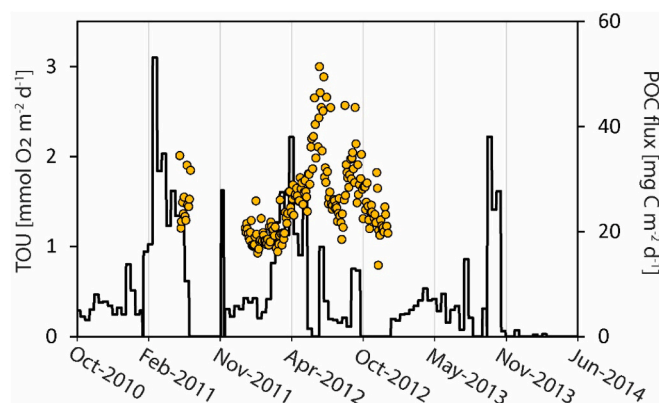


Fig. 12. Particulate organic carbon (POC) flux (black curve) and total benthic O_2 uptake (orange symbols) measured in the NE Pacific at 4000 m water depth at station M in the Monterey Deep-Sea Fan (N 34° 50' W 123° 06'). The strong variability is shown at high temporal resolution from fall 2010 to summer 2014 (Modified after Smith Jr. et al., 2016; courtesy of Ken Smith Jr.).

resolution and long-term studies by autonomous instruments (Fig. 1) are required to meet this challenge (Wenzhöfer et al., 2016a; Lemburg et al., 2018; Sherman and Smith Jr., 2009) and to supplement deep ocean observation data (Levin et al., 2019; MBARI, 2009).

4.4. Mid-oceanic gyres

Ocean gyres are large systems of circular ocean currents driven by global wind patterns and by forces caused by Earth's rotation. Due to these Coriolis forces, the circular currents run clockwise in the northern hemisphere and counter-clockwise in the southern hemisphere. There are five major gyre systems, located in the North and South Pacific, the North and South Atlantic, and the Indian Ocean. The gyres isolate nutrient-poor, central parts of the upper ocean and are distinct by remote sensing due to their low chlorophyll concentration (see Fig. 17b). Gyres have very low phytoplankton productivity and a low export of sinking particulate material, either of POC derived from the photic zone or of clastic material derived from the continents. The underlying seabed therefore has extremely low sedimentation rates, low rates of organic matter degradation, and deep oxygen penetration.

While measurements of total oxygen uptake (TOU) and oxygen penetration depth (OPD) are abundant along the ocean margins, measurements are scarce in the central, low-productive parts of the oceans. This may be due to their remoteness, to less scientific interest in these regions, and to the difficulty of measuring very low O_2 consumption rates and very deep O_2 penetration. Chamber landers for measuring *in situ* flux can barely detect the extremely slow depletion of O_2 in the chamber within useful incubation periods. Most *in situ* O_2 measurements with microsensors using benthic landers have had a depth range limited to the top 5-10 cm (Chapter 2).

In order to overcome the latter limitation, Wenzhöfer et al. (2001) constructed a benthic lander with O_2 optodes that could penetrate half a meter into the sediment. In the western Atlantic they recorded O_2 down to 8-26 cm depth. In large areas of the ocean, however, O_2 reaches much further down and it is necessary to retrieve cores and perform measurements on board ship (e.g., Grundmanis and Murray, 1982; Fischer et al., 2009; Roy et al., 2012; D'Hondt et al., 2015). This can be done by drilling small holes in the side of the core liner and pushing microsensors into the sediment core to let them equilibrate at *in situ* temperature. Although pressure drop and transient heating of the cores tend to affect the O_2 consumption rates, these rates are so low in the deep-sea cores that the O_2 distribution hardly has time to change before measurements are done. The deep diffusive oxygen uptake (DOU) can therefore be calculated by diffusion-reaction modeling of the measured O_2 distribution.

An example from the North Atlantic gyre of such a deep O_2 profile is shown in Fig. 13A. The data reaching 25 m into the seabed were obtained during RV *Knorr* Expedition KN223. We calculated the diffusive O_2 flux using the O_2 gradient in the top 0.4 m and assuming a porosity of 0.75, a temperature of 2 °C, a salinity of 35, and a molecular diffusion coefficient of $1.05 \times 10^{-9} \text{ m}^2 \text{ s}^{-1}$ (Schulz and Zabel, 2006). The resulting flux is $0.0045 \text{ mmol } O_2 \text{ m}^{-2} \text{ d}^{-1}$. This is ca. 100-fold lower than the globally mean DOU in abyssal sediments ($0.6 \text{ mmol } O_2 \text{ m}^{-2} \text{ d}^{-1}$; Table 4). The linear gradient below 5 m depth shows even a 30-fold lower O_2 flux of $0.00014 \text{ mmol } O_2 \text{ m}^{-2} \text{ d}^{-1}$. However, neither of these fluxes represents the O_2 uptake of the seabed, as the following example shows.

The South Pacific Gyre is a global extreme with respect to low sedimentation rates and low O_2 consumption. In the central gyre, oxygen and aerobic respiration persist through the entire sediment column, even reaching down to the crustal basement, tens of meters below (Fischer et al., 2009; D'Hondt et al., 2009). Fig. 13B shows an example of O_2 data from a 5-m long piston core with a distinct drop in concentration in the upper 0-1 m. The O_2 flux modeled from these data was $0.014 \text{ mmol m}^{-2} \text{ d}^{-1}$ in the top 10 cm and $0.00018 \text{ mmol m}^{-2} \text{ d}^{-1}$ across 1.5 m depth. However, the main zone of oxygen consumption is not revealed at

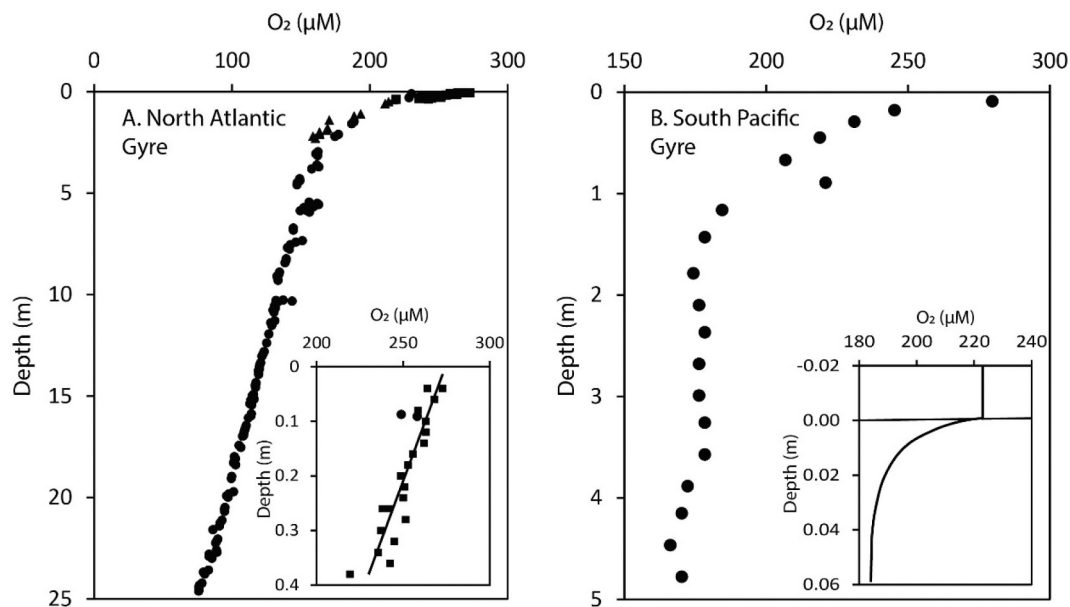


Fig. 13. A) Deep O₂ penetration in sediment from the North Atlantic gyre at 5400 m water depth. The graph combines data from a 0.4-m long multicorer, a 3-m long gravity corer, and a 28-m long piston corer. The insert shows data from the multicorer, from which a linear regression was used to estimate the O₂ flux into the sediment. (Data from D'Hondt et al., 2015; Station 12; data courtesy of Steven D'Hondt). B) Deep O₂ penetration in a piston core from the South Pacific Gyre. The insert shows a modelled curve fitted to an *in situ* microsensor profile from the same site. (Data from Fischer et al., 2009; Station 10).

this depth resolution. The insert presents the model fit to an O₂ micro-profile measured directly *in situ* by a benthic microsensor lander at the same site. By this resolution, the calculated DOU was 0.23 mmol O₂ m⁻² d⁻¹ in the top 0-4 cm (Fischer et al., 2009).

Together with several *ex situ* measurements, these data from Fischer et al. (2009) reveal that nearly the entire O₂ consumption in the South Pacific gyre sediments takes place within a few-cm thick surface layer and only 1% takes place in the 10-20-m deep sediment column below. Fig. 14 shows that this is apparently a general phenomenon in the ocean gyres. The high-resolution DOU at the sediment surface is roughly 100-fold higher than the O₂ flux calculated from measurements in retrieved sediment cores. The much higher oxygen consumption in the surface layer (0.12-1.32 mmol O₂ m⁻² d⁻¹) corresponds quite well to the multiple regression of DOU in the global seabed for the same water depths and sea-surface primary productivity (ca. 0.4 mmol O₂ m⁻² d⁻¹) (see

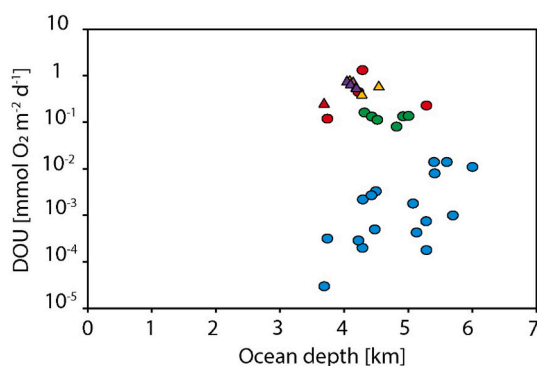


Fig. 14. Ocean gyre data: Diffusive oxygen uptake (DOU) of sediments calculated from microsensor measurements at several-cm resolution from the side of retrieved cores (blue symbols) or at sub-mm resolution at the sediment surface (other colored symbols). Data from *in situ* measurements directly on the seafloor are indicated by triangles. The graph illustrates that nearly all O₂ consumption in these gyre sediments takes place right at the sediment surface. Source: D'Hondt et al. (2009, 2015), Fischer et al. (2009), Røy et al. (2012), Vuillemin et al. (2019), Orcutt et al. (2013), Wenzhöfer et al. (unpubl.), Volz et al. (2018), Vonnahme et al. (2020).

Fig. 21b). Honjo et al. (2008) synthesized time-series sediment trap data from the world ocean and concluded that the POC flux across 2000 m water depth in the North Pacific subtropical/tropical gyre was 39 mmol C_{org} m⁻² yr⁻¹. With a C_{org}:O₂ mineralization ratio of 0.75:1 (see Table 5), this corresponds to a potential oxygen consumption rate of 0.14 mmol O₂ m⁻² d⁻¹.

The sedimentation rates in the central gyre are extremely low, 0.1-1 mm per 1000 years, bioturbation is negligible, and the thin surface layer of recently deposited organic matter is therefore the main oxygen sink. Oxygen that is not consumed in this layer, on the other hand, may diffuse far down into the underlying deposits that are many millions of years old and in which the buried organic matter is extremely resistant to further degradation (Estes et al., 2019). If such an extreme displacement of oxygen consumption towards the sediment surface is generally characteristic of abyssal sediments from low-productivity regions, it means that O₂ data measured at several-cm resolution in retrieved sediment cores may grossly underestimate the benthic oxygen uptake. There is clearly a need for further *in situ* microsensor data to understand how oxygen consumption is controlled in ocean gyre sediments.

D'Hondt et al. (2015) used data on total sediment thickness and mean sediment accumulation rates to develop a global map of regions where O₂ is likely to penetrate through the entire sediment column and thereby exclude anaerobic microorganisms and anaerobic processes (Fig. 15). These regions coincide to a large degree with the geographic extent of the ocean gyres. D'Hondt and co-authors estimated that O₂ penetrates all the way to the basaltic crust in 15-44% of the Pacific seabed and in 9-37% of the global seabed.

Modeling of sediment O₂ profiles in the central South Pacific Gyre yielded calculated O₂ consumption rates per sediment volume that ranged from 6 × 10⁻¹¹ mol O₂ cm⁻³ yr⁻¹ in the upper few meters to a minimum of 3 × 10⁻¹³ mol O₂ cm⁻³ yr⁻¹ at 50 m depth (Site U1370; D'Hondt et al., 2015). At that specific site, the residual O₂ concentration was 8 μM at 50 m depth. This means that the *in situ* turnover time of the small O₂ pool at that depth was 20,000 years. A similar calculation for a deep sediment core from the North Pacific Gyre indicated an O₂ turnover time of 40,000 years at 25 m depth (Røy et al., 2012). This extremely slow aerobic respiration is driven by deeply buried organic matter that becomes increasingly persistent with depth and age, but continues to be

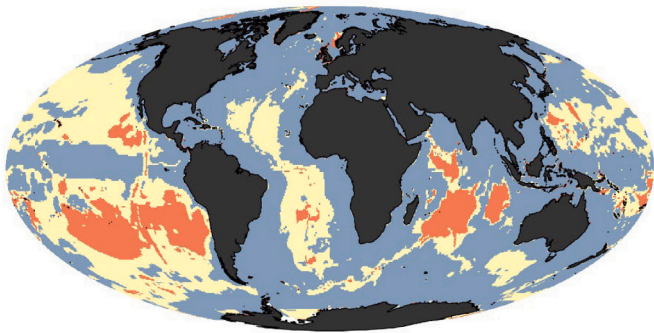


Fig. 15. Regions in the ocean where dissolved O_2 and aerobic activity in the seabed may occur from the sediment surface to the crustal basement. The red areas mark the estimated minimum extent and yellow areas the estimated maximum extent of these regions based on model calculations. (Data from D'Hondt et al., 2015; courtesy of Steven D'Hondt and Robert Pockalny).

slowly degraded and to feed the deep sub-seafloor biosphere (Estes et al., 2019). The slow respiration is also driven by H_2 and oxidants produced *in situ* by radiolysis of water due to high-energy radiation by the natural, long-lived radionuclides ^{40}K , ^{232}Th and ^{238}U (Blair et al., 2007; Sauvage et al., 2021). However, this radiolysis-fueled respiration may not contribute to net O_2 reduction, since oxidants are produced in stoichiometric balance with the H_2 (Sauvage et al., 2021). In the fully oxic sediments underlying the South Pacific Gyre, the extremely low energy availability maintains viable communities of aerobic microorganisms in deep sediments of up to 100 million years age (Morono et al., 2020).

It was a striking observation in the periphery of the South Pacific Gyre (Site U1371) that O_2 penetrated 0.9 m down into the sediment, but that O_2 was also supplied from the underlying ocean crust and penetrated 15 m up into the sediment from below (D'Hondt et al., 2015). A similar observation of a deep O_2 and nitrate flux from the underlying crust was observed in the tropical eastern Pacific (D'Hondt et al., 2004). It was explained by a slow, thermohaline circulation of deep, oxic seawater that entered and vented the crust through seamounts. This long-distance circulation caused a lateral seepage of seawater through the crustal aquifer that slowly leaked O_2 up into the overlying sediment (Jørgensen et al., 2006; Bekins et al., 2007). A deep O_2 source was also observed on the western flank of the Mid-Atlantic Ridge, driven by a hydrothermal circulation through the ridge crust (Orcutt et al., 2013). While these inverted O_2 fluxes are interesting and geochemically and hydrologically important, they are insignificant for the global seabed O_2 budget.

4.5. Hadal trenches

The hadal zone is the deepest part of the global ocean, stretching from 6 km to almost 11 km water depth at the bottom of the Challenger Deep in the Mariana trench. The hadal zone represents 45% of the oceanic depth range and covers an area of 3.44×10^6 km², corresponding to 1.1% of the global seabed (Harris et al., 2014). It includes 47 individual trench systems and is dominated by 27 large trenches that extend along tectonic subduction zones, mainly in the Pacific Ocean (Stewart and Jamieson, 2018).

It is a general observation that biological activity declines with increasing ocean depth. The hadal trenches were therefore originally believed to be largely deprived of life, but it has now been documented that the trench systems act as depo-centers for organic material. Hadal sediments often harbor surprisingly high abundances of meiofauna and microorganisms that thrive at the extremely high hydrostatic pressure of 10^3 bar (Danovaro et al., 2002, 2003; Itoh et al., 2011; Schaubberger et al., 2021). The biogeochemical function of hadal trenches therefore cannot be assessed by simply extrapolating relations to water depth, which otherwise appears to be a robust procedure for most other oceanic

settings.

Trenches have in cross-section a distinct V-shaped bathymetry and are situated in regions of high seismic activity. Thus, material deposited along the trench slopes is frequently translocated to the bottom of the trench (the trench axis) during mass wasting, typically triggered by earthquakes (Itoh et al., 2000; Bao et al., 2018). Using bathymetric mapping, Parasound profiling, and sediment TOC measurements it was estimated that 1 Tg of organic carbon was re-deposited to the interior of the Japan Trench during the Tohoku-oki earthquake in 2011 (Kioka et al., 2019). This corresponds to 1% of the total annual TOC deposition on the deep global seabed (>4000 m). Based on preliminary assessments using specific biomarkers, signatures of carbon stable isotopes, and thermochemical analysis of deposited TOC, it appears that trench sediments represent a globally significant marine storage of resilient terrigenous organic material (Luo et al., 2017; Xu et al., 2020, 2021). Hadal trenches may thus play an important role for the long-term burial of organic material in the deep sea, much beyond their areal contribution to the seafloor (Glud et al., 2021).

In situ measurements of DOU document 2-5 times higher benthic O_2 consumption along hadal trench axes as compared to the adjacent abyssal plain (Fig. 16; Glud et al., 2013; Wenzhöfer et al., 2016b; Luo et al., 2018). Together with elevated cell abundances, this indicates that it is not just relict organic carbon that accumulates in the hadal trenches, but deposition also includes labile organic material that can sustain a relatively high level of microbial activity. Generally, the average benthic O_2 consumption in the trenches correlates well to the regional surface primary production, but measurements within individual trenches also show extensive variations, indicating that the linkage to surface production is modulated by other factors (Glud et al., 2021).

Sediment mass wasting is a catastrophic event for mega- and macrofauna within the trenches, and their carcasses tend to be deposited along the trench axis, representing highly labile nutrition for the hadal communities (Oguri et al., 2013). Four months after the Tohoku-oki earthquake and the associated tsunami, the bottom water in the Japan Trench was still turbid and contained high levels of suspended detrital material (Oguri et al., 2013). Recovered sediment cores from the trench axis revealed recent, but highly variable, deposition of labile organic material, even within relatively short distances of a few kilometres. Surprisingly, a high level of the short-lived ^{134}Cs isotope, which could only originate from the flooded Fukushima nuclear power plant, was found at the trench axis (Oguri et al., 2013). Thus, large seismic events can efficiently transport terrigenous and labile coastal material to the trench interior. Variability in benthic O_2 uptake within the trench might thus reflect the deposited amount and the time since the last mass deposition.

The distinct V-shaped bathymetry of subducting trenches facilitates tidally induced internal waves (Van Haren, 2020), which cause local erosion of the trench slopes. Such waves may also cause focusing or winnowing of sediment material along the trench axis and enhance transport of surface derived material towards the trench bottom (Turnewitsch et al., 2014). This further contributes to the relatively high benthic deposition and large spatio-temporal variations in benthic O_2 consumption in hadal trenches (Glud et al., 2021).

The benthic O_2 uptake is generally a robust proxy for total benthic carbon mineralization, which includes the efficient re-oxidation of reduced products of anaerobic mineralization. However, trench sediments with frequent mass wasting and little bioturbation driven by macrofauna might be the exception to this rule. Trench sediments may not show a simple decline in TOC availability with increasing sediment depth (Glud et al., 2013; Wenzhöfer et al., 2016b). They may even have an inverted distribution of sediment layers with old and sparse TOC overlying layers with younger and more abundant TOC (Xu et al., 2021). Thus, mass wasting may facilitate burial of labile organic material well below the oxic surface layer. A recent study at 7000 m water depth in the Atacama Trench showed high levels of iron(III) reduction and sulfate reduction, well below the sediment surface, and deep layers

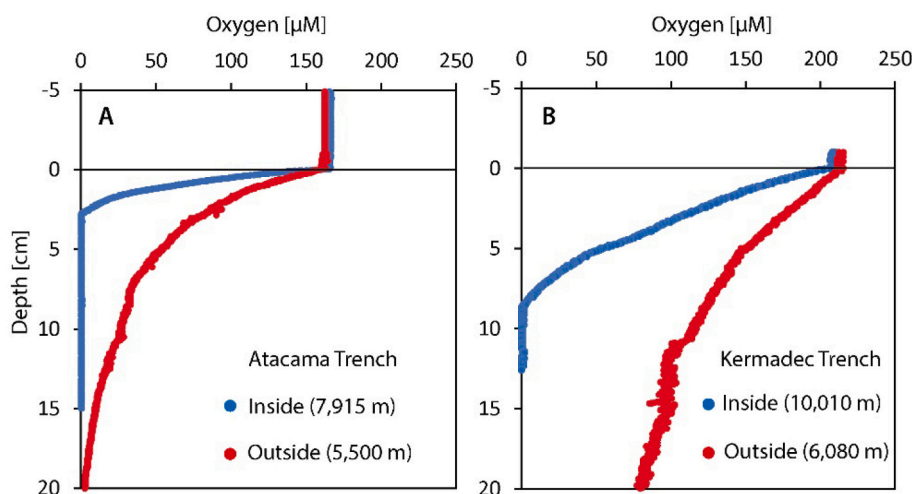


Fig. 16. Oxygen profiles measured *in situ* in the deep sea. A) The Atacama Trench off northern Chile. B) The Kermadec Trench north of New Zealand. Blue profiles are from inside the deep trench while red profiles are from the abyssal plain just outside the trench. (From Glud et al., 2021).

of reduced iron sulfides (Glud et al., 2021). Given frequent mass-wasting, as apparent by distinct sediment layering and lack of efficient bioturbation, the reduced products from anaerobic degradation may be buried and never be re-oxidized in such settings. In that case, the benthic O_2 consumption includes only a fraction of the total carbon mineralization (Glud et al., 2021). Yet, the importance of anaerobic carbon mineralization in hadal trenches remains largely unknown.

Hadal trenches also act as depositional centers for persistent pollutants. The hadal biota appear to hold high levels of anthropogenic organic pollutants and heavy metals, presumably transported to the trench interior by sinking carrions (Jamieson et al., 2017; Blum et al., 2020; Sun et al., 2020). Recent studies from the Atacama and Kermadec trench regions show benthic mercury accumulation rates that are 30-50 times higher than the average for the deep ocean (Sanei et al., 2021). Hadal trenches are thus important sites for oceanic deposition, possibly even of global importance. At the same time, trenches function as deep-sea hot spots for early diagenesis, mediated by largely unexplored microbial communities.

5. Global distribution of seabed O_2 uptake

In this chapter, the extensive database described in Chapter 2.2 is used to analyze the multiple correlations to environmental parameters and to develop a global map of the seabed O_2 uptake rates. We also discuss, which environmental factors play the most important role for the O_2 uptake.

5.1. From database to global map

We analyzed data for total oxygen uptake (TOU) and diffusive oxygen uptake (DOU) collected from a total of 3904 stations. Due to potential problems with *ex situ* measurements, described in Chapter 2, we used only data from *in situ* measurements for depths >10 m by our multiple regression analysis. We also excluded measurements according to other defined criteria, as explained in Chapter 2. Multiple measurements from the same station were averaged before our multiple regression analyses.

This selection removed 70% of all data from the original database and resulted in a total of 798 data from stations distributed throughout the world oceans. These *in situ* data were used for a global quantification of seabed O_2 uptake. Fig. 17a shows the geographic distribution of available data, plotted on a map of ocean depths. It is apparent that the highest data density is strongly skewed towards the continental shelves and slopes along the ocean margins, and towards the northern

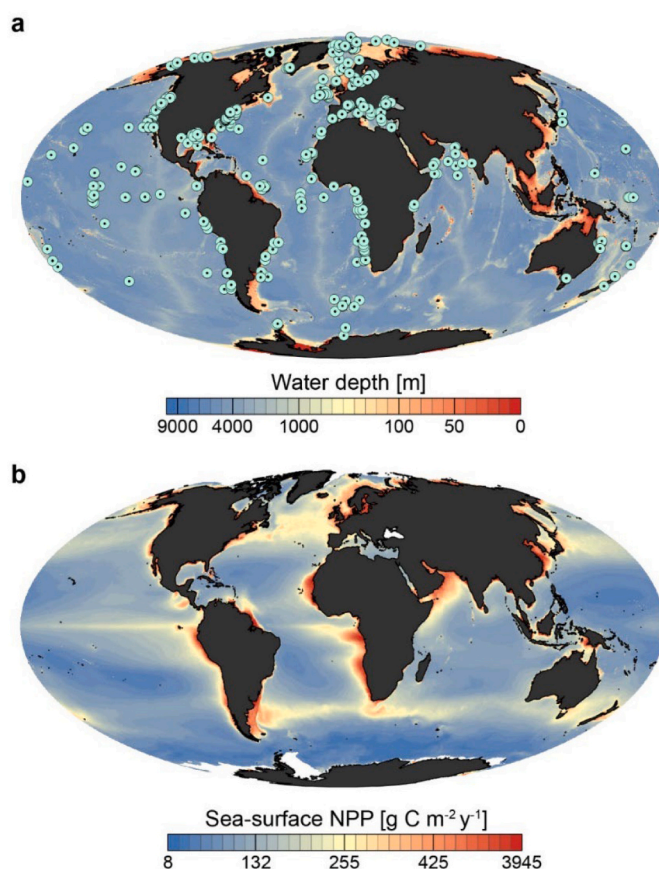


Fig. 17. A) Global distribution of sites ($n = 798$; blue dots) used to derive global estimates of sediment oxygen uptake rates. Many sites are so close that symbols overlap. The underlying map depicts ocean water depths in m (Amante and Eakings, 2009). B) Global map showing the time-averaged (1998-2007) sea-surface net primary production (NPP) distribution (for reference, see text). Note that color scales are non-linear.

hemisphere. The data density is low in the open Pacific Ocean and Atlantic Ocean and data are largely missing from the Indian Ocean.

Table 1 shows the geographic area of seven depth zones in the ocean, the number of total observations of TOU and DOU in each zone, and the density of observations per million km^2 . The shelf region out to 200 m

Table 1

Geographic area of different depth zones in the global ocean. The number of *in situ* data for total oxygen uptake (TOU) and diffusive oxygen uptake (DOU) from each zone is shown and the number of observations per 10^6 km^2 is calculated.

Region (water depth)	Seafloor area [10^6 km^2]	Number of observations		Observations per 10^6 km^2	
		TOU	DOU	TOU	DOU
Inner shelf (0-10 m)	2.3	43	3	18.3	1.3
Inner shelf (10-50 m)	8.8	127	15	14.4	1.7
Outer shelf (50-200 m)	12.5	101	37	8.1	3.0
Upper slope (200-1000 m)	14.4	73	31	5.1	2.2
Lower slope (1000-2000 m)	15.5	60	58	3.9	3.8
Rise (2000-4000 m)	109.7	77	68	0.7	0.6
Abyss (>4000 m)	190.8	63	43	0.3	0.2
Total	354.0	544	255	1.5	0.7

water depth covers 7% of the global ocean and has a data density of 8-18 TOU and 1.3-3.0 DOU measurements per 10^6 km^2 . The abyssal plains at >4000 m depth cover 54% of the global ocean and have a mean data density of 0.3 TOU and 0.2 DOU per 10^6 km^2 . That corresponds to 3 and 2 data points, respectively, per area the size of the USA or Europe. There is clearly a need for more *in situ* data, in particular from the deep sea, to reach a representative data coverage and reduce the large statistical uncertainty of global estimates.

Fig. 17b shows the distribution of net primary production (NPP) in the surface ocean monitored by remote sensing. We used the NPP data available through the Oregon State University (www.science.oregonstate.edu/ocean.productivity/custom.php) on monthly climatologically averaged physical data computed over a 10-yr period (1998-2007). The distribution based on calculations from remote sensing data was processed with the vertically generalized production model, VGPM, of Behrenfeld and Falkowski (1997). The map shows that the highest phytoplankton primary production is strongly skewed towards the higher latitudes and towards the ocean margins with westward extensions along the Equator in the Pacific and the Atlantic Ocean.

This coincidence between the highest data density, the shallowest ocean depths, and the highest sea-surface NPP means that deep and oligotrophic regions of the ocean are statistically poorly represented by the data distribution. This is illustrated in Fig. 18, where the white bars correspond to the frequency distribution of observations in our database relative to (a) the ocean depths and (b) the sea-surface NPP. The blue bars show the actual, global distribution of (a) ocean depths and (b) sea-surface NPP. Fig. 18 shows that the frequency of data is strongly skewed towards shallow depths and high sea-surface NPP. This confirms that the seabed O_2 uptake remains poorly constrained in large, central parts of the ocean. Yet, correlation plots of TOU and DOU versus ocean depth and versus sea surface primary production indicate that the available data from abyssal plains in low productivity regions fall along the general trend of the entire seafloor dataset (see Chapter 5.2).

For the global mapping of oxygen uptake rates in the seabed we

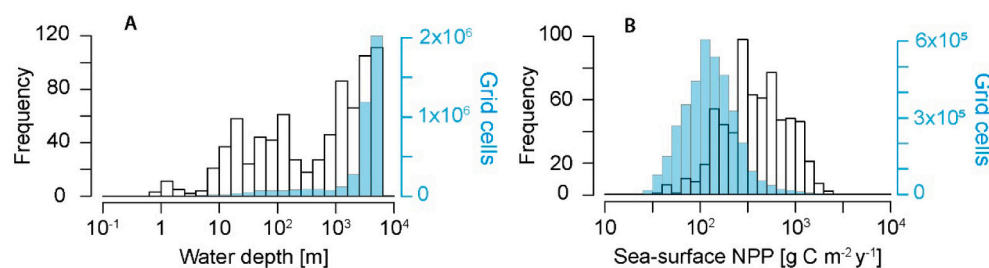


Fig. 18. Geographic distribution of TOU data relative to ocean data. Histograms show frequency of observations and number of grid cells vs. A) water depth and B) sea-surface net primary production (NPP). White bars correspond to the frequency of observations in our database ($n = 798$). Blue bars represent distributions for the global ocean (0.1×0.1 -degree grid), with values for water depths ($n = 4,276,617$) extracted from Amante and Eakings (2009) and values for sea-surface NPP ($n = 3,689,276$) derived from annual mean (1998-2007) satellite

observations (see text).

developed a multicomponent linear regression model to derive an empirical relationship between the log-transformed data for oxygen uptake ($\text{mmol O}_2 \text{ m}^{-2} \text{ d}^{-1}$), water depth (m), and sea-surface net primary production ($\text{NPP, g C m}^{-2} \text{ y}^{-1}$). Annual mean (1998-2007) sea-surface NPP data were extracted from the above reference for each station using Esri ArcGIS software. Further parameters tested in the regression model were distance to nearest coast and annual mean (1997-2010) sea-surface POC (<https://oceancolor.gsfc.nasa.gov/data/seawifs/>). These parameters did not show a statistically significant improvement of the model (significance level < 0.05).

For each depth region, as defined in Table 1 (excluding data from depths $< 10 \text{ m}$) we calculated the mean value of log transformed TOU and DOU data versus log depth and versus log NPP (Fig. 21) and determined the standard error of the mean. We then performed a multicomponent linear regression analysis of the log-log-transformed mean values and derived the following empirical relationships for TOU and DOU:

$$\log(\text{TOU}) = A_{\text{TOU}} + B_{\text{TOU}} \times \log(z) + C_{\text{TOU}} \times \log(\text{NPP}) \quad (\text{Eq. 5.1})$$

$$\log(\text{DOU}) = A_{\text{DOU}} + B_{\text{DOU}} \times \log(z) + C_{\text{DOU}} \times \log(\text{NPP}) \quad (\text{Eq. 5.2})$$

where z is ocean depth and NPP is net primary productivity. The model parameters A, B, and C for TOU and DOU, as well as the 5% and 95% confidence interval (CI), the coefficients of determination (R^2), and the P values are shown in Table 2. A confidence interval was calculated for each depth interval from the mean $\pm 2 \times$ standard error. The CI's for each depth interval were used to run a multiple regression and calculate the 5% and 95% values for the model fit. The model parameters show, as expected, that the $\log(\text{TOU})$ and $\log(\text{DOU})$ are negatively correlated with ocean depth and positively correlated with sea-surface NPP. The coefficient of determination, R^2 , is high, 0.995 and 0.998 for TOU and DOU, respectively, with a significance level, $P < 0.001$.

When using Eq. 5.1 and 5.2 for geographic extrapolation and mapping, a correction factor was applied to account for the skewness bias inherent in the back conversion from a log-log transformed linear regression model to arithmetic units. As described by Middelburg et al.

Table 2

Multiple linear regression model parameters (see Eq. 5.1 and Eq. 5.2) for seabed TOU and DOU. The 5% CI and 95% CI are confidence intervals of the multiple linear regression. R^2 is the coefficient of determination, while P is the test of significance level.

Coefficient	Fit	5% CI	95% CI	R^2	P value
TOU				0.995	<0.001
A_{TOU} (intercept)	0.563	0.680	0.446		
B_{TOU} ($\log[z]$)	-0.549	-0.568	-0.529		
C_{TOU} ($\log[\text{NPP}]$)	0.561	0.513	0.609		
DOU				0.998	<0.001
A_{DOU} (intercept)	1.728	1.950	1.507		
B_{DOU} ($\log[z]$)	-0.631	-0.661	-0.600		
C_{DOU} ($\log[\text{NPP}]$)	0.138	0.064	0.211		

(1997), high values lose significance relative to low values in a log-log linear regression, which therefore results in a bias towards lower values. The correction factor (CF) takes this bias into account and can be calculated using the variance of the data, $CF = e^{2.65 \times \text{variance}}$ (Middelburg et al., 1997). The variance was calculated for each ocean depth interval and used to correct the mean value for that interval. The correction factors for TOU ranged from 1.22 to 1.61, lowest on the inner shelf and highest on the upper slope.

Using the power law equations derived from the multiple linear regression of log-log transformed mean values per ocean depth (Eq. 5.1 and 5.2), we predict the modeled TOU and DOU for each observation site based on the corresponding water depths and sea-surface NPP values. To test the validity of this model, the predicted (modeled) values are compared to the actual value for each observation site. In general, the predicted oxygen uptake rates are in good agreement with the observed values (Fig. 19a, c), with the predicted oxygen uptake rates generally deviating much less than one order of magnitude from the observations and with the median values matching 1:1 (Fig. 19 b,d).

To create a global map of sediment oxygen uptake on a geographically highly resolved $0.1^\circ \times 0.1^\circ$ grid, the predictive relationships for TOU and DOU were combined with a gridded global dataset of water depth (Amante and Eakings, 2009) and annual mean sea-surface NPP (see text above). For each $0.1^\circ \times 0.1^\circ$ grid cell of the world ocean, we predicted TOU and DOU by applying Eq. 5.1 and 5.2, respectively. We also applied the correction factors mentioned above to account for the skewness bias inherent in the back conversion from a log-log transformed linear regression model to arithmetic units. TOU and DOU for coastal sediments at 0-10 m water depth were not calculated from this multiple regression but were calculated separately using only the arithmetic mean of data from that depth interval.

The resulting map of global TOU distribution is shown in Fig. 20. A separate map of global DOU distribution is shown in Supplementary Fig. S1. The DOU map is graphically very similar to the TOU map. The color scale is arithmetic and covers a TOU range from 0 to 119 $\text{mmol O}_2 \text{ m}^{-2} \text{ d}^{-1}$. The scale is designed to provide high color sensitivity by the low

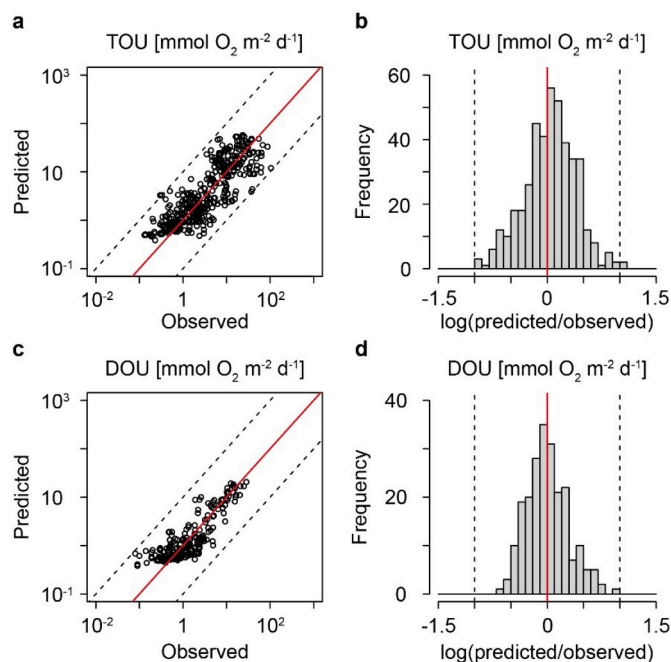


Fig. 19. Observed vs. predicted values of (a) TOU and (c) DOU based on Eq. 5.1 and 5.2. Histograms show the same comparison of predicted vs. observed (b) TOU and (d) DOU values. Notice log-log scales. Solid red lines represent a 1:1 fit (i.e., a perfect model). Dashed lines indicate ± 1 order of magnitude deviation from the 1:1 fit.

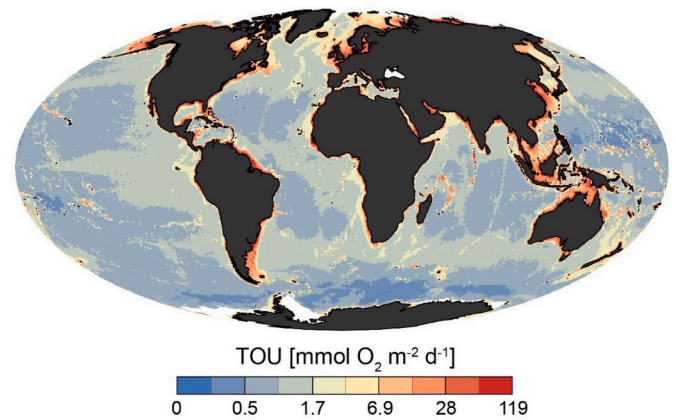


Fig. 20. Global map of the total oxygen uptake (TOU) of the seabed at 0.1×0.1 degree resolution. The map was calculated by applying the multicomponent linear regression model in Eq. 5.1.

TOU values in the open ocean and low color sensitivity by the high TOU values along the ocean margins. The map shows a very strong focus of seabed O_2 uptake towards the continental shelves and upper slopes. In the deep sea, the O_2 uptake reflects the distribution of sea surface net primary production (cf. Fig. 17B).

5.2. Controls on O_2 uptake

5.2.1. Water depth and sea-surface net primary production

Water depth is the most important factor controlling the flux of organic matter to the seabed and, thereby, its oxygen uptake rate. Fig. 21a and b show the total and the diffusive O_2 uptake as a function of water depth, ranging from 1 m to the abyss. The TOU and DOU data have been fitted by a log-log linear correlation for mean values per corresponding depth region as defined in Table 1, and excluding water depths < 10 m. The R^2 of these correlations is high (> 0.99 ; Table 2). In shallow water of < 10 m there is no apparent depth dependence of TOU or DOU. We have therefore fitted a constant mean rate for each parameter (dashed horizontal lines in Fig. 21a and b) and used this for the global budget in Chapter 6.3. Sea-surface primary production is the second-most important factor controlling benthic O_2 uptake (Fig. 21c and d). All data in Fig. 21 are from *in situ* measurements, except for the DOU from 0 to 10 m where very few *in situ* data exist and where also *ex situ* data were included.

The large scatter of data in Fig. 21 is partly due to the fact that these data are snapshots of processes that vary strongly in both time and space. As described in Chapter 4.2, the deposition of fresh phytoplankton detritus is often a brief event lasting only a few days or weeks of the year, even in the deep sea. During such deposition events, the O_2 consumption rate can be very high right at the sediment surface, while most of the year the rate is moderate and more constant. Depending on whether *in situ* measurements catch such events, the measured rates of TOU and DOU can show strong variability and conceal the importance of sea-surface NPP in data scatter. Furthermore, the degradation rate of deposited organic matter depends on a complex interplay of biological, geochemical and physical properties of the sediment (e.g., LaRowe et al., 2020).

5.2.2. Oxygen penetration depth (OPD)

The oxygen penetration depth (OPD) into the seabed is determined as the depth where O_2 profiles appear to reach zero concentration. The OPD and the diffusive oxygen uptake rate are mutually coupled, although not in a simple manner. The relationship depends on the depth distribution of volumetric O_2 consumption rates, especially when O_2 penetrates deeper than a cm. Such deeper O_2 profiles show highest

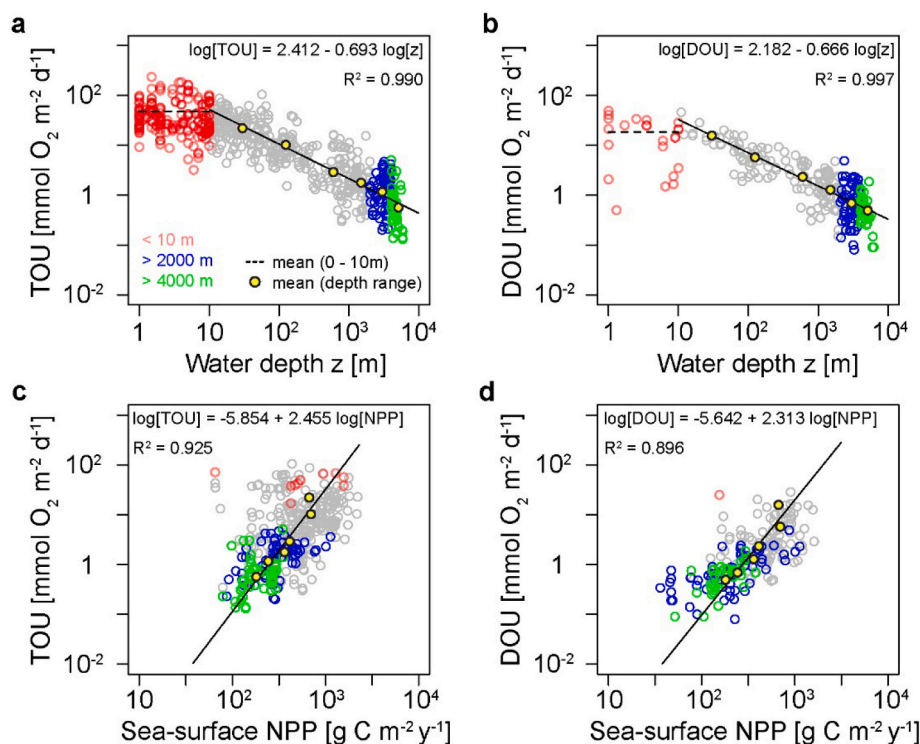


Fig. 21. Observed global relationship between (a) TOU (total oxygen uptake; $n = 544$) and (b) DOU (diffusive oxygen uptake; $n = 255$) and water depth. Similar relationships are shown between (c) TOU and (d) DOU and sea-surface net primary production (NPP) for the same number of data. Solid lines represent log-log linear regressions for water depths >10 m, based on the mean values (yellow points) per corresponding depth region, i.e., the inner shelf (10–50 m), outer shelf (50–200 m), upper slope (200–1000 m), lower slope (1000–2000 m), rise (2000–4000 m) and abyss (> 4000 m). Mean values are calculated for data from 0 to 10 m water depth (dashed lines). Colored symbols indicate different water depths as explained in (a).

respiration rate at the sediment surface, where fresh detritus settles, and at the bottom of the oxic zone, where reduced products of anaerobic degradation become oxidized (Fig. 5). The relationship also depends on the porosity of the sediment and on the molecular diffusion coefficient of O_2 , which is a function of temperature. Revsbech et al. (1980) tested a simple relationship for a depth-independent O_2 respiration in a coastal marine sediment with 1–5 mm O_2 penetration:

$$OPD = 2D_s \times C_0 \times \varphi / DOU \quad (\text{Eq. 5.3})$$

where D_s is the molecular diffusion coefficient in the sediment and φ is sediment porosity, both considered to be constant within the depth interval. They found a relatively deeper OPD than predicted by Eq. 5.3 and explained this as a result of bioturbation, perhaps by meio- and microfauna. Others have tested the same relationship on sediment O_2 profiles from different stations, e.g. off the SW coast of Japan (Glud et al., 2009a), in the South Atlantic (Hensen et al., 2006), and off the east and west coast of the USA (Cai and Sayles, 1996). Cai and Sayles (1996) found that the relationship holds well for O_2 profiles along the continental margin but that it underestimates the OPD in the open ocean. Seitaj et al. (2016) tested the relationship in a saline coastal reservoir and found that the pronounced oxidation of products from anaerobic mineralization at the bottom of the oxic zone tended to reduce the oxygen penetration to half of the penetration calculated from Eq. 5.3.

Our database indicates a log-log linear correlation between DOU (in $\text{mmol } O_2 \text{ m}^{-2} \text{ d}^{-1}$) and OPD (in mm) (Fig. 22a):

$$\log(OPD) = 1.470 - 0.877 \times \log(DOU) \quad (\text{Eq. 5.4})$$

with an R^2 of 0.64 and a P value of <0.001 . A similar relationship has been observed in earlier analyses (Wenzhöfer and Glud, 2002; Glud, 2008). One single data point, which was not included in the log-log linear regression, shows extremely deep O_2 penetration relative to the DOU (Fig. 22A). This data point by Fischer et al. (2009) originates from the central gyre in the South Pacific and is discussed in Chapter 4.4. The general goodness of the fit is illustrated in Fig. 22B, which shows the ratio between predicted and observed OPD. The peak of this frequency distribution nearly coincides with the perfect 1:1 fit ($\log = 0$) between

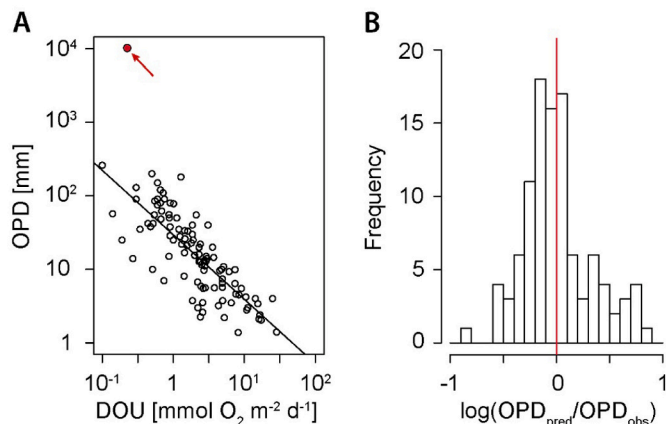


Fig. 22. A) Log-log plot of observed oxygen penetration depth (OPD) versus observed diffusive oxygen uptake (DOU). Oxygen profiles visually affected by bioirrigation were excluded from this analysis. The line represents the log-log linear regression (Eq. 5.4). A strongly deviating data point is marked by a red arrow (see text). B) Histogram of predicted OPD (OPD_{pred}) versus observed OPD (OPD_{obs}) relative to the log-log linear regression in (A). The red line indicates a perfect model fit (predicted/observed OPD = 1).

OPD_{pred} and OPD_{obs} .

As discussed in Chapter 4.4, the relationship in Eq. 5.4 breaks down in the deep sea, in particular in the mid-oceanic gyres where bioirrigation is practically absent and the O_2 consumption rate in the uppermost few cm of the sediment may be orders of magnitude higher than in the subsurface. An example from the South Pacific Gyre presented in Fig. 13B shows O_2 penetration to the ocean crust ($OPD > 10$ m), i.e. $\log OPD$ (mm) > 4 , while the DOU was $0.23 \text{ mmol } O_2 \text{ m}^{-2} \text{ d}^{-1}$, i.e. $\log DOU = -0.63$ (Fischer et al., 2009). This illustrates how the extremely deep O_2 penetration in oceanic gyre sediments gives a misleading expectation that the DOU must also be extremely low. Data in Fig. 13, 14 and 22 suggest that this is not the case.

5.2.3. Temperature

Temperature has a fundamental impact on the metabolic rates of benthic microorganisms and fauna. Temperature is also a major environmental variable that selects for the predominant biotic communities. The temperature of deep-sea sediments is low, 0–3 °C, and generally very stable for each ocean region. Short-term experiments with the oxygen consumption rate of marine sediments from the temperate inner shelf show maximum rates at 20 °C both summer and winter but relatively higher rates at low temperature at the end of winter (Fig. 23). Similar experiments with Arctic sediments showed maximum rates at 10 °C (Thamdrup and Fleischer, 1998). However, the true adaptation of sediment bacteria to permanently low temperature is not clearly detected by such short-term respiration measurements but rather from the temperature dependence of the growth yield of the microbial communities, which may be highest at the low *in situ* temperature (Scholze et al., 2021).

Sediments from tropical, temperate and polar latitudes are exposed to temperatures that may differ by 20–30 °C on the inner shelf. It is not clear to which extent this large temperature difference controls the rate of oxygen uptake or the efficiency of organic matter mineralization. Experiments on the degradation of kelp across a wide range of geographic latitudes and temperatures of coastal sediments showed enhanced mineralization rates and shorter retention times of degrading biomass in warmer climates (Filbee-Dexter et al., 2021). The accumulation rate of POC is relatively high in Arctic sediments that receive a large contribution of terrestrial organic matter (Wallmann et al., 2012). Yet, we are not aware of data that indicate that the fraction of deposited, plankton-derived organic matter, which becomes buried, is controlled by long-term temperature. Benthic microbial and faunal communities in different regimes are well adapted to the ambient temperature, and bacteria in polar sediments have relatively high cell-specific respiration rates at the low *in situ* temperature (Knoblauch et al., 1999).

The situation is different in temperate coastal sediments with a strong seasonal temperature variation. Here, the sediment oxygen uptake tends to vary over the year together with the ambient temperature. The variation is a combined effect of accelerated respiration rate of the benthic organisms at higher temperature and accelerated influx of fresh organic matter to feed their respiration during spring and summer. In many coastal waters this potentially enhanced oxygen consumption is counteracted by hypoxia during summer, which limits the oxygen flux

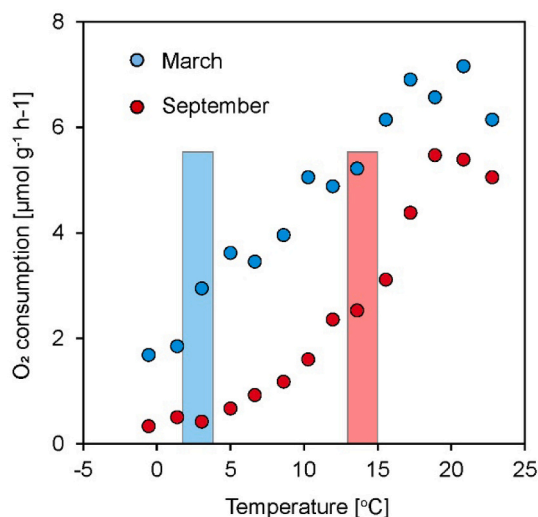


Fig. 23. Temperature dependence of oxygen uptake rate in a coastal marine sediment (Aarhus Bay) during short-term experiments lasting about ten hours. Measurements were done in late winter by 2–4 °C *in situ* temperature and in late summer by 13–15 °C *in situ* temperature. Rates are expressed per g wet sediment. (Data from Thamdrup et al., 1998).

and may result in a rather constant oxygen uptake throughout the year (Rasmussen and Jørgensen, 1992; Glud et al., 2003). The sediment may instead build up an oxygen debt in the form of iron sulfide minerals that are gradually oxidized during fall and winter (Seitaj et al., 2015).

5.2.4. O₂ concentration in bottom water

Sediment oxygen uptake in oxygen minimum zones along the ocean margins is discussed in Chapter 4.2. Since benthic O₂ uptake is a poor proxy for mineralization rates during permanent or transient hypoxia, we decided to exclude data from our multiple correlation analysis when the bottom water O₂ concentration was below 25 μM. Benthic mineralization of organic carbon in oxygen minimum zones was therefore assumed to be similar to oxic regions with similar surface productivity and similar water depth. Sediments underlying such oxygen minimum zones constitute only 4% of the outer shelf and upper slope.

5.2.5. Fauna

Benthic animals play important roles for the oxygen uptake in marine sediments, as discussed in Chapter 3.3. Apart from their own respiration, they increase the extent of the sediment-water interface and of the diffusive oxygen flux through their burrow structures. They also increase the advective oxygen flux by ventilating their burrows and enhance the degradation of organic matter by particle fragmentation and sediment reworking, so that a smaller fraction of the deposited organic carbon is buried.

The importance of fauna for the benthic O₂ exchange is often assessed by the difference between TOU and DOU (see Chapter 3.3). Previous data compilations of *in situ* TOU and DOU, have demonstrated that, while TOU exceeded DOU by a factor of 2–4 in coastal settings, values converge beyond the shelf and become similar at abyssal water depths (Archer and Devol, 1992; Glud, 2008).

This may partly reflect that the O₂ penetration depth increases with water depth from mm in the coastal areas to cm or dm in abyssal settings and faunal activity in the upper sediment layers therefore has little impact on the benthic O₂ uptake in the deep sea (Glud et al., 1994, 1999). Furthermore, the biomass of benthic macrofauna generally drops relatively faster with water depth than the biomass of microorganisms (Rex et al., 2006; Wei et al., 2010), implying that the relative importance of microbially driven O₂ consumption increases with water depth. Exceptions to this include sponge grounds and cold-water coral reefs, which act as deep-sea hotspots for organic carbon mineralization (Beazley et al., 2013; Rovelli et al., 2015).

This general depth trend was not observed in the extended database of the current study. This could imply a depth-independent contribution of fauna to the benthic O₂ exchange rate. However, the scatter is extensive by inclusion of all the non-coordinated data (Fig. 21). Indeed, when selecting only the *in situ* studies where both TOU and DOU were measured in parallel at the same site at the same time, the fauna contribution clearly declines with increasing water depth. This is apparent from the calculated decrease in mean TOU:DOU ratio from >2.2:1 on the inner shelf to 1.2:1 in the abyss (Fig. 24).

5.2.6. Physical factors

A range of physical factors affect the mechanisms of sediment oxygen uptake and potentially also of the resulting total oxygen uptake, as described in Chapter 3.1. Sediment topography enhances the effective area of the sediment-water interface at different scales and thereby the surface area through which oxygen may diffuse. In very shallow waters, this should be taken into account by oxygen flux calculations based on microsensor measurements of vertical O₂ gradients in the diffusive boundary layer or in the sediments. That is rarely done, which may cause an underestimation of the true diffusive oxygen uptake when the topography is distinct and the O₂ penetration depth is shallow. Examples from coastal sediments show that the underestimation is generally only about 10% or less, but it can also be higher (Gundersen and Jørgensen, 1990; Røy et al., 2002; Glud et al., 2003).

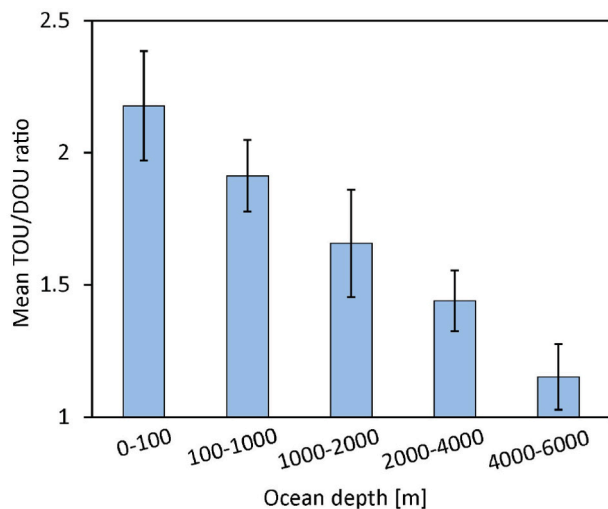


Fig. 24. Mean ratio between concurrently measured TOU and DOU by five depth ranges (total $n = 108$). The error bars indicate standard error of the mean.

Bottom currents and wave motion on the inner shelf affect the sediment oxygen uptake. Higher current speeds cause a thinner diffusive boundary layer, which may transiently enhance the O_2 diffusive flux into sediments with high potential oxygen consumption rate (Glud et al., 2007; Chapter 3.1). Currents combined with sediment topography generate lateral pressure gradients that induce pore water advection in sand and in other porous sediments. Such an advective flow within the sediment has been documented in experimental flumes and is also pronounced in coastal sands with, e.g. ripple marks or faunal casts and feeding pits (Huettel and Webster, 2001; McGinnis et al., 2014). By increasing current speeds, sediment resuspension plays an increasing role by lifting freshly deposited organic particles up into the benthic boundary layer where oxic mineralization rates are enhanced (Holtappels and Lorke, 2011; Holtappels et al., 2011; Camillini et al., 2021).

In conclusion, the oxygen uptake of the seafloor is controlled by multiple parameters that complicate the accurate measurement of TOU and DOU. Some of these parameters affect how and where the oxygen consumption takes place but do not affect the resulting total oxygen uptake. Yet, the ultimate control on benthic TOU is the flux of particulate organic matter, of which most is completely mineralized in the sediment at the expense of O_2 and only 6% is buried, as an estimated global mean (Stolpovsky et al., 2015).

6. Role of the seabed in the oceanic carbon cycle

The map of benthic O_2 consumption rates presented in Chapter 5.1 enables us to assess the quantitative importance of the seabed for the global marine carbon cycle. This requires that O_2 consumption rates are converted to benthic carbon mineralization rates assuming a respiratory quotient for early diagenesis in marine sediments. However, the nature of organic matter reaching the seabed depends on the sources and age of the material, which differ substantially with water depth and distance to terrestrial sources. The relative amount of O_2 required to oxidize deposited organic matter therefore differs across the seascape (Williams and del Giorgio, 2004). In addition, the extent to which anaerobic mineralization is included in the O_2 consumption depends on the degree of recycling of the anaerobic pathways and the burial rate of reduced products from anaerobic diagenesis (Canfield, 1993; Chapter 3.5). In this chapter, we discuss sources of organic matter and qualify the applied benthic respiratory quotient used to assess the benthic carbon mineralization from our TOU data base. The calculated budgets for benthic carbon mineralization of different oceanic depth horizons is discussed and compared with previous assessments as derived from

sediment incubations and sediment trap studies. Finally, the quantitative importance of the seabed for the global marine carbon cycle is assessed and discussed.

6.1. Sources of organic carbon in marine sediments

Rivers deliver large quantities of terrigenous organic material to the coastal ocean, where it is retained, mineralized or transported onwards to the open ocean (Burdige, 2005; Kandasamy and Nath, 2016). Current estimates have considerable uncertainties, but are in the order of 35 Tmol $C_{org} yr^{-1}$ of terrigenous organic material entering the coastal zone where 40% is mineralized, 50% is sequestered in the sediment while 10% is exported to the open ocean (Schlesinger and Melack, 1981; Regnier et al., 2013). The relatively low estimated mineralization efficiency in the coastal zone reflects the complex and recalcitrant nature of terrigenous organic material with high content of nitrogen-poor humic substances. Vegetated estuarine habitats such as salt marshes, mangroves, seagrass beds and macroalgae represent other important marine sources of organic carbon. Also here, assessments are highly uncertain. It has been estimated that between 95 and 280 Tmol $C_{org} yr^{-1}$ is exported from vegetated estuarine habitats to the coastal ocean and beyond (Duarte et al., 2005). Most of this material is presumably mineralized and deposited in coastal and shelf sediments, but recent studies based on e-DNA sequencing from deep sea sediments suggest a significant export of organic material from coastal vegetated habitats to the deep ocean (Ortega et al., 2019). Yet, the above estimate of organic carbon export appears to be exceedingly high compared to the total oxygen consumption of continental shelf sediments (Table 5).

More specific, it has been estimated that approximately 40% of the organic material produced in macroalgal beds is exported, corresponding to 50 Tmol $C_{org} yr^{-1}$ (Krause-Jensen and Duarte, 2016). Most of this material is retained and mineralized in shelf settings, but 3 Tmol $C_{org} yr^{-1}$ reaches deep sea sediments as particulate organic material (Krause-Jensen and Duarte, 2016). A similar export has been proposed for the estimated 40 Tmol $C_{org} yr^{-1}$ of organic material produced in seagrass meadows (Duarte and Krause-Jensen, 2017). Thus, the benthic supply of organic material from rivers and from coastal marine vegetated habitats is substantial, but despite its high C:N ratio and refractory nature, a considerable fraction of these organic sources is degraded in coastal, shelf and even deep-sea sediments (Burdige, 2005). The benthic imprint of refractory organic material from vegetated habitats clearly attenuates with distance from the continents (Hedges and Keil, 1995; Regnier et al., 2013; Li et al., 2017).

Benthic microphytes also contribute to the primary production of shallow settings (0-10 m) (Cahoon, 1999; Glud et al., 2009b) and represent a quantitatively important and nutritious food source for coastal food webs (Miller et al., 1996; Glud et al., 2002; Christiansen et al., 2017). Benthic primary production may be detected even down to ~200 m water depth, but in most coastal settings light attenuates more steeply and benthic primary production rarely contributes to the benthic carbon supply beyond 20-30 m water depth (Gattuso et al., 2006; Rovelli et al., 2019; Attard et al., 2014).

The distribution of phytoplankton in the ocean is very heterogeneous, with high concentrations along the ocean margins, in tropical and subtropical upwelling regions, and at high latitudes, and with extremely low concentrations in the central gyres of the Pacific, Atlantic and Indian Oceans (Fig. 17b). Estimates of the depth-integrated net primary productivity have been made from remote sensing of ocean color coupled to general circulation models and biogeochemical models. Global estimates vary by a factor of two between models, with 4300 Tmol $C_{org} yr^{-1}$ as a recent, mean value (Field et al., 1998; Carr et al., 2006; Westberry and Behrenfeld, 2014; Silsbe et al., 2016).

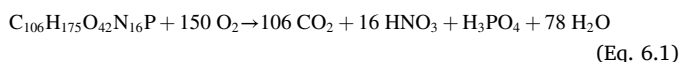
The export of organic matter from the photic surface waters, which feeds the flux of particulate organic carbon (POC) sinking towards the seafloor, has high spatial and temporal variability. Different data and models have been used, and estimates of the export efficiency differ

considerably among studies (e.g., Laufkötter et al., 2016). As examples, Najjar et al. (2007) estimated a global POC export flux of 1400 ± 500 (\pm s.d.) Tmol C_{org} yr^{-1} across a 75 m depth boundary, while Dunne et al. (2007) estimated a global export flux of 800 ± 300 Tmol C_{org} yr^{-1} with a flexible lower boundary of the photic surface water.

The nutritious value of sinking POC generally declines with increasing ocean depth leading to a relatively higher fraction of recalcitrant organic material reaching the deeper realm (Loh and Bauer, 2000). Yet, pulses of relatively fresh phytodetritus are observed at great water depth and on abyssal sediments (Billett et al., 1983; Beaulieu, 2002). The quantity and quality of organic material reaching the seabed therefore vary extensively across the global seascape. Inter-annual and seasonal variation in ocean productivity and riverine run-off combined with extensive horizontal transport complicate the linkage between the estimated deposition of organic material and the measured benthic O_2 consumption at any given location.

6.2. Conversion of O_2 consumption to organic carbon oxidation – the Respiratory Quotient

The conversion of seabed oxygen consumption to organic carbon mineralization is not straightforward. The export production from the photic surface ocean has an elemental composition close to the originally proposed Redfield ratio of P:N:C = 1:16:106. Different authors have estimated that the respiratory quotient (RQ), linking the O_2 required for the complete oxidation of this organic carbon and nitrogen to CO_2 and NO_3^- , is P:N:C:- O_2 = 1:16:103:-172 (Takahashi et al., 1985) or 1:16:117:-170 (Anderson and Sarmiento, 1994). The stoichiometry between organic C oxidized and O_2 consumed by the respiration of phytoplankton biomass may vary, but is mostly in the range of 0.67–0.78, depending on the growth phase and composition of the algae and their content of protein, carbohydrate, lipid and nucleic acid (Finkel et al., 2016; Tanioka and Matsumoto, 2020). Based on a mean composition of phytoplankton, Anderson (1995) derived the following equation for a complete mineralization:



This corresponds to an RQ of 0.71. By this oxidation, the N mineralization stoichiometry is assumed to be:



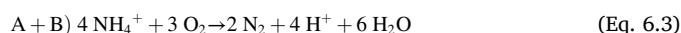
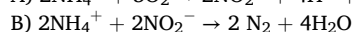
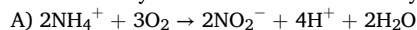
This implies that the oxidation of organic N to nitrate consumes 13% of the O_2 . If the organic N were released as ammonium and not being oxidized to nitrate, less O_2 would be required and the RQ would increase to 0.82.

Körtzinger et al. (2001) estimated an RQ of 0.75 for the Northeast Atlantic, while Tanioka and Matsumoto (2020) compiled data from the global ocean and determined a mean RQ of 0.7 for the complete mineralization of export production in the upper ocean. They noted that the C:N ratio of sinking POC increases systematically with depth in the ocean, but so does the H:C ratio, thus maintaining a rather constant RQ of 0.7 into the abyss.

As stated in Chapter 6.1, the coastal ocean receives a large contribution of organic matter from terrestrial runoff and from vegetated coastal ecosystems. These POC sources have a higher C:N ratio than the Redfield ratio of 7:1 and are much richer in structural carbohydrates than phytoplankton. As carbohydrate has the highest mean oxidation state among the main cellular components, these POC sources require relatively less O_2 to oxidize the organic carbon and therefore have a higher $C_{org}:O_2$ ratio by mineralization than the phytoplankton RQ of 0.7. This implies that the $C_{org}:O_2$ ratio of freshly deposited organic matter is relatively high in the coastal zone and on the inner shelf and declines offshore.

The fate of NH_4^+ released from organic matter degradation in marine

sediments complicates this $C_{org}:O_2$ stoichiometry (e.g., Li and Katsev, 2014). Deeply oxygenated offshore sediments tend to be nitrate sources, as ammonium released from the mineralized organic nitrogen is quantitatively oxidized to nitrate, so that the $C_{org}:O_2$ ratio approaches that of complete aerobic mineralization. The oxygen consumption by nitrification may thereby account for up to 12% of the total oxygen uptake (Li and Katsev, 2014). Coastal sediments, in contrast, tend to be nitrate sinks, where ammonium from organic nitrogen mineralization is oxidized to nitrate, which is recycled within the sediment by reduction to N_2 during denitrification. Nitrate from the overlying water diffuses into the sediment and is also denitrified to N_2 . Ammonium and nitrite may be used by anammox bacteria near the sediment surface and converted to N_2 . It is not important for the $C_{org}:O_2$ stoichiometry whether the conversion to N_2 takes place via anammox or via nitrification-denitrification. By anammox the stoichiometry is:



By nitrification-denitrification, more O_2 is consumed per ammonium than by anammox but, at the same time, additional organic carbon is oxidized during denitrification. Seitzinger et al. (2006) estimated that 80% of the global denitrification in shelf sediments is due to coupled nitrification-denitrification (or anammox) and 20% is due to nitrate uptake from the water column. As a result, the $C_{org}:O_2$ ratio of shelf sediments is relatively high and approaches a stoichiometry without NH_4^+ oxidation. This reinforces the above mentioned effect of terrestrially derived POC towards a higher RQ in shelf sediments.

Another complication of the $C_{org}:O_2$ stoichiometry is the fact that much of the degradation of sediment organic matter takes place below the oxic zone and involves fermentation processes and anaerobic respiration with alternative electron acceptors, as described in Chapter 3.5. This anaerobic respiration produces NH_4^+ , Mn^{2+} , Fe^{2+} and H_2S as well as CH_4 and a range of solid-phase minerals such as pyrite (FeS_2). Bioturbation and upwards diffusion of the dissolved species drive a redox cascade of oxidation processes by which most of these reduced products becomes oxidized with O_2 as the ultimate oxidant. As an example, for coastal sediments, 50% of the oxidation of the organic matter may be due to sulfate reduction from which 90% of the produced sulfide is re-oxidized at the expense of O_2 (Jørgensen, 1982). This means that, in such a case, only 5% of the total organic carbon oxidation is not included in the O_2 uptake. If an RQ of 0.85 were assumed for the aerobic mineralization, then a $C_{org}:O_2$ stoichiometry closer to 0.90 should be chosen for the complete mineralization in order to convert sediment oxygen uptake to total organic C oxidation in the seabed.

An alternative approach to determine the $C_{org}:O_2$ ratio is to directly measure the fluxes of O_2 into the sediment and dissolved inorganic carbon (DIC, total CO_2) out of the sediment using benthic *in situ* incubation chambers. Table 3 compiles data from such concurrent DIC and

Table 3

Respiratory quotient (RQ) of marine sediments determined as the ratio between DIC outflux and O_2 influx across the sediment surface measured by *in situ* flux chamber incubations. The RQ values are qualified by the number of stations (n) or by the standard deviation of multiple data (\pm s.d.).

Location	Water depth [m]	RQ (DIC: O_2) [mol/mol]	Reference
New Caledonia	10-17	1.17 (n = 14)	Boucher et al. (1994)
NE Greenland fjord	40	1.25 (\pm 0.45)	Glud et al. (2002)
Scottish Sea Loch	ca. 25	0.85 (\pm 0.32)	Cathalot et al. (2012)
Scottish Sea Loch	56-70	1.04 (n = 7)	Glud et al. (2016)
Svalbard fjords	155-329	1.17 (n = 3)	Glud et al. (1998)
Mediterranean Sea	80-350	0.90 (\pm 0.35)	Ståhl et al. (2004a)
Skagerrak	112-562	1.31 (\pm 0.50)	Ståhl et al. (2004b)
Slope off Chile	580-2470	1.18 (n = 4)	Glud et al. (1999)
Central tropical Pacific	3300-4300	0.69 (\pm 0.08)	Hammond et al. (1996)

O₂ flux measurements. The resulting RQ shows large variations between 0.69 and 1.31 with no clear trend with ocean depth. A reason for this large variation is probably that carbonate dissolution in the sediment enhances the DIC flux and requires concurrent analysis of alkalinity production or modeling of the Ca²⁺ and Mg²⁺ fluxes to enable a correction of this source (e.g., Berelson et al., 1994; Hammond et al., 1996). Another reason may be that the DIC and O₂ fluxes are not closely coupled in time due to episodic events in the POC influx (Therkildsen and Lomstein, 1993; Smith Jr. et al., 2018).

It is striking how different authors have chosen different RQ values for local or global conversions from oxygen data to carbon budgets. For example, Smith Jr. (1987) assumed an RQ of 0.85 for the deep sea and used this number in later publications (Smith Jr. et al., 2018). Jahnke (1996) assumed a rather low RQ of 0.6 based on a Redfield stoichiometry determined by Takahashi et al. (1985). Dunne et al. (2007) cited the RQ of 0.6 of Jahnke (1996) and used this value in their calculation of the global marine carbon budget. Other RQ values used for the global seabed include 0.77 (Seiter et al. (2005) and 1.0 (Snelgrove et al., 2018).

Based on the above discussion, we conclude that the RQ on the continental shelf is expectedly higher than the 0.82 estimate for a mineralization that does not include organic N oxidation, while in the deep sea it is lower. As our best estimate, we will in the following use an RQ of 0.90 for the inner shelf, 0.85 for the outer shelf, 0.80 for the slopes, and 0.75 for the deep sea. As seen from Table 3, these values are all within the relatively large standard deviations of estimates from *in situ* flux chamber measurements.

6.3. A global budget of O₂ uptake and organic carbon mineralization

To quantify the global oxygen uptake of marine sediments, we calculated the areal depth-integrated TOU and DOU values for every 0.1° × 0.1° grid cell of the seafloor and summed these for specific water depths. Table 1 shows the seafloor area covered by each of the seven depth regions used. The total seafloor area covered equals 354 × 10⁶ km², corresponding to ~98% of the total ocean. Table 4 shows the mean areal TOU and DOU for each depth region, as predicted from the multicomponent regression analysis described in Chapter 5.1. These data are compared to the mean TOU and DOU for the same depth regions calculated from the observed *in situ* data in the database. A plot of the two sets of data, predicted versus observed, was shown in Fig. 19.

The mean, observed areal TOU drops with ocean depth from about 45 mmol O₂ m⁻² d⁻¹ on the inner shelf to 0.8 mmol O₂ m⁻² d⁻¹ on the abyssal seafloor (Table 4). The similar drop in mean, observed areal DOU is from 20 to 0.6 mmol O₂ m⁻² d⁻¹. The standard deviations are calculated for each depth region for both predicted and observed TOU and DOU. Table 4 shows model predictions for both the entire global seabed and for the specific sites of observation. There is a good agreement between the predicted and the mean observed values of TOU and DOU of the measurement sites within each depth interval. The relative standard deviations are generally 20-50% of the mean for the predicted values and 50-90% of the mean for the observed values. The difference

Table 4

Predicted and observed, mean areal TOU and DOU for different depth regions with corresponding standard deviations in parentheses. Predicted (global) rates are the mean values modelled for the global ocean (i.e., for every 0.1° × 0.1° grid cell of the seafloor). Predicted (sites) rates are the mean values modelled for the sites of observation. For the 0-10 m depth region, the mean values of observed TOU and DOU are used for our prediction (see text).

Region (water depth)	TOU [mmol O ₂ m ⁻² d ⁻¹]			DOU [mmol O ₂ m ⁻² d ⁻¹]		
	Predicted (global)	Predicted (sites)	Observed (sites)	Predicted (global)	Predicted (sites)	Observed (sites)
Inner shelf (0-10 m)	–	–	45 (± 22)	–	–	20 (± 5)
Inner shelf (10-50 m)	25 (± 13)	35 (± 15)	27 (± 16)	20 (± 7)	21 (± 6)	17 (± 9)
Outer shelf (50-200 m)	9 (± 5)	16 (± 6)	14 (± 14)	8 (± 2)	9 (± 2)	7 (± 4)
Slope (200-1000 m)	3.5 (± 1.6)	5.6 (± 2.3)	4.3 (± 3.8)	3.1 (± 1.0)	3.4 (± 1.2)	3.1 (± 2.1)
Slope (1000-2000 m)	1.6 (± 0.6)	2.7 (± 1.0)	2.5 (± 2.6)	1.4 (± 0.3)	1.6 (± 0.2)	1.6 (± 1.0)
Rise (2000-4000 m)	0.9 (± 0.3)	1.4 (± 0.6)	1.5 (± 1.1)	0.8 (± 0.1)	1.0 (± 0.2)	1.0 (± 0.8)
Abyss (>4000 m)	0.7 (± 0.3)	0.9 (± 0.2)	0.8 (± 0.8)	0.6 (± 0.1)	0.7 (± 0.1)	0.6 (± 0.4)

between predicted and observed values is generally much less than the standard deviation for each depth region. The mean predicted values for the global seabed are on average 75% of the mean observed values for TOU and 100% for DOU. This means that a simple arithmetic mean of the observed values for each depth interval would slightly overestimate the global seabed O₂ uptake by ca. 30% for the TOU but would correspond to the DOU calculated from the modeled values. The lower predicted values for the global ocean compared to the sites of observation is due to the bias of sampling sites towards regions with high net primary production (Fig. 18b).

It should be noted that the multicomponent linear regression models for TOU and DOU were only applied for water depths greater than 10 m. For the coastal waters of the inner shelf (0-10 m water depth), the data showed no significant correlation with water depth or sea-surface POC. We therefore used the arithmetic mean of all observations from this shallow depth range in Table 4, corresponding to 45 mmol O₂ m⁻² d⁻¹ for TOU and 20 mmol O₂ m⁻² d⁻¹ for DOU.

Based on the predicted TOU and DOU of all the 0.1° × 0.1° grid cells in the ocean, a global budget of seabed oxygen uptake was calculated for each of the seven selected depth intervals Table 5. To evaluate the uncertainties of the global estimates, we present 5% and 95% confidence intervals (CI). These values were derived by subtracting (5% CI) or adding (95% CI) 2 times the standard error of the mean oxygen uptake rates per depth region and subsequently run the multicomponent linear regression with these uptake rates (Table 2). The lower global estimate was then calculated using the 5% CI values for all three coefficients in Eq. 4.1 and 4.2. The upper global estimate was derived by similarly using the 95% CI values for all three coefficients. The results show that the global estimates have relatively wide confidence intervals as a result of the relatively large scatter in measured rates. The 5% and 95% CI for water depths <10 m were derived using the 5% and 95% percentiles of the observations.

Table 5 shows that the calculated total oxygen uptake (TOU) of the

Table 5

Global budget of oxygen uptake rates in marine sediments calculated by adding up all the modeled TOU values in each 0.1° - by - 0.1° grid cell within the defined depth regions. Based on the TOU data, the rate of organic carbon oxidation to CO₂ has been calculated, using the specified respiratory quotients (RQ) for each depth region. The 5%-95% confidence intervals (CI) are shown in parenthesis.

Region (water depth)	TOU [Tmol O ₂ yr ⁻¹]	RQ	Corg [Tmol C yr ⁻¹]
	(5% - 95% CI)	(C _{org} :O ₂)	(5% - 95% CI)
Inner shelf (0-10 m)	38 (15–65)	0.90	34 (14–59)
Inner shelf (10-50 m)	70 (63–77)	0.90	63 (57–69)
Outer shelf (50-200 m)	42 (38–46)	0.85	36 (32–39)
Slope (200-1000 m)	15 (14–17)	0.80	12 (11–14)
Slope (1000-2000 m)	8 (8–10)	0.80	6 (6–8)
Rise (2000-4000 m)	35 (31–40)	0.75	26 (23–30)
Abyss (>4000 m)	47 (42–54)	0.75	35 (32–41)
Total	255 (218–299)		212 (175–260)

global seabed is 255 Tmol O₂ yr⁻¹ (1 teramol = 10¹² mol), with a 5-95% confidence interval of 218-299 Tmol O₂ yr⁻¹. The calculated diffusive oxygen uptake (DOU) of the global seabed is about 80% of this, 201 Tmol O₂ yr⁻¹, with a 5-95% confidence interval of 187-215 Tmol O₂ yr⁻¹. An estimated 59% of the global seabed TOU and 53% of the DOU take place on the continental shelf out to 200 m water depth. The abyssal sediments deeper than 4.000 m account for 18% of the TOU.

Using the specified RQ values, the TOU was converted to benthic carbon mineralization rates for each of the defined depth regions. The integrated value for all regions expressing the global benthic carbon mineralization is 212 Tmol C yr⁻¹ (Table 5). The regional and global integrals have a 5-95% confidence interval of ca. ±20%. This underscores that, despite all efforts during the past decades and despite an ever-growing data base of high-quality *in situ* assessments of benthic carbon mineralization, the global and regional budgets are still moderately constrained. This mainly reflects the extensive spatial heterogeneity and temporal variability in diagenetic activity at the seabed. To further constrain the budget, more measurements are needed, in particular in regions that are poorly represented in the data base, such as the open oceanic gyres where there are still very few available *in situ* measurements. Regions with extensive spatio-temporal dynamics are also poorly represented in the database, and slope and abyssal sediments are under-sampled.

The shelf region is clearly highly important for the global oceanic carbon budget. Although the inner shelf (0-50 m) covers only 3% of the global seabed, it accounts for an estimated 45% of the global benthic carbon mineralization (Table 5), not including sediments of vegetated ecosystems. This activity is to a large extent sustained by benthic primary production and supply of organic material exported from shallow vegetated ecosystems and from terrigenous run off (Chapter 6.1). The inner shelf region is characterized by a mosaic of diverse habitats and high seasonal variability, so despite a relatively good spatial data coverage, we still have only a moderate quantitative assessment of carbon turnover (and productivity) in shelf sediments.

To constrain the organic carbon export from the surface ocean, several studies have assessed the benthic carbon requirements from benthic O₂ consumption rates in the deep sea (>1000 m). Values range over a factor of three, from 33 Tmol C yr⁻¹ (Jahnke, 1996) to 97 Tmol C yr⁻¹ (Andersson et al., 2004) bracketing our own current estimate of 67 Tmol C yr⁻¹ (Table 6). The bottom-up assessments of benthic mineralization rates of the entire global seabed range from 99 Tmol C yr⁻¹ to the 212 Tmol C yr⁻¹ of the current study. Different regression analyses have been applied and, considering the extreme variation of data on benthic O₂ consumption, the assessments are remarkably similar. In fact, the difference between the deep-sea estimates is to some extent explained by the range of RQ values used. This, however, does not mean that the global benthic mineralization of organic material is well constrained. Not all studies acknowledge the large uncertainty or confidence interval of the average (or median) values derived. Further, the studies largely use the same - albeit gradually increasing - database and apply similar

Table 6

Compiled values of benthic carbon mineralization of deep sea sediments (>1000 m) and of global ocean sediments, respectively. All values have been derived by a bottom-up approach using assessment of the benthic O₂ consumption rates but using different RQ values as indicated.

Reference	C _{org} [Tmol C yr ⁻¹]	C _{org} [Tmol C yr ⁻¹]	RQ
	>1000 m	Global seabed	
Jahnke (1996)	33	–	0.6
Christensen (2000)	62	–	0.75
Andersson et al. (2004)	97	–	0.75
Seiter et al. (2005)	32-42	–	0.77
Glud (2008)	75	–	1
Snelgrove et al. (2018)	–	139	1
Stratmann et al. (2019)	–	99	1
This study*	67	212	0.75-0.90

relations to water depth and surface production for areal extrapolation.

6.4. Constraints on the oceanic carbon budget

As stated before, particulate organic carbon that sinks down through the water column from the photic surface waters or is transported laterally from the coastal zone and into the ocean exerts the primary control on seabed oxygen uptake. While a net primary production of about 4300 Tmol C yr⁻¹ has been estimated from satellite measurements of ocean color and modeling, the export production and the flux into the deep ocean are determined from the POC captured by multiple sediment traps. The fraction of produced POC that sinks out of the photic zone corresponds to a global export efficiency of 20-30%. As the sinking organic particles are gradually broken down and mineralized, the POC flux drops with depth. Based on multiple data from bottom-tethered time-series sediment traps at 134 globally distributed stations, Honjo et al. (2008) estimated a mean POC flux of 0.33 mmol C m⁻² d⁻¹ at an ocean depth of 2000 m.

This estimate is compared in Fig. 25 to published data on the POC flux in the ocean determined from multiple free-floating sediment traps. Data from different authors and different ocean regions show large scatter but a clear depth trend of steeply decreasing flux with depth in the upper ocean. This drop in organic particle flux indicates which fraction of the sinking POC is mineralized in the water column. The sediment trap data were fitted by different models that all assume an exponential decrease in POC flux with depth (Fig. 25). The model of Antia et al. (2001) also took the sea surface net primary production into account. It is striking how closely the estimate by Honjo et al. (2008) at 2000 m water depth matches these models, although they are based on different data sets from different sediment trap systems.

Since these sediment trap data describe the vertical POC flux that feeds the O₂ consumption of the global seabed, we integrated the sediment TOU beneath different ocean depths according to our multiple regression analysis. This was done by adding up the TOU calculated for all the 0.1° × 0.1° grid cells of the world ocean beneath each ocean depth. The TOU data were recalculated to organic carbon using the RQ values stated in Chapter 6.2. The results are plotted in Fig. 25 and show

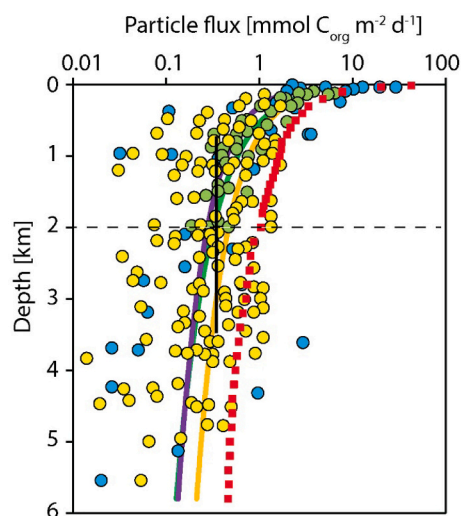


Fig. 25. Flux of particulate organic carbon (POC) down through the water column. Data points show POC collected by free-floating sediment traps, while curves show model fits to these data (blue circles: Suess, 1980; green circles and green curve: Martin et al., 1987; orange curve: Pace et al., 1987; yellow circles: Lutz et al., 2002; purple curve: Antia et al., 2001). The mean POC flux at 2000 m depth estimated by Honjo et al. (2008) based on bottom-tethered time-series traps is shown as a vertical black line. The total oxygen uptake of the global seabed below different water depths, modeled from our study, was converted to C_{org} as described in the text and is shown as a red, dotted curve.

that a POC flux higher than that determined by modeled sediment trap data is required to account for the calculated organic carbon oxidation in the seabed.

Stolpovsky et al. (2018) also used a global database of benthic O_2 and NO_3^- fluxes to estimate POC rain rates at different depths in the ocean using a multi-G model. Although the calculated depth distribution was comparable to the Martin et al. (1987) curve, they found a similar mismatch between POC trap flux data and higher organic matter mineralization rates in the sediment as shown in Fig. 25. Several other studies have noted that trap-derived POC sedimentation rates were insufficient to account for the TOU-based organic carbon demand (Wenzhöfer and Glud, 2002; Smith Jr. and Kaufmann, 1999; Smith Jr. et al., 2016; Witte and Pfannkuche, 2000).

The mean fluxes per m^2 shown in Fig. 25 can be extrapolated to the global ocean to calculate the total organic carbon flux across a depth of 2000 m. The ocean area deeper than 2000 m is $301 \times 10^6 km^2$ (Honjo et al., 2008; Table 1). Honjo et al. (2008) calculated a mean flux of $0.33 mmol C m^{-2} d^{-1}$ at an ocean depth of 2000 m, which corresponds to a global flux of $36 Tmol C_{org} yr^{-1}$ across that depth. Henson et al. (2012) combined models of export and transfer efficiencies with remote sensing data to estimate a global POC flux at 2000 m water depth of $55 Tmol C_{org} yr^{-1}$. Our estimated mean organic carbon demand needed to cover the global seabed oxygen consumption below 2000 m is $61 Tmol C_{org} yr^{-1}$ (Table 5). An additional 1-8 $Tmol C_{org} yr^{-1}$ is buried in the seabed beneath 2000 m ocean depth (Muller-Karger et al., 2004; Dunne et al., 2007), which requires a global carbon flux to the seabed beneath 2000 m of 62-69 $Tmol C_{org} yr^{-1}$. As only $36 Tmol C_{org} yr^{-1}$ was estimated to sink down across 2000 m depth, ca. $30 Tmol C_{org} yr^{-1}$, corresponding to half of the seabed C_{org} mineralization, remain unaccounted for by the sediment trap data.

Why is there such an apparent discrepancy between the measured organic carbon flux in the water column and the organic carbon oxidation and burial in the global seafloor? There are several possibilities: A) the sediment trap data underestimate the POC flux, B) the TOU data overestimate the mineralization rates, C) the estimated RQ values are too high, D) there is lateral transport down along the continental shelf, E) there is an additional flux of dissolved organic carbon (DOC) to the deep sea, and F) the discrepancy is within the uncertainty of the different estimates and is therefore statistically not significant.

A) Sediment traps may be biased relative to the total flux of POC due to factors related to hydrodynamics, lateral particle advection, zooplankton swimmers, and POC solubilization (Buesseler et al., 2007). Approaches to calibrate sediment traps include corrections using natural radionuclides (e.g., $^{234}Th/^{238}U$, $^{210}Po/^{210}Pb$) or mass balance of stable elements. Such calibrations have indicated a significant under-trapping, in particular in the mesopelagic zone (e.g., Buesseler et al., 2007; Burd et al., 2010; Wiedmann et al., 2020). Long time series with concurrent measurements of sedimentation rates and sediment oxygen consumption at specific deep-sea locations have also shown that sediment traps tend to underestimate the total POC flux (Chapter 4.3).

B) It is well documented that the retrieval of sediment cores from the deep sea and the measurement of O_2 uptake on board ships tends to overestimate TOU and DOU relative to measurements *in situ* (Glud, 2008; Chapter 2.1). We have therefore used only *in situ* data in our model analysis for all depths >10 m.

C) The RQ values used here decrease from 0.90 on the inner shelf to 0.75 in the deep sea and fall within the published range of 0.6-1.0 (Chapter 6.2). A recalculation to an extreme value of 0.6 for the deep sea would reduce the C_{org} oxidation of deep-sea sediments by 20%, which is still far from the apparent discrepancy.

D) The lateral transport of POC is well documented for many regions, in particular for the continental slopes where it was suggested to account for an 80% deficit between the vertical POC flux and the sediment oxygen consumption (Lampitt et al., 1995).

E) There is a huge reservoir of DOC in the ocean, which is partly refractory material derived from rivers and coastal ecosystems and from

old DOC originally excreted from plankton communities. There is also labile DOC that is continuously released by plankton organisms. This labile DOC may globally account for 17% of the net primary productivity, but it is mostly turned over in the upper ocean (Hansell and Carlson, 1998). DOC is also released from sinking POC in the ocean, but this fraction is largely included in the POC flux determined by sediment traps. In contrast, there is a flux of DOC from the seabed and into the overlying water column, which would add to the POC flux required to balance the sediment TOU and would exacerbate the discrepancy between sediment trap and TOU data. Burdige et al. (1999) estimated that such a DOC flux may globally correspond to up to 10% of the DIC flux from the sediments.

F) The 5-95% confidence interval of our $61 Tmol C_{org} yr^{-1}$ estimate is 55- to $71 Tmol C_{org} yr^{-1}$. We do not know the confidence interval of the sediment trap estimates, but it is possibly larger. It is therefore not clear whether the two estimates are statistically different.

A potential bias between POC flux data from sediment traps and sediment C_{org} oxidation data from TOU measurements could possibly arise because the two data sets are obtained from different ocean regions with different water depths and different sea-surface productivity. Fig. 26 shows the geographic distribution of stations occupied by free-floating sediment traps and by bottom-tethered time-series traps. All stations included in Fig. 25 and in Honjo et al. (2008) are presented in Fig. 26. The world map shows that the sediment trap positions tend to be skewed towards the ocean margins.

In order to compare this geographic distribution of sediment trap data with the distribution of sediment TOU data (Fig. 17a) we have analyzed the frequency distribution of both data sets relative to the distribution of ocean depths and sea-surface net primary productivity. The sediment trap distributions are shown in Fig. 27 (white bars). Their geographic distribution matches the global distribution of ocean depths very well. They also match the global distribution of net primary productivity fairly well, with some bias towards highly productive regions. A comparison of Fig. 27 with Fig. 18 shows that the global TOU data are much more biased towards shallow water and high productivity regions than are the sediment trap data. We have not been able to distinguish the role of such a selectivity in depth and NPP in our analysis of sediment TOU and DOU data, but it remains a potential bias.

6.5. Role of other benthic habitats

In our global budget of seabed O_2 consumption we have generally excluded vegetated coastal ecosystems such as salt marshes, mangroves and seagrass beds. We have also excluded advective systems, such as cold seeps and hot vents, and we excluded the hadal trenches. Here we will briefly touch upon their potential role in the global marine carbon cycle and how they compare to the role of non-vegetated marine sediments.

The export of organic carbon from vegetated coastal ecosystems was discussed in Chapter 6.1. Canfield et al. (2005) estimated the average O_2 uptake rates of sediments within these ecosystems. Considering that the source of organic matter here is rich in structural carbohydrates, we will assume a respiratory quotient of 1.0. The total organic carbon oxidation calculated from Canfield et al. (2005) is then $34 Tmol C yr^{-1}$ in salt marshes, $6 Tmol C yr^{-1}$ in mangroves, and $16 Tmol C yr^{-1}$ in seagrass beds. Intertidal flats add only $0.7 Tmol C yr^{-1}$ to this. Crossland et al. (1991) estimated the export production from coral reefs to be $1.7 Tmol C yr^{-1}$. This all adds up to $58 Tmol C yr^{-1}$, which exceeds our estimate of $34 Tmol C yr^{-1}$ for all other sediments on the inner shelf at 0-10 m water depth (Table 5). The fluxes cited in Chapter 6.1 of $35 Tmol C yr^{-1}$ from rivers and $95-280 Tmol C yr^{-1}$ from vegetated estuarine habitats to the coastal ocean exceeds the total organic carbon mineralization of $97 Tmol C yr^{-1}$, calculated for continental shelf sediments out to 50 m depth (Table 5). Although these estimates have wide error margins, they illustrate the extremely high productivity of ecosystems along the coastal margin (Najjar et al., 2018). They also illustrate the need to

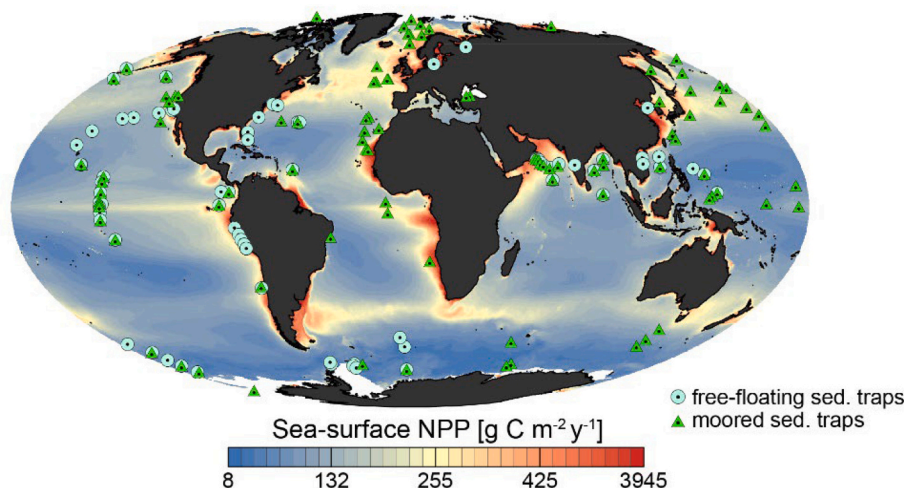


Fig. 26. Global map of sediment trap positions: Free-floating traps (light-green circles, see Fig. 25 legend); bottom-tethered traps (dark-green triangles; from Honjo et al., 2008).

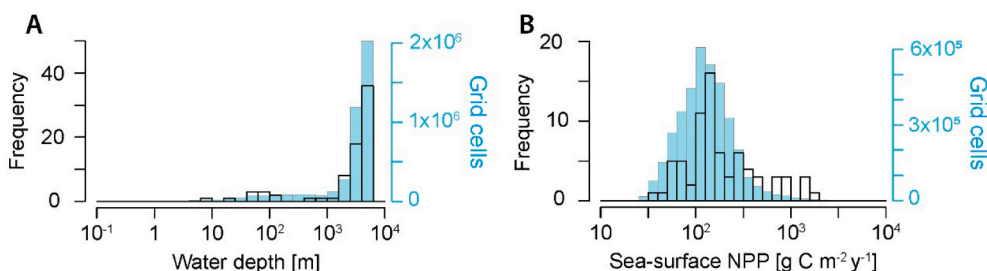


Fig. 27. Geographic distribution of sediment trap data relative to ocean data. Histograms of the relative number of observations versus, A) water depth and B) sea-surface net primary production (NPP). White bars show to the relative frequency of sediment trap data. Blue bars represent the actual distributions in the global ocean (0.1×0.1 -degree grids; see legend to Fig. 18).

better constrain current estimates of sources and sinks of organic carbon along the ocean margins.

Boetius and Wenzhöfer (2013) reviewed the tectonically driven cold seeps on the continental slopes that leak methane-rich fluids from subsurface reservoirs to the sea floor. They compiled data from seeps at 700 to 3000 m water depth. They estimated that a few tens of thousands of active cold seep systems exist on continental slopes worldwide and that seep-fueled benthic communities consume on average two orders of magnitude more O_2 per area than the surrounding seabed. They estimated a methane flux of up to 3 Tmol C yr^{-1} , of which two thirds are emitted into the overlying seawater while one third, up to 1 Tmol C yr^{-1} , is oxidized by the benthic community of free-living and symbiotic microorganisms, thus consuming 2 Tmol O_2 yr^{-1} ($CH_4 + 2O_2 \rightarrow CO_2 + 2H_2O$). While this is only a few percent of the organic carbon oxidation on the lower slope and rise, it exceeds the estimated global methane production of 0.5 Tmol CH_4 yr^{-1} in marine sediments at that depth range (Egger et al., 2018). Boetius and Wenzhöfer (2013) suggested that some of the methane may originate from dissolving gas hydrate or from the deep, hot subsurface at >1 km depth.

Bach and Edwards (2003) quantified the low-temperature alterations of upper ocean crust in the flanks of mid-ocean ridges and estimated an annual oxidation of 1.7 Tmol Fe and 0.1 Tmol S. These reactions could, directly or indirectly, consume up to 0.6 Tmol O_2 yr^{-1} and support a chemolithoautotrophic biomass production of 0.1 Tmol C yr^{-1} . Elderfield and Schultz (1996) reviewed the hydrothermal fluid flux along the mid-ocean ridges whereby a complete thermochemical reduction of seawater sulfate takes place. From this fluid flux they estimated a hydrothermal venting of 0.1-1 Tmol H_2S yr^{-1} , which by oxidation to sulfate in cold deep-sea water would consume 0.2-2 Tmol O_2 yr^{-1} .

Together, these oxygen sinks by seawater circulation through cold or hot ocean crust are of the order of 2-4 Tmol O_2 yr^{-1} in the deep sea. For comparison, the estimated global seabed oxygen uptake below 1000 m depth is 90 Tmol O_2 yr^{-1} (Table 5).

Hadal trenches cover about 0.8×10^6 km² (Stewart and Jamieson, 2018), corresponding to 0.4% of the seabed area beneath 4000 m depth (Table 1). Their O_2 uptake rate is 4-5-fold higher than that of the surrounding abyssal seabed (Chapter 4.5), which implies that their contribution to the global deep sea carbon budget is about 2%.

7. Conclusions and future perspectives

The present global budget of oxygen uptake and organic matter mineralization in the seabed started out with a database with nearly 4000 entries on benthic O_2 uptake rates. The budget was then calculated from a multiple regression analysis of data relative to key environmental parameters, of which ocean depth and sea surface primary productivity explained most of the variation. The aim was to understand the controls on *in situ* sediment O_2 uptake rates of the seafloor. We therefore needed to perform a critical selection of the data according to well-defined criteria, which discarded 70% of all data. The remaining data showed mean TOU rates that dropped with ocean depth from about 45 mmol O_2 m^{-2} d^{-1} on the inner shelf to 0.8 mmol O_2 m^{-2} d^{-1} on the abyssal seafloor. The relative standard deviations of the corresponding modeled rates were generally 20-50% of the mean. The calculated organic carbon oxidation in the global seabed was 212 Tmol C yr^{-1} with a 5-95% confidence interval of 175-260 Tmol C yr^{-1} . This confidence interval is probably of similar magnitude as by other published estimates and is important to keep in mind when comparing global budgets in the

literature.

A potential quality criterion for published TOU data, which would be hard to quantify and use, is how the measurement of sediment O₂ uptake was actually performed, i.e. how carefully the sediment was treated and the experiment was done. Each measurement of total seabed O₂ uptake is indeed a sensitive experiment on a biologically, chemically, and physically complex system. The correct *in situ* data therefore depend strongly on minimum disturbance and use of the best techniques. Unfortunately, the optimal techniques tend to be technically complex and costly, and there is a need for simpler and more robust instruments that are easier to use.

One such candidate is the non-invasive eddy covariance technique, which has the potential to become much more widely used, once standardized instruments, software packages, and data treatment procedures are developed (Berg et al., 2003, 2022). The technique is non-invasive and does not disturb the natural flow in the benthic boundary layer or the natural bioirrigation of benthic fauna. It also enables measurements of O₂ flux across the surface of permeable sandy sediments, whereby it integrates a relatively large area of the seabed, but it provides only limited insight into the spatial variability within a habitat. Benthic crawlers are much more complex instruments but have the unique capability to perform repeated measurements and generate time-series data for a range of parameters within an area of the seafloor (Lemburg et al., 2018; Smith Jr. et al., 2021). An increased capacity to combine “snapshot” measurements and long-term observatories will strongly improve our understanding of seabed dynamics.

The combination of several techniques is important because each approach tends to reveal only one aspect of the complex and dynamic processes. As an example, from the South Pacific gyre, where O₂ penetrates tens of meters down into the sediment, the combination of *in situ* O₂ microprofiles from a free-falling lander and *ex situ* O₂ measurements in retrieved sediment cores revealed that 99% of the oxygen respiration took place in the top few cm, which are generally missed by the coring technique (Fischer et al., 2009). As another example, sediment O₂ uptake and sediment trap deployments on the same stations have shown a several-fold discrepancy. It is therefore important to combine time-series of both in order to reconcile bottom-up and top-down measures of POC flux to the seafloor (Smith Jr. et al., 2018).

The seafloor constitutes a global interface between the oxic ocean and the anoxic subsurface biosphere. Both aerobic and anaerobic processes in the seabed are strongly focused towards the ocean margins and the organic-rich sediments of the coastal zone. If vegetated coastal ecosystems are included in the global budgets, about 75% of both the oxygen respiration and the sulfate reduction takes place in continental shelf sediments at 0–200 m water depth, covering about 7% of the total ocean area. In these shelf sediments, benthic fauna plays an important role for the O₂ respiration, and the re-oxidation of sulfide produced during sulfate reduction consumes 25–50% of the total O₂ uptake. In our model, we correlated the rates of seafloor O₂ uptake to sea-surface primary productivity. However, in estuaries and on the inner shelf there is a large contribution of organic matter from continental run-off and from the vegetated coastal zone (Regnier et al., 2013; Duarte et al., 2005). Recent estimates suggest that these sources may exceed the plankton productivity on the inner shelf and that they also export POC down the continental slopes, yet their contributions are poorly constrained.

This balance between aerobic and anaerobic processes is very sensitive to the organic loading of the sediment and to the availability of O₂ in the bottom water. The large oxygen minimum zones in the ocean are currently expanding, driven by ocean warming, which reduces ventilation of deeper waters due to stronger stratification in the upper ocean and decreases O₂ solubility (Levin, 2018). This causes an impoverished bottom fauna, a shift from bioirrigation towards diffusive O₂ uptake, and a relative enhancement of anaerobic degradation processes. Coastal seas are today the most strongly affected by this change due to the combination of anthropogenic eutrophication and the general ocean warming (e.g., Meier et al., 2018; Ni et al., 2019). Polar regions have the fastest

warming, which results in reduced sea ice cover and enhanced pelagic and benthic photosynthesis over the year (e.g., Arrigo et al., 2008; Gattuso et al., 2020). Thus, about 20% of the global shelf area is in the Arctic, with a considerable potential for benthic primary production as the open water period is expanding. It is critical to understand the extent and the time scale of these changes that are a result of global warming and anthropocene CO₂ emission. Predicted changes will affect the biological pump and the sequestering of organic carbon in the seabed, with significant effects on the benthic fauna and the mechanisms of O₂ consumption, both in the coastal seas and in the deep sea.

Data availability

Data are available in Supplementary Table S1, which includes all data from *in situ* and *ex situ* measurements. Data were filtered according to selection criteria outlined in Chapter 2.2 and specified in the table. The globally gridded TOU model data will be uploaded to Figshare and thereby made publicly available upon acceptance of this review.

Declaration of Competing Interest

None.

Acknowledgments

We thank Steven D’Hondt, Jack J. Middelburg, Robert Pockalny, Kenneth L. Smith and Paul Wintersteller for providing data to support our analyses and graphs. We thank Alejandro Ordonez Gloria for helpful discussion on the spatial modeling. We also thank Moritz Holtappels and Steven D’Hondt for helpful comments and references. Reviews by Andy Dale and an anonymous reviewer provided constructive suggestions to improve the manuscript.

This work was supported by (a) The Danish National Research Foundation via the Danish Center for Hadal Research (DNRF145), The European commission via an Advanced Grant HADES-ERC (669947), and the Independent Research Fund Denmark (FNU 7014-00078) to RNG, and (b) the Helmholtz Infrastructure Initiative FRAM (“Frontiers of Arctic Marine Monitoring”), the Helmholtz Alliance ROBEX (Robotic Exploration of Extreme Environments), and the Helmholtz Research Program “Changing Earth – Sustaining our Future” to FW.

Appendix A. Supplementary data

Supplementary data to this article can be found online at <https://doi.org/10.1016/j.earscirev.2022.103987>.

References

- Ahmerkamp, S., Winter, C., Janssen, F., Kuypers, M.M.M., Holtappels, M., 2015. The impact of bedform migration on benthic oxygen fluxes. *J. Geophys. Res. Biogeosci.* 120, 2229–2242.
- Aller, R.C., 1990. Bioturbation and manganese cycling in hemipelagic sediments. *Phil. Trans. Royal Soc. London A* 331, 51–58.
- Aller, R.C., 1994. Bioturbation and remineralization of sedimentary organic matter: effects of redox oscillation. *Chem. Geol.* 114, 331–345.
- Aller, R.C., 2004. Conceptual models of early diagenetic processes: the muddy seafloor as an unsteady, batch reactor. *J. Mar. Res.* 62, 815–835.
- Aller, R.C., Aller, J.Y., 1992. Meiofauna and solute transport in marine muds. *Limnol. Oceanogr.* 37, 1018–1033.
- Aller, R.C., Aller, J.Y., 1998. The effect of biogenic irrigation intensity and solute exchange on diagenetic reaction rates in marine sediments. *J. Mar. Res.* 56, 905–936.
- Aller, R.C., Rude, P.D., 1988. Complete oxidation of solid phase sulfides by manganese and bacteria in anoxic marine sediments. *Geochim. Cosmochim. Acta* 52, 751–765.
- Amante, C., Eakings, B.W., 2009. ETOPO 1 Arc-Minute Global Relief Model: Procedures, Data Sources and Analysis. NOAA Tech. Memo. NESDIS NGDC-24. Natl. Geophys. Data Center, NOAA. <https://doi.org/10.7289/V5C8276M>.
- Andersen, J.H., Carstensen, J., Conley, D.J., Dromph, K., Fleming-Lehtinen, V., Gustafsson, B.G., Josefson, A.B., Norkko, A., Villnäs, A., Murray, C., 2017. Long-term temporal and spatial trends in eutrophication status of the Baltic Sea. *Biol. Rev.* 92, 135–149.

- Anderson, L.A., 1995. On the hydrogen and oxygen content of marine phytoplankton. *Deep-Sea Res. I* 42, 1675–1680.
- Anderson, L.A., Sarmiento, J.L., 1994. Redfield ratios of remineralization determined by nutrient data-analysis. *Glob. Biogeochem. Cycles* 8, 65–80.
- Andersson, J.H., Wijsman, J.W.M., Herman, P.M.J., Middelburg, J.J., Soetaert, K., Heip, C., 2004. Respiration patterns in the deep sea. *Geophys. Res. Lett.* 31, L03304.
- Andrews, D., Bennett, A., 1981. Measurements of diffusivity near the sediment-water interface with a fine-scale resistivity probe. *Geochim. Cosmochim. Acta* 45, 2169–2175.
- Antia, A.N., Koeve, W., Fischer, G., Blanz, T., Schulz-Bull, D., Scholten, J., et al., 2001. Basin-wide particulate carbon flux in the Atlantic Ocean: Regional export patterns and potential for atmospheric CO₂ sequestration. *Glob. Biogeochem. Cycles* 15, 845–862.
- Archer, R.C., Devol, A., 1992. Benthic oxygen fluxes on the Washington shelf and slope: a comparison of in situ microelectrode and chamber flux measurements. *Limnol. Oceanogr.* 37, 614–629.
- Archer, D., Emerson, S., Smith, C.R., 1989. Direct measurement of the diffusive sublayer at the deep sea floor using oxygen microelectrodes. *Nature* 340, 623–626.
- Arrigo, K.R., van Dijken, G., Pabi, S., 2008. Impact of a shrinking Arctic ice cover on marine primary production. *Geophys. Res. Lett.* 35, L19603.
- Attard, K.M., Glud, R.N., McGinnis, D.F., Rysgaard, S., 2014. Seasonal rates of benthic primary production in a Greenland fjord measured by aquatic eddy correlation. *Limnol. Oceanogr.* 59, 1555–1569.
- Attard, K.M., Rodil, I.F., Berg, P., Mogg, A.O.M., Westerbomb, M., Norkko, A., Glud, R.N., 2020. Rocky mussel reefs as C processing hotspots: pathways of organic C flow in a high-temperature setting undergoing large-scale environmental change. *Mar. Ecol. Prog. Ser.* 645, 41–54.
- Bach, W., Edwards, K.J., 2003. Iron and sulfide oxidation within the basaltic ocean crust: implications for chemolithoautotrophic microbial biomass production. *Geochim. Cosmochim. Acta* 67, 3871–3887.
- Bacon, M.P., Anderson, R.F., 1982. Distribution of Thorium isotopes between dissolved and particulate forms in the deep-sea. *J. Geophys. Res. Oceans* 87, 2045–2056.
- Bao, R., Strasser, M., McNichol, A.P., Hagipour, N., McIntyre, C., Wefer, G., Eglinton, T.I., 2018. Tectonically-triggered sediment and carbon export to the Hadal zone. *Nature Com.* 9, 121.
- Barnett, P.R.O., Watson, J., Connelly, D., 1984. A multiple corer for taking virtually undisturbed samples from shelf, bathyal and abyssal sediments. *Oceanol. Acta* 7, 399–408.
- Baroni, I.R., Palastanga, V., Slomp, C.P., 2020. Enhanced organic burial in sediments of oxygen minimum zones upon ocean deoxygenation. *Front. Mar. Sci.* 6, 839.
- Bauer, J.E., Druffel, E.R.M., 1998. Ocean margins as a significant source of organic matter to the deep open ocean. *Nature* 392, 482–485.
- Bauerfeind, E., Nöthig, E.-M., Beszczynska, A., Fahl, K., Kaleschke, L., Kreker, K., Klages, M., Soltwedel, T., Lorenzen, C., Wegner, J., 2009. Variations in vertical particle flux in the Eastern Fram Strait (79° N/4° E) during 2000–2005. Results from the Deep-Sea Long-Term Observatory HAUSGARTEN. *Deep-Sea Res.* 156, 1471–1487.
- Beaulieu, S., 2002. Accumulation and fate of phytodetritus on the sea floor. *Oceanogr. Mar. Biol.* 40, 171–232.
- Beazley, L.L., Kenchington, E.L., Murillo, F.J., Mar Sacau, M., 2013. Deep-sea sponge grounds enhance diversity and abundance of epibenthic megafauna in the North Atlantic. *ICES Mar. Sci.* 70, 1471–1490.
- Becker, M., Schrottko, K., Bartholomä, A., Ernstsen, V., Winter, C., Hebbeln, D., 2013. Formation and entrainment of fluid mud layers in troughs of subtidal dunes in an estuarine turbidity zone. *J. Geophys. Res. Oceans* 118, 2175–2187.
- Behrenfeld, M.J., Falkowski, P.G., 1997. Photosynthetic rates derived from satellite-based chlorophyll concentration. *Limnol. Oceanogr.* 42, 1–20.
- Bekins, B., Spivack, A.J., Davis, E.E., Mayer, L.A., 2007. Dissolution of biogenic ooze over basement edifices in the equatorial Pacific with implications for hydrothermal ventilation of the oceanic crust. *Geology* 35, 679–682.
- Belley, R., Snelgrove, P.V.R., 2016. Relative contributions of biodiversity and environment to benthic ecosystem functioning. *Front. Mar. Sci.* 3, 242.
- Bender, M., Jahnke, R., Weiss, R., Martin, W., Heggie, D.T., Orchard, J., Sowers, T., 1989. Organic carbon oxidation and benthic nitrogen and silica dynamics in San Clemente Basin, a continental borderland site. *Geochim. Cosmochim. Acta* 53, 685–697.
- Berelson, W.M., Hammond, D.E., 1986. The calibration of a new free-vehicle benthic flux chamber for use in the deep sea. *Deep-Sea Res.* 33, 1439–1454.
- Berelson, W.M., Hammond, D.E., Johnson, K.S., 1987. Benthic fluxes and the cycling of biogenic silica and carbon in two southern California borderland basins. *Geochim. Cosmochim. Acta* 51, 1345–1363.
- Berelson, W.M., Hammond, D.E., McManus, J., Kilgore, T.E., 1994. Dissolution kinetics of calcium carbonate in Equatorial Pacific sediments. *Glob. Biogeochem. Cycles* 8, 219–235.
- Berg, P., Huettel, M., 2008. Monitoring the seafloor using the noninvasive eddy correlation technique: integrated benthic exchange dynamics. *Oceanography* 21, 164–167.
- Berg, P., Risgaard-Petersen, N., Rysgaard, S., 1998. Interpretation of measured concentration profiles in sediment pore water. *Limnol. Oceanogr.* 43, 1500–1510.
- Berg, P., Roy, H., Janssen, F., Meyer, V., Jørgensen, B.B., Hüttl, M., de Beer, D., 2003. Oxygen uptake by aquatic sediments measured with a novel non-invasive EDDY-correlation technique. *Mar. Ecol. Prog. Ser.* 261, 75–83.
- Berg, P., Roy, H., Wiberg, P.L., 2007. Eddy correlation flux measurements: the sediment surface area that contributes to the flux. *Limnol. Oceanogr.* 52, 1672–1684.
- Berelson, W.M., McManus, J., Severmann, S., Rollins, N., 2019. Benthic fluxes from hypoxia-influenced Gulf of Mexico sediments: impact on bottom water acidification. *Mar. Chem.* 209, 94–106.
- Berg, P., Glud, R.N., Hume, A., Stahl, H., Oguri, K., Meyer, V., Kitazato, H., 2009. Eddy correlation measurements of oxygen uptake in deep ocean sediments. *Limnol. Oceanogr. Methods* 7, 576–584.
- Berg, P., Huettel, M., Glud, R.N., Reimers, C.E., Attard, K., 2022. Aquatic Eddy Covariance: the method and its contribution to defining oxygen and carbon fluxes in marine environments. *Annu. Rev. Mar. Sci.* 14, 431–455.
- Bertics, V.J., Ziebis, W., 2009. Biodiversity of benthic microbial communities in bioturbated coastal sediments is controlled by geochemical microniches. *ISME J.* 3, 1269–1285.
- Billett, D.S.M., Lampitt, R.S., Rice, A.L., Mantoura, R.F.C., 1983. Seasonal sedimentation of phytoplankton to the deep-sea benthos. *Nature* 302, 520–522.
- Billett, D.S.M., Bett, B.J., Jacobs, C.L., Rouse, I.P., Wigham, B.D., 2006. Mass deposition of jellyfish in the deep Arabian Sea. *Limnol. Oceanogr.* 51, 2077–2083.
- Björck, S., 1995. A review of the history of the Baltic Sea, 13.0–8.0 ka BP. *Quat. Int.* 27, 19–40.
- Blair, C.C., D'Hondt, S., Spivack, A.J., Kingsley, R.H., 2007. Radiolytic hydrogen and microbial respiration in subsurface sediments. *Astrobiology* 7, 951–970.
- Blum, J.D., Drazen, J.C., Johnson, M.W., Popp, B.N., Motta, L.C., Jamieson, A.J., 2020. Mercury isotopes identify near-surface marine mercury in deep-sea trench biota. *Proc. Natl. Acad. Sci. U. S. A.* 117, 29292–29298.
- Boetius, A., Wenzhöfer, F., 2013. Seafloor oxygen consumption fueled by methane from cold seeps. *Nat. Geosci.* 6, 725–734.
- Boetius, A., Albrecht, S., Bakker, K., Bienhold, C., Felden, J., Fernández-Méndez, M., Hendricks, S., Katlein, C., Lalanda, C., Krumpal, T., Nicolaus, M., Peeken, I., Rabe, B., Rogacheva, A., Rybakova, E., Somavilla, R., Wenzhöfer, F., the RV Polarstern ARK27-3-Shipboard Science Party, 2013. Export of algal biomass from the melting Arctic sea ice. *Science* 339, 1430–1432.
- Bonaglia, S., Nascimato, F.J.A., Bartoli, M., Klawonn, I., Brüchert, V., 2014. Meiofauna increases bacterial denitrification in marine sediments. *Nat. Commun.* 5, 5133.
- Bonaglia, S., Hedberg, J., Marzocchi, U., Iburg, S., Glud, R.N., Nascimato, F.J.A., 2020. Meiofauna improve oxygenation and accelerate sulfide removal in the seasonally hypoxic seabed. *Mar. Environ. Res.* 159, 104968.
- Boucher, G., Clavier, J., Garrigue, C., 1994. Oxygen and carbon dioxide fluxes at the water-sediment interface of a tropical lagoon. *Mar. Ecol. Prog. Ser.* 107, 185–193.
- Boudreau, B.P., 1998. Mean mixed depth of sediments: The wherefore and the why. *Limnol. Oceanogr.* 43, 524–526.
- Boudreau, B.P., 2001. Solute transport above the sediment-water interface. In: Boudreau, B., Jørgensen, B.B. (Eds.), *The Benthic Boundary Layer*. Oxford University Press, pp. 104–123.
- Boudreau, B.P., Jørgensen, B.B. (Eds.), 2001. *The Benthic Boundary Layer: Transport Processes and Biogeochemistry*. Oxford University Press.
- Bradley, J.A., Amend, J.P., LaRowe, D.E., 2018. Necromass as a limited source of energy for microorganisms in marine sediments. *J. Geophys. Res. Biogeosci.* 123, 577–590.
- Bradley, J.A., Arndt, S., Amend, J.P., Burwicz, E., Dale, A.W., Egger, M., LaRowe, D.E., 2020. Widespread energy limitation to life in global subseafloor sediments. *Sci. Adv.* 6, eaba0697.
- Breitburg, D., Levin, L.A., Oschlies, A., Grégoire, M., Chavez, F.P., Conley, D.J., et al., 2018. Declining oxygen in the global ocean and coastal waters. *Science* 359, eaam7240.
- Brüchert, V., Jørgensen, B.B., Neumann, K., Riechmann, D., Schlösser, M., Schulz, H., 2003. Regulation of bacterial sulfate reduction and hydrogen sulfide fluxes in the central Namibian coastal upwelling zone. *Geochim. Cosmochim. Acta* 67, 4505–4518.
- Buchholtz-ten Brink, M.R., Gust, G., Chavis, C., 1989. Calibration and performance of a stirred benthic chamber. *Deep-Sea Res. I* 36, 1083–1101.
- Buesseler, K.O., Antia, A.N., Chen, M., Fowler, S.W., Gardner, W.D., Gustafsson, O., et al., 2007. An assessment of the use of sediment traps for estimating upper ocean particle fluxes. *J. Mar. Res.* 65, 345–416.
- Burd, A.B., Hansell, D.A., Steinberg, D.K., Anderson, T.R., Aristegui, J., Baltar, F., et al., 2010. Assessing the apparent imbalance between geochemical and biochemical indicators of meso- and bathypelagic biological activity: What the @#! is wrong with present calculations of carbon budgets? *Deep-Sea Res. II* 57, 1557–1571.
- Burdige, D.J., 2005. Burial of terrestrial organic matter in marine sediments: A re-assessment. *Glob. Biogeochem. Cycles* 19, GB4011.
- Burdige, D.J., Berelson, W.M., Coale, K.H., McManus, J., Johnson, K.S., 1999. Fluxes of dissolved organic carbon from California continental margin sediments. *Geochim. Cosmochim. Acta* 63, 1507–1515.
- Cahoon, L.B., 1999. The role of benthic microalgae in neritic ecosystems. *Oceanogr. Mar. Biol. Annu. Rev.* 37, 47–86.
- Cai, W.-J., Sayles, F.L., 1996. Oxygen penetration depths and fluxes in marine sediments. *Mar. Chem.* 52, 123–131.
- Camillini, N., Larsen, M., Glud, R.N., 2019. Behavioral patterns of soft-shell clam *Mya arenaria* (L): Implications for benthic oxygen and nitrogen dynamics. *Mar. Ecol. Prog. Ser.* 622, 103–199.
- Camillini, N., Attard, K.M., Eyre, B.D., Glud, R.N., 2021. Resolving community metabolism of eelgrass (*Zostera marina*) meadows by benthic flume-chambers and eddy covariance in dynamic coastal environments. *Mar. Ecol. Prog. Ser.* 661, 97–114.
- Canfield, D.E., 1993. Organic matter oxidation in marine sediments. In: Wollast, R., Mackenzie, F.T., Chou, L. (Eds.), *Interactions of C, N, P and S Biogeochemical Cycles and Global Change*. Springer, Berlin, pp. 333–363.
- Canfield, D.E., 1994. Factors influencing organic carbon preservation in marine sediments. *Chem. Geol.* 114, 315–329.

- Canfield, D.E., Kristensen, E., Thamdrup, B., 2005. Aquatic geomicrobiology. *Advances in Marine Biology*, vol. 48. Elsevier, London.
- Carr, M.-E., Friedrichs, M.A.M., Schmetz, M., Aita, M.N., Antoine, D., Arrigo, K.R., et al., 2006. A comparison of global estimates of marine primary production from ocean color. *Deep-Sea Res. II* 53, 741–770.
- Carstensen, J., Andersen, J.H., Gustafsson, B.G., Conley, D.J., 2014. Deoxygenation of the Baltic Sea during the last century. *Proc. Natl. Acad. Sci. U. S. A.* 111, 5628–5633.
- Cathalot, C., Lansard, B., Hall, P.O.J., Tengberg, A., Almroth-Rosell, E., Apler, A., Calder, L., Bell, E., Rabouille, C., 2012. Spatial and temporal variability of benthic respiration in a Scottish Sea Loch impacted by fish farming: a combination of in situ techniques. *Aquat. Geochem.* 18, 515–541.
- Chen, H., Xie, X., Van Rooij, D., Vandorpe, T., Huang, L., Guo, L., Su, M., 2013. Depositional characteristics and spatial distribution of deep-water sedimentary systems on the northwestern middle-lower slope of the Northwest Sub-Basin, South China Sea. *Mar. Geophys. Res.* 34, 239–257.
- Christensen, J.P., 2000. A relationship between deep-sea benthic oxygen demand and ocean primary productivity. *Oceanol. Acta* 23, 65–82.
- Christiansen, M.J.A., Middelburg, J.J., Holthuijsen, S.J., Jouta, J., Compton, T.J., van der Heide, T., Piersma, T., Sinnighe Damsté, J.S., van der Veer, H.W., Olf, H., 2017. Benthic primary producers are key to sustain the Wadden Sea food web: stable carbon isotope analysis at landscape scale. *Ecology* 95, 1498–1512.
- Clough, L.M., Renaud, P., Ambrose, W.G., 2005. Impacts of water depths, sediment pigment concentration, and benthic macrofaunal biomass on sediment oxygen demand in the western Arctic Ocean. *Can. J. Fish. Aquat. Sci.* 62, 1756–1765.
- Conley, D.J., Stockenberg, A., Carman, R., Johnstone, R.W., Rahm, L., Wul, F., 1997. Sediment-water nutrient fluxes in the Gulf of Finland, Baltic Sea. *Estuar. Coast. Shelf Sci.* 45, 591–598.
- Conley, D.J., Björck, S., Bonsdorff, E., Carstensen, J., Destouni, G., Gustafsson, B.G., Heitanen, S., Kortekaas, M., et al., 2009. Hypoxia-related processes in the Baltic Sea. *Environ. Sci. Technol.* 43, 3412–3420.
- Cook, P.L.M., Wenzhöfer, F., Glud, R.N., Janssen, F., Huettel, M., 2007. Benthic solute exchange and carbon mineralization in two shallow subtidal sandy sediments: Effect of advective pore-water exchange. *Limnol. Oceanogr.* 52, 1943–1963.
- Crossland, C.J., Hatcher, B.G., Smith, S.V., 1991. Role of coral reefs in global ocean production. *Coral Reefs* 10, 55–64.
- D'Hondt, S., Jørgensen, B.B., Miller, D.J., the ODP Leg 201 Scientific Party, 2004. Distributions of microbial activities in deep subseafloor sediments. *Science* 306, 2216–2221.
- D'Hondt, S., Spivack, A.J., Pockalny, R., Ferdelman, T.G., Fischer, J.P., Kallmeyer, J., Abrams, L.J., Smith, D.C., Graham, D., Hasiuk, F., Schrum, H., Stancin, A.M., 2009. Subseafloor sedimentary life in the South Pacific Gyre. *Proc. Natl. Acad. Sci. U. S. A.* 106, 11651–11656.
- D'Hondt, S., Inagaki, F., Zarikian, C.A., Abrams, L.J., Dubois, N., Engelhardt, T., Evans, H., Ferdelman, T., et al., 2015. Presence of oxygen and aerobic communities from sea floor to basement in deep-sea sediments. *Nat. Geosci.* 8, 299–304.
- Dade, W.B., 1993. Near-bed turbulence and hydrodynamic control of diffusional mass transfer at the sea floor. *Limnol. Oceanogr.* 38, 52–69.
- Dade, W.B., Hogg, A.J., Boudreau, B.P., 2001. Physics of flow above the sediment-water interface. In: Boudreau, B.P., Jørgensen, B.B. (Eds.), *The Benthic Boundary Layer*. Oxford University Press, pp. 4–43.
- Dale, A.W., Sommer, S., Ryabenko, E., Noffke, A., Bohlen, L., et al., 2014. Benthic nitrogen fluxes and fractionation of nitrate in the Mauritanian oxygen minimum zone (Eastern Tropical North Atlantic). *Geochim. Cosmochim. Acta* 134, 234–256.
- Dale, A.W., Sommer, S., Lomnitz, U., Montes, I., Treude, T., Liebetrau, V., et al., 2015. Organic carbon production, mineralisation and preservation on the Peruvian margin. *Biogeosciences* 12, 1537–1559.
- Dale, A.W., Sommer, S., Lomnitz, U., Bourbonnais, A., Wallmann, K., 2016. Biological nitrate transport in sediments on the Peruvian margin mitigates benthic sulfide emissions and drives pelagic N loss during stagnation events. *Deep-Sea Res. I* 112, 123–136.
- Danovaro, R., Gambi, C., Della Croce, N., 2002. Meiofauna hotspot in the Atacama Trench, eastern South Pacific Ocean. *Deep-Sea Res. I* 49, 843–857.
- Danovaro, R., Della Croce, N., Dell'Anno, A., Pusceddu, A., 2003. A decoupler of organic matter at 7800 m depth in the SE Pacific Ocean. *Deep-Sea Res. I* 50, 1411–1420.
- Deuser, W.G., Ross, E.H., 1980. Seasonal change in the flux of organic carbon to the deep Sargasso Sea. *Nature* 283, 364–365.
- Donis, D., McGinnis, D.F., Holtappels, M., Felden, J., Wenzhoefer, F., 2016. Assessing benthic oxygen fluxes in oligotrophic deep sea sediments (HAUSGARTEN observatory). *Deep-Sea Res. I* 111, 1–10.
- Duarte, C.M., Krause-Jensen, D., 2017. Export from seagrass meadows contributes to marine carbon sequestration. *Front. Mar. Sci.* 4, 13.
- Duarte, C.M., Middelburg, J.J., Caraco, N., 2005. Major role of marine vegetation on the oceanic carbon cycle. *Biogeosciences* 2, 1–8.
- Dunne, J.P., Sarmiento, J.L., Gnanadesikan, A., 2007. A synthesis of global particle export from the surface ocean and cycling through the ocean interior and on the seafloor. *Glob. Biogeochem. Cycles* 21, GB4006.
- Dupont, E., Stora, G., Tremblay, P., Gilbert, F., 2006. Effects of population density on the sediment mixing induced by the gallery-diffuser *Hediste (Neries) diversicolor* O.F. Muller, 1776. *J. Mar. Biol. Ecol.* 336, 33–41.
- Durden, J.M., Bett, B.J., Huffard, C.L., Pebody, C., Ruhl, H.A., Smith Jr., K.L., 2020. Response of deep-sea deposit-feeder to detrital inputs: A comparison of two abyssal time-series sites. *Deep-Sea Res. II* 173, 104677.
- Egger, M., Riedinger, N., Mogollón, J.M., Jørgensen, B.B., 2018. Global diffusive fluxes of methane in marine sediments. *Nat. Geosci.* 11, 421–425.
- Elderfield, H., Schultz, A., 1996. Mid-ocean ridge hydrothermal fluxes and the chemical composition of the ocean. *Annu. Rev. Earth Planet. Sci.* 24, 191–224.
- Estes, E.R., Pockalny, R., D'Hondt, S., Inagaki, F., Morono, Y., Murray, R.W., Nordlund, D., Spivack, A.J., Wankel, S.D., Xiao, N., Hansel, C.M., 2019. Persistent organic matter in oxic subseafloor sediment. *Nat. Geosci.* 12, 126–131.
- Ferrón, S., Alonso-Pérez, F., Castro, C.G., Ortega, T., Pérez, F.F., Ríos, A.F., Gómez-Parra, A., Forja, J.M., 2008. Hydrodynamic characterization and performance of an autonomous benthic chamber for use in coastal systems. *Limnol. Oceanogr. Methods* 6, 558–571.
- Fettweis, M., Baeye, M., 2014. Seasonal variation in concentration, size, and settling velocity of muddy marine flocs in the benthic boundary layer. *J. Geophys. Res. Oceans* 120, 5648–5667.
- Field, C.B., Behrenfeld, M.J., Randerson, J.T., Falkowski, P., 1998. Primary production of the biosphere: Integrating terrestrial and oceanic components. *Science* 281, 237–240.
- Filbee-Dexter, K., Feehan, C., Smale, D., Krumhansl, K., Augustine, S., de Bettignies, F., et al., 2021. Ocean temperature controls kelp decomposition and carbon sink potential. <https://doi.org/10.21203/rs.3.rs-38503/v1>.
- Findlay, A.J., Pellerin, A., Lauffer, K., Jørgensen, B.B., 2020. Quantification of sulphide oxidation rates in sediment. *Geochim. Cosmochim. Acta* 280, 441–452.
- Finkel, Z.V., Follows, M.J., Liefer, J.D., Brown, C.M., Benner, I., Irwin, A.J., 2016. Phylogenetic diversity in the macromolecular composition of microalgae. *PLoS One* 11, e0155977.
- Fischer, J.P., Ferdelman, T.G., D'Hondt, S., Røy, H., Wenzhöfer, F., 2009. Oxygen penetration deep into the sediment of the South Pacific gyre. *Biogeosciences* 6, 1467.
- Flury, S., Røy, H., Dale, A.W., Fossing, H., Tóth, Z., Spiess, V., Jensen, J.B., Jørgensen, B. B., 2016. Controls on subsurface methane fluxes and shallow gas formation in Baltic Sea sediment (Aarhus Bay). *Geochim. Cosmochim. Acta* 188, 297–309.
- Forster, S., Graf, G., 1995. Impact of irrigation on oxygen flux into the sediment: intermittent pumping by *Callianassa* subterranean and 'piston-pumping' by *Janicea conchilega*. *Mar. Biol.* 123, 335–346.
- Forster, S., Glud, R.N., Gundersen, J.K., Huettel, M., 1999. In situ study of bromide tracer and oxygen flux in coastal sediments. *Estuar. Coast. Shelf Sci.* 49, 813–827.
- Fossing, H., Gallardo, V.A., Jørgensen, B.B., Hüttl, M., Nielsen, L.P., et al., 1995. Concentration and transport of nitrate by the mat-forming sulphur bacterium *Thioploca*. *Nature* 374, 713–715.
- Froelich, P.N., Klinkhammer, G.P., Bender, M.L., Luedtke, N.A., Heath, G.R., Cullen, D., Dauphin, P., Hammond, D., Hartman, B., Maynard, V., 1979. Early oxidation of organic matter in pelagic sediments of the eastern equatorial Atlantic: suboxic diagenesis. *Geochim. Cosmochim. Acta* 43, 1075–1090.
- Funkey, C.P., Conley, D.J., Reuss, N.S., Humborg, C., Jilbert, T., Slomp, C.P., 2014. Hypoxia sustains cyanobacteria blooms in the Baltic Sea. *Environ. Sci. Technol.* 48, 2598–2602.
- Gattuso, J.-P., Gentili, B., Duarte, C.M., Kleypas, J.A., Middelburg, J.J., 2006. Light availability in the coastal ocean: impact on the distribution of benthic photosynthetic organisms and their contribution to primary production. *Biogeosciences* 3, 489–513.
- Gattuso, J.-P., Gentili, B., Antoine, D., Doxaran, D., 2020. Global distribution of photosynthetically available radiation on the seafloor. *Earth Syst. Sci. Data* 12, 1697–1709.
- Ghedini, G., White, C.R., Marshall, D.J., 2018. Metabolic scaling across succession: Do individual rates predict community-level energy use? *Funct. Ecol.* 32, 1447–1456.
- Gilbert, F., Hulth, S., Grossi, V., Poggiale, J.C., et al., 2007. Sediment reworking by marine benthic species from the Gullmar Fjord (western Sweden): importance of faunal biovolume. *J. Exp. Mar. Biol. Ecol.* 348, 133–144.
- Gilly, W.F., Beman, J.M., Litvin, S.Y., Robinson, B.H., 2013. Oceanographic and biological effects of shoaling of the oxygen minimum zone. *Annu. Rev. Mar. Sci.* 5, 393–420.
- Glud, R.N., 2008. Oxygen dynamics of marine sediments. *Mar. Biol. Res.* 4, 243–289.
- Glud, R.N., Blackburn, N., 2002. The effects of chamber size on benthic oxygen uptake measurements: A simulation study. *Ophelia* 56, 23–31.
- Glud, R.N., Gundersen, J.K., Jørgensen, B.B., Revsbech, N.P., Schulz, H.D., 1994. Diffusive and total oxygen uptake of deep-sea sediments in the eastern South Atlantic Ocean: *in situ* and laboratory measurements. *Deep-Sea Res.* 41, 1767–1788.
- Glud, R.N., Jensen, K., Revsbech, N.P., 1995. Diffusivity in surficial sediments and benthic mats determined by use of a combined N₂O-O₂ microsensor. *Geochim. Cosmochim. Acta* 59, 231–237.
- Glud, R.N., Gundersen, J.K., Revsbech, N.P., Jørgensen, B.B., Huettel, M., 1995a. Calibration and performance of the stirred flux chamber from the benthic lander Elinor. *Deep-Sea Res. I* 42, 1029–1042.
- Glud, R.N., Ramsing, N.B., Gundersen, J.K., Klimant, I., 1996. Planar optodes, a new tool for fine scale measurements of two-dimensional O₂ distribution in benthic communities. *Mar. Ecol. Prog. Ser.* 140, 217–226.
- Glud, R.N., Holby, O., Hoffmann, F., Canfield, D.E., 1998. Benthic mineralization and exchange in Arctic sediments (Svalbard, Norway). *Mar. Ecol. Prog. Ser.* 173, 237–251.
- Glud, R.N., Gundersen, J.K., Holby, O., 1999. Benthic *in situ* respiration in the upwelling area off central Chile. *Mar. Ecol. Prog. Ser.* 186, 9–18.
- Glud, R.N., Tengberg, A., Kühl, M., Hall, P.O.J., Klimant, I., Holst, G., 2001. An *in situ* instrument for planar O₂ optode measurements at benthic interfaces. *Limnol. Oceanogr.* 46, 2073–2080.
- Glud, R.N., Kühl, M., Wenzhöfer, F., Rysgaard, S., 2002. Benthic diatoms of a high Arctic fjord (Young Sound, NE Greenland): importance for ecosystem primary production. *Mar. Ecol. Prog. Ser.* 238, 15–29.

- Glud, R.N., Gundersen, J.K., Roy, H., Jørgensen, B.B., 2003. Seasonal dynamics of benthic O₂ uptake in a semi-enclosed bay: importance of diffusion and faunal activity. *Limnol. Oceanogr.* 48, 1265–1276.
- Glud, R.N., Berg, P., Fossing, H., Jørgensen, B.B., 2007. Effect of the diffusive boundary layer on benthic mineralization and O₂ distribution: a theoretical model analysis. *Limnol. Oceanogr.* 52, 547–557.
- Glud, R.N., Stahl, H., Berg, P., Wenzhöfer, F., Oguri, K., Kitazato, H., 2009a. In situ microscale variation in distribution and consumption of O₂: A case study from a deep ocean margin sediment (Sagami Bay, Japan). *Limnol. Oceanogr.* 54, 1–12.
- Glud, R.N., Woelfel, J., Karsten, U., Kühl, M., Rysgaard, S., 2009b. Benthic microalgal production in the Arctic: applied methods and status of the current database. *Bot. Mar.* 52, 559–571.
- Glud, R.N., Wenzhöfer, F., Middelboe, M., Oguri, K., Turnewisch, R., Canfield, D.E., Kitazato, H., 2013. High rates of microbial carbon turnover in sediments in the deepest oceanic trench on Earth. *Nat. Geosci.* 9, 284–288.
- Glud, R.N., Berg, P., Stahl, H., Hume, A., Larsen, M., Eyre, B.D., Cook, P.L.M., 2016. Benthic carbon mineralization and nutrient turn-over in a Scottish sea loch: an integrative in situ study. *Aquat. Geochem.* 22, 443–467.
- Glud, R.N., Berg, P., Thamdrup, B., Larsen, M., Stewart, H.A., Jamieson, A.J., Glud, A., Oguri, K., Saneil, H., Rowden, A.A., Wenzhöfer, F., 2021. Hadal trenches are dynamic hotspots for early diagenesis in the deep sea. *Comm. Earth Environ.* 2, 21.
- Gooday, A.J., Bett, B.J., Escobar, E., Ingole, B.S., 2010. Benthic biodiversity and habitat heterogeneity in oxygen minimum zones. *Mar. Ecol.* 31, 125–147.
- Gorska, B., Soltwedel, T., Schewe, I., Wlondarska-Kowalczyk, M., 2020. Bathymetric trends in biomass size spectra, carbon demand, and production of Arctic benthos (76–5561 m, Fram Strait). *Prog. Oceanogr.* 186, 102370.
- Grundmanis, V., Murray, J.W., 1982. Aerobic respiration in pelagic marine sediments. *Geochim. Cosmochim. Acta* 46, 1101–1120.
- Gundersen, J.K., Jørgensen, B.B., 1990. Microstructure of diffusive boundary layers and the oxygen uptake of the sea floor. *Nature* 345, 604–607.
- Hall, S.J., 2002. The continental shelf benthic ecosystem: current status, agents for change and future prospects. *Environ. Conserv.* 29, 350–374.
- Hall, P.O.J., Anderson, L.G., Rutgers van der Loeff, M.M., Sundby, B., Westerlund, S.F.G., 1989. Oxygen uptake kinetics in the benthic boundary layer. *Limnol. Oceanogr.* 34, 734–746.
- Hall, P.O.J., Brunnegard, J., Hulthe, G., Martin, W.R., Stahl, H., Tengberg, A., 2007. Dissolved organic matter in abyssal sediments; core recovery artifacts. *Limnol. Oceanogr.* 52, 19–31.
- Hällfors, G., Niemi, Å., Ackefors, H., Lassig, J., Leppäkoski, E., 1981. Biological oceanography. In: Voipio, A. (Ed.), *The Baltic Sea*, Elsevier Oceanography Series 30. Elsevier, Amsterdam, pp. 219–274.
- Hammond, D.E., McManus, J., Berelson, W.M., Kilgore, T.E., Pope, R.H., 1996. Early diagenesis of organic material in equatorial Pacific sediments: stoichiometry and kinetics. *Deep-Sea Res. II* 43, 1365–1412.
- Han, X., Fang, H., He, G., Reible, D., 2018. Effects of roughness and permeability on solute transfer at the sediment water interface. *Water Res.* 129, 39–50.
- Hansell, D.A., Carlson, C.A., 1998. Net community production of dissolved organic carbon. *Glob. Biogeochem. Cycles* 12, 443–453.
- Hansen, K., Kristensen, E., 1997. Impact of macrofaunal recolonization on benthic metabolism and nutrient fluxes in a shallow marine sediment previously overgrown with macroalgal mats. *Estuar. Coast. Shelf Sci.* 45, 613–628.
- Harnett, H.E., Devol, A.H., 2003. Role of a strong oxygen-deficient zone in the preservation and degradation of organic matter: A carbon budget for the continental margins of northwest Mexico and Washington State. *Geochim. Cosmochim. Acta* 67, 247–264.
- Harnett, H.E., Keil, R.G., Hedges, J.L., Devol, A.H., 1998. Influence of oxygen exposure time on organic carbon preservation in continental margin sediments. *Nature* 391, 572–574.
- Harris, P.T., Macmillan-Lawler, M., Rupp, J., Barker, E.K., 2014. Geomorphology of the Oceans. *Mar. Geol.* 352, 4–24.
- Hedges, J.L., Keil, R.G., 1995. Sedimentary organic matter preservation: an assessment and speculative synthesis. *Mar. Chem.* 49, 81–115.
- Heip, C., Herman, P., Middelburg, J.J., 2001. The role of the benthic biota in sedimentary metabolism and sediment-water exchange processes in the Goban Spur area (NE Atlantic). *Deep-Sea Res. II* 48, 3223–3243.
- Heiskanen, A.-S., Leppänen, J.-M., 1995. Estimation of export production in the coastal Baltic Sea: effect of resuspension and microbial decomposition on sedimentation measurements. *Hydrobiologia* 316, 211–224.
- Helly, J.J., Levin, L.A., 2004. Global distribution of naturally occurring marine hypoxia on continental margins. *Deep Sea Res. I* 51, 1159–1168.
- Hensen, C., Zabel, M., Schulz, H.N., 2006. Benthic cycling of oxygen, nitrogen and phosphorus. In: Schulz, H.D., Zabel, M. (Eds.), *Marine Geochemistry*, 2nd ed. Springer, Berlin, pp. 207–240.
- Henson, S.A., Sanders, R., Madsen, E., 2012. Global patterns in efficiency of particulate organic carbon export and transfer to the deep ocean. *Glob. Biogeochem. Cycles* 26, GB1028.
- Holt, J., Schrum, C., Cannaby, H., Daewel, U., Allen, I., Artioli, Y., Bopp, L., Butenschon, M., et al., 2016. Potential impacts of climate change on the primary production of regional seas: a comparative analysis of five European seas. *Prog. Oceanogr.* 140, 91–115.
- Holtappels, M., Lorke, A., 2011. Estimating turbulent diffusion in a benthic boundary layer. *Limnol. Oceanogr. Methods* 9, 29–41.
- Holtappels, M., Kuypers, M.M.M., Schlüter, M., Brüchert, V., 2011. Measurement and interpretation of solute concentration gradients in the benthic boundary layer. *Limnol. Oceanogr. Methods* 9, 1–13.
- Honjo, S., Manganini, S.J., Krishfield, R.A., Francois, R., 2008. Particulate organic carbon fluxes to the ocean interior and factors controlling the biological pump: a synthesis of global sediment trap programs since 1983. *Prog. Oceanogr.* 76, 217–285.
- Huang, K., Boudreau, B.P., Reed, D.C., 2007. Simulated fiddler crab sediment mixing. *J. Mar. Res.* 65, 491–522.
- Huettel, M., Gust, G., 1992a. Solute release mechanisms from confined cores in stirred benthic chambers and flume flows. *Mar. Ecol. Prog. Ser.* 82, 187–197.
- Huettel, M., Gust, G., 1992b. Impact of bioirrigation on interfacial solute exchange in permeable sediments. *Mar. Ecol. Prog. Ser.* 89, 253–267.
- Huettel, M., Rusch, A., 2000. Transport and degradation of phytoplankton in permeable sediment. *Limnol. Oceanogr.* 45, 534–549.
- Huettel, M., Webster, I.T., 2001. Porewater flow in permeable sediments. In: Boudreau, B.P., Jørgensen, B.B. (Eds.), *The Benthic Boundary Layer: Transport Processes and Biogeochemistry*. Oxford University Press, pp. 144–179.
- Huettel, M., Berg, P., Kostka, J.E., 2014. Benthic exchange and biogeochemical cycling in permeable sediments. *Annu. Rev. Mar. Sci.* 6, 23–51.
- Huffard, C.L., Kuhnz, L.A., Lemon, L., Sherman, A.D., Smith Jr., K.L., 2016. Demographic indicators of change in a deposit-feeding abyssal holothurian community (Station M, 4000m). *Deep-Sea Res. I* 109, 27–39.
- Inoue, T., Nakamura, Y., Sayama, M., 2007. A new method for measuring flow structure in the benthic boundary layer using an acoustic Doppler velocimeter. *J. Atmos. Ocean. Technol.* 25, 822–830.
- International Council for the Exploration of the Sea, 2018. *ICES Ecosystem Overviews. Baltic Sea Ecoregion*. <https://doi.org/10.17895/ices.pub.4665>.
- Itoh, M., Matsumura, I., Noriki, S.A., 2000. Large flux of particulate matter in the deep Japan Trench observed just after the 1994 Sanriku-Oki earthquake. *Deep-Sea Res. I* 47, 1987–1998.
- Itoh, M., Kawamura, K., Kitahashi, T., Kojima, S., Katagiri, H., Shimanaga, M., 2011. Bathymetric patterns of meiofaunal abundance and biomass associated with the Kuril and Ryukyu trenches, western North Pacific Ocean. *Deep-Sea Res. I* 58, 86–97.
- Iversen, N., Jørgensen, B.B., 1993. Diffusion coefficients of sulfate and methane in marine sediments: influence of porosity. *Geochim. Cosmochim. Acta* 57, 571–578.
- Jahnke, R.A., 1996. The global ocean flux of particulate organic carbon: a real distribution and magnitude. *Glob. Biogeochem. Cycles* 10, 71–88.
- Jahnke, R.A., Craven, D.B., McCorkle, D.C., Reimers, C.E., 1997. CaCO₃ dissolution in California continental margin sediments: the influence of organic matter remineralization. *Geochim. Cosmochim. Acta* 61, 3587–3604.
- Jahnke, R., Jackson, G., 1992. The spatial distribution of sea floor oxygen consumption in the Atlantic and Pacific Oceans. In: Rowe, G., Pariente, V. (Eds.), *Deep-Sea Food Chains and the Global Carbon Cycle*. Kluwer Academic Publishers, The Netherlands, pp. 295–308.
- Jahnke, R.A., Reimers, C., Craven, D.B., 1990. Intensification of recycling of organic matter at the sea floor near ocean margins. *Nature* 348, 50–54.
- Jahnke, R.A., Nelson, J.R., Marinelli, R.L., Eckman, J.E., 2000. Benthic flux of biogenic elements on the southeastern US continental shelf: influence of pore water advective transport and benthic microalgae. *Cont. Shelf Res.* 20, 109–127.
- Jamieson, A.J., Malkocs, T., Piertney, S.B., Fujii, T., Zhang, Z., 2017. Bioaccumulation of persistent organic pollutants in the deepest ocean fauna. *Nat. Ecol. Evol.* 3, 0051.
- Janssen, F., Faerber, P., Huettel, M., Meyer, V., Witte, U., 2005. Porewater advection and solute fluxes in permeable marine sediments (I): calibration and performance of a novel benthic chamber system. *Sandy. Limnol. Oceanogr.* 50, 768–778.
- Jilbert, T., Conley, D.J., Gustafsson, B.G., Funkey, C.P., Slomp, C.P., 2015. Glacio-isostatic control on hypoxia in a high-latitude shelf basin. *Geology* 43, 427–430.
- Jonsson, P., Carman, R., 1994. Changes in deposition of organic matter and nutrients in the Baltic Sea during the twentieth century. *Mar. Pollut. Bull.* 28, 417–426.
- Jørgensen, B.B., 1977a. Distribution of colorless sulfur bacteria (*Beggiatoa* spp.) in a coastal marine sediment. *Mar. Biol.* 41, 19–28.
- Jørgensen, B.B., 1977b. Bacterial sulfate reduction within reduced microniches of oxidized marine sediments. *Mar. Biol.* 41, 7–17.
- Jørgensen, B.B., 1982. Mineralization of organic matter in the sea bed - the role of sulphate reduction. *Nature* 296, 643–645.
- Jørgensen, B.B., 2006. Bacteria and marine biogeochemistry. In: Schulz, H.D., Zabel, M. (Eds.), *Marine Geochemistry*, 2nd ed. Springer, Berlin, pp. 169–206.
- Jørgensen, B.B., 2021. Sulfur biogeochemical cycle of marine sediments. *Geochem. Perspect.* 10, 145–307.
- Jørgensen, B.B., Des Marais, D.J., 1990. The diffusive boundary layer of sediments: oxygen microgradients over a microbial mat. *Limnol. Oceanogr.* 35, 1343–1355.
- Jørgensen, B.B., Nelson, D.C., 2004. Sulfide oxidation in marine sediments: Geochemistry meets microbiology. In: Amend, J.P., Edwards, K.J., Lyons, T.W. (Eds.), *Sulfur Biogeochemistry – Past and Present*. Geological Society of America Special Paper 379, pp. 63–81. Boulder, Colorado.
- Jørgensen, B.B., Revsbech, N.P., 1983. Colorless sulfur bacteria, *Beggiatoa* spp. and *Thiovulum* spp., in O₂ and H₂S microgradients. *Appl. Environ. Microbiol.* 45, 1261–1270.
- Jørgensen, B.B., Revsbech, N.P., 1985. Diffusive boundary layers and the oxygen uptake of sediments and detritus. *Limnol. Oceanogr.* 30, 111–122.
- Jørgensen, B.B., Glud, R.N., Holby, O., 2005. Oxygen distribution and bioirrigation in Arctic fjord sediments (Svalbard, Barents Sea). *Mar. Ecol. Prog. Ser.* 292, 85–95.
- Jørgensen, B.B., D'Hondt, S.L., Miller, D.J. (Eds.), 2006. *Proc. ODP, Sci. Res.* 201. Ocean Drilling Program, Texas A&M University, College Station TX 77845-9547. USA.
- Jørgensen, B.B., Findlay, A.J.L., Pellerin, A., 2019. The biogeochemical sulfur cycle of marine sediments. *Front. Microbiol.* 10, 849.
- Kalvelage, T., Lavik, G., Lam, P., Contreras, S., Arteaga, L., et al., 2013. Nitrogen cycling driven by organic matter export in the South Pacific oxygen minimum zone. *Nat. Geosci.* 6, 228–234.

- Kandasamy, S., Nath, B.N., 2016. Perspectives on the terrestrial organic matter transport and burial along the land-deep sea continuum: Caveats in our understanding of biogeochemical processes and future needs. *Front. Mar. Sci.* 3, 259.
- Kelly-Gerrey, B.A., Hydes, D.J., Wanik, J.J., 2005. Control of the diffusive boundary layer on benthic fluxes: a model study. *Mar. Ecol. Prog. Ser.* 292, 61–74.
- Khalili, A., Javadi, K., Saidi, A., Goharzadeh, A., Huettel, M., Jørgensen, B.B., 2008. On generating uniform bottom shear stress. Part I: a quantitative study of microcosm chambers. *Recent Patents Chem. Eng.* 1, 174–191.
- Kioka, A., Schwestermann, T., Moernaut, J., Ikehara, K., Kanamatsu, T., McHugh, C.M., Ferreira, C.D., Wiemer, G., Haghpour, N., Kopf, A.J., Eglinton, T.I., Strasser, M., 2019. Megathrust earthquake drives drastic organic carbon supply to the hadal trench. *Sci. Rep.* 9, 1553.
- Klimant, I., Meyer, V., Kühl, M., 1995. Fiber-optic oxygen microsensors, a new tool in aquatic biology. *Limnol. Oceanogr.* 40, 1159–1165.
- Knoblauch, C., Jørgensen, B.B., Harder, J., 1999. Community size and metabolic rates of psychrophilic sulfate-reducing bacteria in Arctic marine sediments. *Appl. Environ. Microbiol.* 65, 4230–4233.
- Kononets, M., Tengberg, A., Nilsson, M., Ekeröth, N., Hylan, A., Robertson, E.K., van de Velde, S., Bonaglia, S., Rütting, T., Blomqvist, S., Hall, P.O.J., 2021. In situ incubations with the Gothenburg benthic chamber landers: Applications and quality control. *J. Mar. Syst.* 214, 103475.
- Koop, K., Boynton, W.R., Wulff, F., Carman, R., 1990. Sediment-water oxygen and nutrient exchanges along a depth gradient in the Baltic Sea. *Mar. Ecol. Prog. Ser.* 63, 65–77.
- Körtzinger, A., Hedges, J.I., Quay, P.D., 2001. Redfield ratios revisited: removing the biasing effect of anthropogenic CO₂. *Limnol. Oceanogr.* 46, 964–970.
- Kotilainen, A.T., Arppe, L., Dobosz, S., Jansen, E., Kabel, K., Karhu, J., Kotilainen, M.M., Kuijpers, A., et al., 2014. Echoes from the past: a healthy Baltic Sea requires more effort. *Ambio* 43, 60–68.
- Krause-Jensen, D., Duarte, C.M., 2016. Substantial role of macroalgae in marine carbon sequestration. *Nat. Geosci.* 9, 737–742.
- Kristensen, E., Holmer, M., 2001. Decomposition of plant materials in marine sediment exposed to different electron acceptors (O₂, NO₃⁻ and SO₄²⁻) with emphasis on substrate origin, degradation kinetics and the role of bioturbation. *Geochim. Cosmochim. Acta* 65, 419–434.
- Kristensen, E., Kostka, J.E., 2006. Macrofaunal burrows and irrigation in marine sediment: microbiological and biogeochemical interactions. In: Kristensen, E., Kostka, J.E., Haese, R. (Eds.), *Interactions Between Macro and Microorganisms in Marine Sediments*. American Geophysical Union, Washington, DC.
- Kristensen, E., Penha-Lopes, G., Delefosse, M., Valdemarsen, T., Quintana, C.Q., 2012. What is bioturbation? The need for a precise definition for fauna in aquatic sciences. *Mar. Ecol. Prog. Ser.* 446, 285–302.
- Lalande, C., Bauerfeind, E., Nöthig, E.-M., Beszczynska-Möller, A., 2013. Impact of a warm anomaly on export fluxes of biogenic matter in the eastern Fram Strait. *Prog. Oceanogr.* 109, 70–77.
- Lam, P., Kuypers, M.M.M., 2011. Microbial nitrogen cycling processes in oxygen minimum zones. *Annu. Rev. Mar. Sci.* 3, 317–345.
- Lampitt, R.S., 1985. Evidence for the seasonal deposition of detritus to the deep-sea floor and its subsequent resuspension. *Deep-Sea Res.* I 32A, 885–897.
- Lampitt, R.S., Raine, R.C.T., Billett, D.S.M., Rice, A.L., 1995. Material supply to the European continental slope: a budget based on benthic oxygen demand and organic supply. *Deep-Sea Res.* I 42, 1865–1880.
- Lampitt, R.S., Salter, I., de Cuevas, B.A., Hartman, S., Larkin, K.E., Pebody, C.A., 2010. Long-term variability of downward particle flux in the deep northeast Atlantic: causes and trends. *Deep-Sea Res.* II 57, 1346–1361.
- LaRowe, D.E., Arndt, S., Bradley, J.A., Estes, E.R., Hoarfrost, A., Lang, S.Q., et al., 2020. The fate of organic carbon in marine sediments – New insights from recent data and analysis. *Earth-Sci. Rev.* 204, 103146.
- Laufkötter, C., Vogt, M., Gruber, N., Aumont, O., Bopp, L., Doney, S.C., Dunne, J.P., Hauck, J., John, J.G., Lima, I.D., Seferian, R., Völker, C., 2016. Projected decreases in future marine export production: the role of the carbon flux through the upper ocean ecosystem. *Biogeosciences* 13, 4023–4047.
- Leduc, D., Rowden, A.A., Glud, R.N., Wenzhöfer, F., Kitazato, H., Clark, M.R., 2016. Comparison between infaunal communities of the deep floor and edge of the Tonga Trench: possible effects in organic matter supply. *Deep-Sea Res.* 116, 264–275.
- Leipe, T., Tauber, F., Vallius, H., Virtasalo, J., Uścińowicz, S., Kowalski, N., Hille, S., Lindgren, S., Myllyvirta, T., 2011. Particulate organic carbon (POC) in surface sediments of the Baltic Sea. *Geo-Mar. Lett.* 31, 175–188.
- Lemburg, J., Wenzhöfer, F., Hofbauer, M., Färber, P., Meyer, V., 2018. Benthic crawler NOMAD – Increasing payload by low-density design. *OCEANS 2018 MTS/IEEE*.
- Levin, L.A., 2018. Manifestation, drivers, and emergence of open ocean deoxygenation. *Annu. Rev. Mar. Sci.* 10, 229–260.
- Levin, L.A., Ekau, W., Gooday, A.J., Jorissen, F., Middelburg, J.J., Naqvi, W., Neira, C., Rabalais, N.N., Zhang, J., 2009a. Effects of natural and human-induced hypoxia on coastal benthos. *Biogeosciences* 6, 3563–3654.
- Levin, L.A., Whitcraft, C.R., Mendoza, G.F., Gonzalez, J.P., Cowie, G., 2009b. Oxygen and organic matter thresholds for benthic faunal activity on the Pakistan margin oxygen minimum zone (700–1100 m). *Deep-Sea Res.* II 56, 449–471.
- Levin, L.A., Bett, B.J., Gates, A.R., Heimback, P., Howe, B.M., Janssen, F., et al., 2019. Global observing needs in the deep ocean. *Front. Mar. Sci.* 6, 241.
- Li, J., Katsev, S., 2014. Nitrogen cycling in deeply oxygenated sediments: results in Lake Superior and implications for marine sediments. *Limnol. Oceanogr.* 59, 465–481.
- Li, X., Zhang, Z., Wade, T.L., Knapp, A.H., Zhang, C.L., 2017. Sources and compositional distribution of organic carbon in surface sediments from the lower Pearl River to the coastal South China Sea. *J. Geophys. Res. Biogeosci.* 122, 2104–2117.
- Loh, A.N., Bauer, J.E., 2000. Distribution, partitioning and fluxes of dissolved and particulate organic C, N and P in the eastern North Pacific and Southern Oceans. *Deep-Sea Res.* I 47, 2287–2316.
- Lohrer, A.M., Thrush, S.E., Hunt, L., Hancock, N., Lundquist, C., 2005. Rapid reworking of subtidal sediments by burrowing spatangoid urchins. *J. Exp. Mar. Biol. Ecol.* 321, 155–169.
- Long, M.H., 2021. Aquatic biogeochemical eddy covariance fluxes in the presence of waves. *J. Geophys. Res.: Oceans* 126 e2020JC016637.
- Long, M.H., Berg, P., de Beer, D., Ziemann, J.C., 2013. In situ coral reef oxygen metabolism: an eddy correlation study. *PLoS One* 8, e58581.
- Loo, L.O., Johnson, P.R., Sköld, M., Karlson, O., 1996. Passive suspension feeding *Amphiuira filiformis* (Echinodermata: Ophiuroidea): feeding behaviour in flume flow and potential feeding rate of field populations. *Mar. Ecol. Prog. Ser.* 139, 143–155.
- Luo, M., Gieskes, J., Chen, L., Shi, X., Chen, D., 2017. Provenances, distribution, and accumulation of organic matter in the southern Mariana Trench rim and slope: Implication for carbon cycle and burial in hadal trenches. *Mar. Geol.* 386, 98–106.
- Luo, M., Glud, R.N., Pan, B., Cui, W., Wenzhöfer, F., Xu, Y., Lin, G., Chen, D., 2018. Benthic carbon mineralization in hadal trenches: Insights from in-situ determination of benthic oxygen consumption. *Geophys. Res. Lett.* 45, 2752–2760.
- Lutz, M., Dunbar, R., Caldeira, K., 2002. Regional variability in the vertical flux of particulate organic carbon in the ocean interior. *Glob. Biogeochem. Cycles* 16, 1037.
- Martin, J.H., Knauer, G.A., Karl, D.M., Broenkow, W.W., 1987. VERTEX: carbon cycling in the northeast Pacific. *Deep-Sea Res.* 34, 267–285.
- MBARI, 2009. <https://www.youtube.com/watch?v=707CQL0rpi4>.
- McCann-Grosvenor, K., Reimers, C.E., Sanders, R.D., 2014. Dynamics of the benthic boundary layer and seafloor contributions to oxygen depletion on the Oregon inner shelf. *Cont. Shelf Res.* 84, 93–106.
- McGinnis, D.F., Cherednichenko, S., Sommer, S., Berg, P., Rovelli, L., Schwarz, R., Linke, P., 2011. Simple, robust eddy correlation amplifier for aquatic dissolved oxygen and hydrogen sulfide flux measurements. *Limnol. Oceanogr. Methods* 9, 340–347.
- McGinnis, D.F., Sommer, S., Lorke, A., Glud, R.N., Linke, P., 2014. Quantifying tidally driven benthic oxygen exchange across permeable sediments: An aquatic eddy correlation study. *J. Geophys. Res.: Oceans* 119. <https://doi.org/10.1002/2014JDC10303>.
- McNichol, A.P., Aluwihare, L.I., 2007. The power of radiocarbon in biogeochemical studies of the marine carbon cycle: Insights from studies of dissolved and particulate organic carbon (DOC and POC). *Chem. Rev.* 107, 443–466.
- Meier, H.E.M., Väli, G., Naumann, M., Eilola, K., Frauen, C., 2018. Recently accelerated oxygen consumption rates amplify deoxygenation in the Baltic Sea. *J. Geophys. Res.: Oceans* 123, 3227–3240.
- Meile, C., Van Cappellen, P., 2003. Global estimates of enhanced solute transport in marine sediments. *Limnol. Oceanogr.* 48, 35–39.
- Meysman, F.J.R., Galaktionov, O.S., Glud, R.N., Middelburg, J.J., 2010. Oxygen penetration around burrows and roots in aquatic sediments. *J. Mar. Res.* 68, 309–336.
- Middelburg, J.J., 2011. Chemoautotrophy in the ocean. *Geophys. Res. Lett.* 38, L24604.
- Middelburg, J.J., 2018. Reviews and Synthesis: To the bottom of carbon processing at the seafloor. *Biogeosci. Discuss.* 15, 413–427.
- Middelburg, J.J., 2019. *Marine Carbon Biogeochemistry*. SpringerBriefs in Earth System Sciences. Springer Open. https://doi.org/10.1007/978-3-030-10822-9_3.
- Middelburg, J.J., Levin, L.A., 2009. Coastal hypoxia and sediment biogeochemistry. *Biogeosciences* 6, 1273–1293.
- Middelburg, J.J., Soetart, K., Herman, P.M.J., 1997. Empirical relationships for use in global diagenetic models. *Deep Sea Res.* I 44, 327–344.
- Miller, D.C., Geider, R.J., MacIntyre, H.L., 1996. Microphytobenthos: the ecological role of the “secret garden” of unvegetated, shallow-water marine habitats. II. Role in sediment stability and shallow-water food webs. *Estuaries* 19, 202–212.
- Moeslund, L., Thamdrup, B., Jørgensen, B.B., 1994. Sulfur and iron cycling in a coastal sediment: radiotracer studies and seasonal dynamics. *Biogeochemistry* 27, 129–152.
- Moodley, L., Heip, C.H.R., Middelburg, J.J., 1998. Benthic activity in sediments of the northwestern Adriatic Sea: sediment oxygen consumption, macrofauna and meiofauna dynamics. *J. Sea Res.* 40, 263–280.
- Morono, Y., Ito, M., Hoshino, T., Terada, T., Hori, T., Ikehara, M., D’Hondt, S., Inagaki, F., 2020. Aerobic microbial life persists in oxic marine sediment as old as 101.5 million years. *Nat. Commun.* 11, 3626.
- Muller-Karger, F.E., Varela, R., Thunell, R., Luerssen, R., Hu, C., Walsh, J.J., 2004. The importance of continental margins in the global carbon cycle. *Geophys. Res. Lett.* 32, L01602.
- Munksby, N., Benthien, M., Glud, R.N., 2002. Flow-induced flushing of relict tube structures in the central Skagerak (Norway). *Mar. Biol.* 141, 939–945.
- Najjar, R.G., Jin, X., Louanchi, F., Aumont, O., Caldeira, K., Doney, S.C., Dutay, J.-C., Follows, M., et al., 2007. Impact of circulation on export production, dissolved organic matter, and dissolved oxygen in the ocean: results from phase II of the ocean carbon-cycle model intercomparison project (OCMP-2). *Glob. Biogeochem. Cycles* 21, GB3007.
- Najjar, R.G., Herrmann, M., Alexander, R., Boyer, E.W., Burdige, D.J., Butman, D., et al., 2018. Carbon budget of tidal wetlands, estuaries, and shelf waters of eastern North America. *Glob. Biogeochem. Cycles* 32, 389–416.
- Nascimento, F.J.A., Laiias, D., Bik, H.M., Creer, S., 2012. Meiofauna enhances organic matter mineralization in soft bottom sediment ecosystems. *Limnol. Oceanogr.* 57, 338–346.
- Ni, W., Li, M., Ross, A.C., Najjar, R.G., 2019. Large projected decline in dissolved oxygen in a eutrophic estuary due to climate change. *J. Geophys. Res.-Oceans* 124, 8271–8289.

- Nilsson, M.M., Kononets, M., Ekeröth, N., Viktorsson, L., Hylén, A., Sommer, S., et al., 2019. Organic carbon recycling in Baltic Sea sediments – an integrated estimate on the system scale based on in situ measurements. *Mar. Chem.* 209, 81–93.
- Nilsson, M.M., Hylén, A., Ekeröth, N., Kononets, M.Y., Viktorsson, L., Almroth-Rosell, E., et al., 2021. Particle shuttling and oxidation capacity of sedimentary organic carbon on the Baltic Sea system scale. *Mar. Chem.* 232, 103963.
- Norkko, J., Gammal, J., Hewitt, J.E., Josefson, A.B., Carstensen, J., Norkko, A., 2015. Seafloor ecosystem function relationships: in situ patterns of change across gradients of increasing hypoxic stress. *Ecosystems* 18, 1424–1439.
- Nowald, N., Iversen, M.H., Fischer, G., Ratmeyer, V., Wefer, G., 2015. Time series of in situ particle properties and sediment trap fluxes in the coastal upwelling filament off Cape Blanc, Mauritania. *Prog. Oceanogr.* 137, 1–11.
- Oguri, K., Kawamura, K., Sakaguchi, A., Toyofuku, T., Kasaya, T., Murayama, M., Fujikura, K., Glud, R.N., Kitazato, H., 2013. Hadal disturbance in the Japan Trench as induced by the 2011 Tohoku-Oki Earthquake. *Sci. Rep.* 3, 1915.
- Ohde, T., Dadou, I., 2018. Seasonal and annual variability of coastal sulphur plumes in the northern Benguela upwelling system. *PLoS One* 13, e0192140.
- Omstedt, A., Edman, M., Claremar, B., Frodin, P., Gustafsson, E., Humborg, C., Mörth, M., Rutgersson, A., et al., 2012. Future changes of the Baltic Sea acid–base (pH) and oxygen balances. *Tellus B* 64, 19586.
- Omstedt, A., Humborg, C., Pempkowiak, J., Perttilä, M., Rutgersson, A., Schneider, B., Smith, B., 2014. Biogeochemical control of the coupled CO₂-O₂ system of the Baltic Sea: a review of the results of Baltic-C. *Ambio* 43, 49–59.
- Orcutt, B.N., Wheat, C.G., Rouxel, O., Hulme, S., Edwards, K.J., Bach, W., 2013. Oxygen consumption rates in subsurface basaltic crust derived from a reaction transport model. *Nat. Commun.* 4, 2539.
- Orsi, W.D., Morard, R., Vuillemin, A., Eitel, M., Wörheide, G., et al., 2020. Anaerobic metabolism of Foraminifera thriving below the seafloor. *ISME J.* 14, 2580–2594.
- Ortega, A., Gerdali, N.R., Alam, I., Kamau, A.A., Acinas, S.G., Logares, R., Gasol, J.M., Massana, R., Krause-Jensen, D., Duarte, C.M., 2019. Important contribution of macroalgae to oceanic carbon sequestration. *Nat. Geosci.* 12, 748–754.
- Pace, M.L., Knauer, G.A., Karl, D.M., Martin, J.H., 1987. Primary production, new production and vertical flux in the eastern Pacific Ocean. *Nature* 325, 803–804.
- Pamatmat, M.M., Fenton, D., 1968. An instrument for measuring subtidal benthic metabolism in situ. *Limnol. Oceanogr.* 13, 537–540.
- Papaspyrou, S., Gregersen, T., Kristensen, E., Christensen, B., Cox, R.P., 2006. Microbial reaction rates and bacterial communities in sediment surrounding burrows of two nereid polychaetes (*Nereis diversicolor* and *N. virens*). *Mar. Biol.* 148, 541–550.
- Paulmier, A., Ruiz-Pino, D., 2009. Oxygen minimum zones (OMZs) in the modern ocean. *Prog. Oceanogr.* 80, 113–128.
- Pelegri, S.P., Blackburn, T.H., 1994. Bioturbation effects of the amphipod *Corophium volutator* on microbial nitrogen transformations in marine sediments. *Mar. Biol.* 121, 253–258.
- Petro, C., Zäncker, B., Starnawski, P., Jochum, L.M., Ferdelman, T.G., Jørgensen, B.B., Røy, H., Kjeldsen, K.U., Schramm, A., 2019. Marine deep biosphere microbial communities assemble in near-surface sediments. *Front. Microbiol.* 10, 758.
- Pfeffer, C., Larsen, S., Song, J., Dong, M., Besenbacher, F., Meyer, R.L., et al., 2012. Filamentous bacteria transport electrons over centimetre distances. *Nature* 491, 218–221.
- Piepenburg, D., Blackburn, T.H., von Dorrien, C.F., Gutt, J., Hall, P.O.J., Hult, S., et al., 1995. Partitioning of benthic community respiration in the Arctic (Northwest Barents Sea). *Mar. Ecol. Prog. Ser.* 118, 199–213.
- Piña-Ochoa, E., Høglund, S., Geslin, E., Cedhagen, T., Revsbech, N.P., et al., 2010. Widespread occurrence of nitrate storage and denitrification among Foraminifera and Gromiida. *Proc. Natl. Acad. Sci. U. S. A.* 107, 1148–1153.
- Polerecky, L., Volkenborn, N., Stief, P., 2006. High temporal resolution oxygen imaging in bioirrigated sediments. *Environ. Sci. Technol.* 40, 5763–5769.
- Quintana, C.O., Tang, M., Kristensen, E., 2007. Simultaneous study of particle reworking, irrigation transport and reaction rates in sediment bioturbated by the polychaetes *Heteromastus* and *Marenzelleria*. *J. Exp. Mar. Biol. Ecol.* 352, 392–406.
- Rasmussen, H., Jørgensen, B.B., 1992. Microelectrode studies of seasonal oxygen uptake in a coastal sediment: role of molecular diffusion. *Mar. Ecol. Prog. Ser.* 81, 289–303.
- Rassmann, J., Eitel, E.M., Lansard, B., Cathalot, C., Brandily, C., et al., 2020. Benthic alkalinity and dissolved inorganic carbon fluxes in the Rhône River prodelta generated by decoupled aerobic and anaerobic processes. *Biogeosciences* 17, 12–33.
- Raymond, P.A., Bauer, J.E., 2001. Use of ¹⁴C and ¹³C natural abundances for evaluating riverine, estuarine, and coastal DOC and POC sources and cycling: a review and synthesis. *Org. Geochem.* 32, 469–485.
- Regnier, P., Friedlingstein, P., Ciais, P., Mackenzie, F.T., Gruber, N., Janssens, I.A., Laruelle, G.G., Lauerwald, R., et al., 2013. Anthropogenic perturbation of the carbon fluxes from land to ocean. *Nat. Geosci.* 6, 597–607.
- Reimers, C.E., 1987. An in situ microprofiling instrument for measuring interfacial pore water gradients: methods and oxygen profiles from the North Pacific Ocean. *Deep-Sea Res.* 34, 2019–2035.
- Reimers, C.E., Fogaren, K.E., 2021. Bottom boundary layer oxygen fluxes during winter on the Oregon Shelf. *J. Geophys. Res.-Oceans* 126, e2020JC016828.
- Reimers, C.E., Glud, R.N., 2000. In situ chemical sensor measurements at the sediment-water interface. In: Varney, M. (Ed.), *Chemical Sensors in Oceanography*. Gordon and Breach Science Publishers, Amsterdam, pp. 249–282.
- Reimers, C.E., Fischer, K.M., Merewether, R., Smith, K.L., Jahnke, R.A., 1986. Oxygen microprofiles measured in situ in deep ocean sediments. *Nature* 320, 741–744.
- Reimers, C.E., Jahnke, R.A., Thomsen, L., 2001. In situ sampling in the benthic boundary layer. In: Boudreau, B., Jørgensen, B.B. (Eds.), *The Benthic Boundary Layer*. Oxford University Press, pp. 245–263.
- Reimers, C.E., Stecher III, H.A., Taghon, G.L., Fuller, C.M., Huettel, M., Rusch, A., Ryckelynck, N., Wild, C., 2004. In situ measurements of advective solute transport in permeable shelf sands. *Cont. Shelf Res.* 24, 183–201.
- Reimers, C.E., Özkan-Haller, H.T., Berg, P., Devol, A., 2012. Benthic oxygen consumption rates during hypoxic conditions on the Oregon continental shelf: Evaluation of the eddy correlation method. *J. Geophys. Res.* 117, C02021.
- Reimers, C.E., Özkan-Haller, H.T., Albright, A.T., Berg, P., 2016. Microelectrode velocity effects and aquatic eddy covariance measurements under waves. *J. Atmos. Ocean. Technol.* 33, 263–282.
- Revsbech, N.P., 1989. An oxygen microelectrode with a guard cathode. *Limnol. Oceanogr.* 34, 474–478.
- Revsbech, N.P., Jørgensen, B.B., Blackburn, T.H., 1980. Oxygen in the sea bottom measured with a microelectrode. *Science* 207, 1355–1356.
- Revsbech, N.P., Nielsen, L.P., Ramsing, N.B., 1998. A novel microsensor for determination of apparent diffusivity in sediments. *Limnol. Oceanogr.* 43, 986–992.
- Revsbech, N.P., Larsen, L.H., Gundersen, J., Dalsgaard, T., Ulloa, O., Thamdrup, B., 2009. Determination of ultra-low oxygen concentrations in oxygen minimum zones by the STOX sensor. *Limnol. Oceanogr. Methods* 7, 371–381.
- Rex, M.A., Etter, R.J., Morris, J.S., Crouse, J., McClain, C.R., Johnson, N.A., Stuart, C.T., Deming, J.W., Thies, R., Avery, R., 2006. Global bathymetric patterns of standing stock and body size in the deep-sea benthos. *Mar. Ecol. Prog. Ser.* 317, 1–8.
- Rheuban, J.E., Berg, P., McGlathery, K.J., 2014. Ecosystem metabolism along a colonization gradient of eelgrass (*Zostera marina*) measured by eddy correlation. *Limnol. Oceanogr.* 59, 1376–1387.
- Riisgård, H.U., 1994. Filter feeding in the polychaete *Nereis diversicolor*: a review. *Neth. J. Aquat. Ecol.* 28, 453–458.
- Riisgård, H.U., Banta, G.T., 1998. Irrigation and deposit feeding by the lugworm *Arenicola marina*, characteristics and secondary effects on the environment. A review of current knowledge. *Vie Milieu* 48, 243–257.
- Riisgård, H.U., Kittner, C., Seerup, D.F., 2003. Regulation of opening state and filtration rate in filter-feeding bivalves (*Cardium edule*, *Mytilus edulis*, *Mya arenaria*) in response to low algal concentration. *J. Exp. Mar. Biol. Ecol.* 284, 105–127.
- Rodil, I.F., Attard, K.M., Norkko, J., Glud, R.N., Norkko, A., 2019. Estimating respiration rates and secondary production of macrobenthos communities across coastal habitats with contrasting structural diversity. *Ecosystems* 8, 1–18.
- Rovelli, L., Attard, K.M., Bryant, L.D., Flögel, S., Stahl, H., Roberts, J.M., Linke, P., Glud, R.N., 2015. Benthic O₂ uptake of two cold-water coral communities estimated with the non-invasive eddy-correlation technique. *Mar. Ecol. Prog. Ser.* 525, 97–104.
- Rovelli, L., Attard, K.M., Cardenas, C.A., Glud, R.N., 2019. Benthic primary production and respiration of shallow rocky habitats: a case study from South Bay (Doumer Island, Western Antarctic Peninsula). *Polar Biol.* 42, 1459–1474.
- Rowe, G.T., 1973. Benthic biomass and surface productivity. In: Costlow, J.D. (Ed.), *Fertility of the Sea*. Gordon and Breach Science Publishers, pp. 441–454.
- Rowe, G.T., 2013. Seasonality in deep-sea food webs - A tribute to the early works of Paul Tyler. *Deep-Sea Res.* 92, 9–17.
- Røy, H., Hüttel, M., Jørgensen, B.B., 2002. The role of small scale sediment topography for oxygen flux across the diffusive boundary layer. *Limnol. Oceanogr.* 47, 837–847.
- Røy, H., Hüttel, M., Jørgensen, B.B., 2005. The influence of topography on the functional exchange surface of marine soft sediments, assessed from sediment topography measured in situ. *Limnol. Oceanogr.* 50, 106–112.
- Røy, H., Kallmeyer, J., Adhikari, R.R., Pockalny, R., Jørgensen, B.B., D'Hondt, S., 2012. Aerobic microbial respiration in 86-million-year-old deep-sea red clay. *Science* 336, 922–925.
- Rysgaard, S., Christensen, P.B., Sørensen, M.V., Funch, P., Berg, P., 2000. Marine meiofauna, carbon and nitrogen mineralization in sandy and soft sediment of Disko Bay, West Greenland. *Aquat. Microb. Ecol.* 21, 59–71.
- Sanei, H., Outridge, P.M., Oguri, K., Stern, G.A., Thamdrup, B., Wenzhöfer, F., Wang, F., Glud, R.N., 2021. High mercury accumulation in deep-ocean hadal sediments. *Sci. Rep.* 11, 10970.
- Santner, J., Larsen, M., Kreuzeder, A., Glud, R.N., 2015. Two decades of chemical imaging of solutes in sediments and soils – a review. *Anal. Chim. Acta* 878, 9–42.
- Sauvage, J.F., Flinders, A., Spivack, A.J., Pockalny, R., Dunlea, A.G., Anderson, C.H., Smith, D.C., Murray, R.W., D'Hondt, S., 2012. The contribution of water radiolysis to marine sedimentary life. *Nat. Commun.* 12, 1297.
- Schauberger, C., Middelboe, M., Larsen, M., Peoples, L.M., Bartlett, D.H., Kirpekar, F., Rowden, A.A., Wenzhöfer, F., Thamdrup, B., Glud, R.N., 2021. Spatial variability of prokaryotic and viral abundances in the Kermadec and Atacama Trench regions. *Limnol. Oceanogr.* 66, 2095–2109.
- Schippers, A., Jørgensen, B.B., 2001. Oxidation of pyrite and iron sulfide by manganese dioxide in marine sediments. *Geochim. Cosmochim. Acta* 65, 915–922.
- Schlesinger, W.H., Melack, J.M., 1981. Transport of organic carbon in the world's rivers. *Tellus* 33, 172–187.
- Schmidtke, S., Stramma, L., Visbeck, M., 2017. Decline in global oceanic oxygen content during the past five decades. *Nature* 542, 335–339.
- Scholze, C., Jørgensen, B.B., Røy, H., 2021. Psychrophilic properties of sulfate reducing bacteria in Arctic sediments. *Limnol. Oceanogr.* 66, S293–S302.
- Schulz, H.D., Zabel, M. (Eds.), 2006. *Marine Geochemistry*. Springer, Berlin.
- Seitaj, D., Schauer, R., Sulu-Gambari, F., Hidalgo-Martinez, S., Malkin, S.Y., Burdorf, L.D.W., Slomp, C.P., Meysman, F.J.R., 2015. Cable bacteria generate a firewall against euxinia in seasonally hypoxic basins. *Proc. Natl. Acad. Sci. U. S. A.* 112, 13278–13283.
- Seitaj, D., Sulu-Gambari, F., Burdorf, L.D.W., Romero-Ramirez, A., Maire, O., Malkin, S.Y., Slomp, C.P., Meysman, F.J.R., 2016. Sedimentary oxygen dynamics in a seasonally hypoxic basin. *Limnol. Oceanogr.* 62, 452–473.
- Seiter, K., Hensen, C., Zabel, M., 2005. Benthic carbon mineralization on a global scale. *Glob. Biogeochem. Cycles* 19, GB1010.

- Seitzinger, S., Harrison, J.A., Böhlke, J.K., Bouwman, A.F., Lowrance, R., Peterson, B., Tobias, C., Van Drecht, G., 2006. Denitrification across landscapes and waterscapes: A synthesis. *Ecol. Appl.* 16, 2064–2090.
- Sherman, A.D., Smith Jr., K.L., 2009. Deep-sea benthic boundary layer communities and food supply: a longterm monitoring strategy. *Deep-Sea Res. II* 56, 1754–1762.
- Silsbe, G.M., Behrenfeld, M.J., Halsey, K.H., Milligan, A.J., Westberry, T.K., 2016. The CAFE model: A net production model for global ocean phytoplankton. *Glob. Biogeochem. Cycles* 30, 1756–1777.
- Smith, C.R., 2006. Bigger is better: the role of whales as detritus in marine ecosystems. In: Estes, J., DeMaster, D.P., Doak, D.F., Williams, T.M., Brownell Jr., R.L. (Eds.), *Whales, Whaling and Ocean Ecosystems*. California University Press, Berkeley, CA, pp. 286–302.
- Smith, K.L., Baldwin, R.J., 1984. Seasonal fluctuations in deep-sea sediment community oxygen consumption: central and eastern North Pacific. *Nature* 307, 624–626.
- Smith Jr., K.L., 1987. Food energy supply and demand: A discrepancy between particulate organic carbon flux and sediment community oxygen consumption in the deep ocean. *Limnol. Oceanogr.* 32, 201–220.
- Smith Jr., K.L., Kaufmann, R.S., 1999. Long-term discrepancy between food supply and demand in the deep eastern North Pacific. *Science* 284, 1174–1177.
- Smith Jr., K.L., Clifford, C.H., Eliason, A.H., Walden, B.W., Rowe, G.T., Teal, J.M., 1976. Free vehicle for measuring benthic community metabolism. *Limnol. Oceanogr.* 21, 164–170.
- Smith Jr., K.L., Kaufmann, R.S., Baldwin, R.J., Carlucci, A.F., 2001. Pelagic–benthic coupling in the abyssal eastern North Pacific: an 8-year time-series study of food supply and demand. *Limnol. Oceanogr.* 46, 543–556.
- Smith Jr., K.L., Ruhl, H.A., Kaufmann, R.S., Kahru, M., 2008. Tracing abyssal food supply back to upper-ocean processes over a 17-year time series in the northeast Pacific. *Limnol. Oceanogr.* 53, 2655–2667.
- Smith Jr., K.L., Ruhl, H.A., Kahru, M., Huffard, C.L., Sherman, A.D., 2013. Deep ocean communities impacted by changing climate over 24 y in the abyssal northeast Pacific Ocean. *Proc. Natl. Acad. Sci. U. S. A.* 110, 19838–19841.
- Smith Jr., K.L., Sherman, A.D., Huffard, C.L., McGill, P.R., Henthorn, R., von Thun, S., Ruhl, H.A., Kahru, M., Ohman, M.D., 2014. Large salp bloom export from the upper ocean and benthic community response in the abyssal northeast Pacific: day to week resolution. *Limnol. Oceanogr.* 59, 745–757.
- Smith Jr., K.L., Huffard, C.L., Sherman, A.D., Ruhl, H.A., 2016. Decadal change in sediment community oxygen consumption in the abyssal Northeast Pacific. *Aquat. Geochem.* 22, 401–417.
- Smith Jr., K.L., Ruhl, H.A., Huffard, C.L., Messié, M., Kahru, M., 2018. Episodic organic carbon fluxes from surface ocean to abyssal depths during long-term monitoring in NE Pacific. *Proc. Natl. Acad. Sci. U. S. A.* 115, 12235–12240.
- Smith Jr., K.L., Sherman, A.D., McGill, P.R., Henthorn, R.G., Ferreira, J., Connolly, T.P., Huffard, C.L., 2021. Abyssal Benthic Rover, an autonomous vehicle for long-term monitoring of deep-ocean processes. *Sci. Robot.* 6, eab14925.
- Smith, C.R., de Leo, F.C., Bernardino, A.F., Sweetman, A.K., Arbizu, P.M., 2008. Abyssal food limitation, ecosystem structure and climate change. *Trends Ecol. Evol.* 23, 518–528.
- Snelgrove, P.R.V., Soetaert, K., Solan, M., Thrush, S., Wei, C.-L., Donavaro, R., Fulweiler, R.W., Kitasato, H., Ingole, B., Norkko, A., Parkes, R.J., Volkenborn, N., 2018. Global carbon cycling on a heterogeneous seafloor. *Trends Ecol. Evol.* 33, 96–105.
- Soltwedel, T., Bauerfeind, E., Bergmann, M., Bracher, A., Budaeva, N., Busch, K., Cherkasheva, A., et al., 2016. Natural variability or anthropogenically-induced variation? Insights from 15 years of multidisciplinary observations at the arctic marine LTER site HAUSGARTEN. *Ecol. Indic.* 65, 89–102.
- Sommer, S., Türk, M., Kriwanek, S., Pfannkuche, O., 2008. Gas exchange system for extended in situ benthic chamber flux measurements under controlled oxygen conditions: First application – Sea bed methane emission measurements at Captain Arutyunov mud volcano. *Limnol. Oceanogr. Methods* 6, 23–33.
- Sommer, S., Gier, J., Treude, T., Lomnitz, U., Dengler, M., et al., 2016. Depletion of oxygen, nitrate and nitrite in the Peruvian oxygen minimum zone cause an imbalance of benthic nitrogen fluxes. *Deep-Sea Res. I* 112, 113–122.
- Ståhl, H., Hall, P.O.J., Tengberg, A., Josefson, A.B., Streftaris, N., Zenetos, A., Karageorgis, A.P., 2004a. Respiration and sequestering of organic carbon in shelf sediments of the oligotrophic northern Aegean Sea. *Mar. Ecol. Prog. Ser.* 269, 33–48.
- Ståhl, H., Tengberg, A., Brunnegård, J., Björnbo, E., Forbes, T.L., Josefson, A.B., Kaberi, H.G., Hasselöv, I.M.K., Olsgard, F., Roos, P., Hall, P.O.J., 2004b. Factors influencing organic carbon recycling and burial in Skagerrak sediments. *J. Mar. Res.* 62, 867–907.
- Stanev, E.V., Poulain, P.-M., Grayek, S., Johnson, K.S., Claustre, H., Murray, J.W., 2018. Understanding the dynamics of the oxic-anoxic interface in the Black Sea. *Geophys. Res. Lett.* 45, 864–871.
- Stewart, H.A., Jamieson, A.J., 2018. Habitat heterogeneity of hadal trenches: considerations and implications for future studies. *Prog. Oceanogr.* 161, 47–65.
- Stolpovsky, K., Dale, A.W., Wallmann, K., 2015. Toward a parameterization of global-scale organic carbon mineralization kinetics in surface marine sediments. *Glob. Biogeochem. Cycles* 29, 812–829.
- Stolpovsky, K., Dale, A.W., Wallmann, K., 2018. A new look at the multi-G model for organic carbon degradation in surface marine sediments for coupled benthic–pelagic simulations of the global ocean. *Biogeosciences* 15, 3391–3407.
- Stratmann, T., Soetaert, K., Wei, C.-L., Lin, Y.-S., van Oevelen, D., 2019. The SCOC database, a large, open, and global database with sediment community oxygen consumption rates. *Scientific Data* 6, 242.
- Stratmann, T., van Oevelen, D., Arbizu, P.M., Wei, C.-L., Liao, J.-X., Cusson, M., et al., 2020. The BenBioDen database, a global database for meio-, macro- and megabenthic biomass and densities. *Scientific Data* 7, 206.
- Suess, E., 1980. Particulate organic carbon flux in the oceans: Surface productivity and oxygen utilization. *Nature* 288, 260–263.
- Sun, R., Yuan, J., Sonke, J.E., Zhang, Y., Zhang, T., Zheng, W., Chen, S., Meng, M., Chen, J., Liu, Y., Peng, X., Liu, C., 2020. Methylmercury produced in upper oceans accumulates in deep Mariana Trench fauna. *Nat. Commun.* 11, 3389.
- Sweetman, A., Norling, K., Gunderstad, C., Haugland, B.T., Dale, T., 2014. Benthic ecosystem functioning beneath fish farms in different hydrodynamic environments. *Limnol. Oceanogr.* 59, 1139–1151.
- Takahashi, T., Broecker, W.S., Langer, S., 1985. Redfield ratio based on chemical data from isopycnal surfaces. *J. Geophys. Res.* 90, 6907–6924.
- Tanioka, T., Matsumoto, K., 2020. Stability of marine organic matter respiration stoichiometry. *Geophys. Res. Lett.* 47, e2019GL085564.
- Tengberg, A., De Bovee, F., Hall, P., Berelson, E., Cicceri, G., Crassous, P., Devol, A., et al., 1995. Benthic chamber and profile landers in oceanography: a review of design, technical solutions and functioning. *Prog. Oceanogr.* 35, 253–294.
- Tengberg, A., Almroth, E., Hall, P., 2003. Resuspension and its effects on organic carbon recycling and nutrient exchange in coastal sediments: in situ measurements using new experimental technology. *J. Exp. Mar. Biol. Ecol.* 285, 119–142.
- Thamdrup, B., Fleischer, S., 1998. Temperature dependence of oxygen respiration, nitrogen mineralization, and nitrification in Arctic sediments. *Aquat. Microb. Ecol.* 15, 191–199.
- Thamdrup, B., Hansen, J.W., Jørgensen, B.B., 1998. Temperature dependence of aerobic respiration in a coastal sediment. *FEMS Microbiol. Ecol.* 25, 189–200.
- Therkildsen, M.S., Lomstein, B.A., 1993. Seasonal variation in net benthic C-mineralization in a shallow estuary. *FEMS Microbiol. Ecol.* 12, 131–142.
- Thouzeau, G., Grall, J., Glavier, J., Chauvaud, L., Jean, F., Leynaert, A., Longphuit, S., Amice, E., Amouroux, D., 2007. Spatial and temporal variability of benthic biogeochemical fluxes associated with macrophytic and macrofaunal distributions in the Thau Lagoon (France). *Estuar. Coast. Shelf. Sci.* 72, 432–446.
- Toussaint, I., Rabouille, C., Cathalot, C., Bombled, B., Abchiche, A., Aouji, O., Buchholtz, G., et al., 2014. A new device to follow temporal variations of oxygen demand in deltaic sediments: the LSCCE benthic station. *Limnol. Oceanogr. Methods* 12, 729–741.
- Treude, T., Smith, C.R., Wenzhöfer, F., Carney, E., Bernardino, A.F., Hannides, A.K., Krüger, M., Boetius, A., 2009. Biogeochemistry of a deep-sea whale-fall: sulfate reduction, sulfide efflux and methanogenesis. *Mar. Ecol. Prog. Ser.* 382, 1–21.
- Trowbridge, J.H., Lentz, S.J., 2018. The bottom boundary layer. *Annu. Rev. Mar. Sci.* 10, 397–420.
- Turnewitsch, R., Falahat, S., Stehlikova, J., Oguri, K., Glud, R.N., Middelboe, M., Kithazato, H., Wenzhöfer, F., Ando, K., Fujio, S., Yanagimoto, D., 2014. Recent sediment dynamics in hadal trenches: evidence for the influence of higher frequency (tidal, near-intertidal) fluid dynamics. *Deep-Sea Res. I* 90, 125–138.
- Ullman, W.J., Aller, R.C., 1982. Diffusion coefficients in nearshore marine sediments. *Limnol. Oceanogr.* 27, 552–556.
- Van Haren, H., 2020. Challenger deep internal wave turbulence events. *Deep-Sea Res. I* 165, 103400.
- Vasquez-Cardenas, D., Meysman, F.J.R., Boschker, T.S., 2020. A cross-system comparison of dark carbon fixation in coastal sediments. *Glob. Biogeochem. Cycles* 34, e2019GB006298.
- Vergara, O., Dewitte, B., Montes, I., Garçon, V., Ramos, M., et al., 2016. Seasonal variability of the oxygen minimum zone off Peru in a high-resolution regional coupled model. *Biogeosciences* 13, 4389–4410.
- Volaric, M.P., Berg, P., Reidenbach, M.A., 2020. Drivers of oyster reef ecosystem metabolism measured across multiple timescales. *Estuar. Coasts* 43, 2034–2025.
- Volkenborn, N., Meile, C., Polerecky, L., Pilditch, C.A., Norkko, A., Norkko, J., Hewitt, J.E., Thrush, S.F., Wetley, D.W., Woodin, S.A., 2012. Intermittent bioirrigation and oxygen dynamics in permeable sediments: an experimental and modeling study of the three tellinid bivalves. *Mar. Res.* 70, 794–823.
- Volz, J.B., Mogollón, J.M., Geibert, W., Arbizu, P.M., Koschinsky, A., Kasten, S., 2018. Natural spatial variability of depositional conditions, biogeochemical processes and element fluxes in sediments of the eastern Clarion-Clipperton Zone, Pacific Ocean. *Deep Sea Res. I* 140, 159–172.
- von Appen, W.-J., Waite, A.M., Bergmann, M., Bienhold, C., Boebel, O., Bracher, A., et al., 2021. Sea ice derived meltwater stratification delays export and favors pelagic secondary production: results from continuous observations. *Nat. Commun.* 12, 7309.
- Vonnahme, T.R., Molari, M., Janssen, F., Wenzhöfer, F., Haeckel, M., Titschack, J., Boetius, A., 2020. Effects of a deep-sea mining experiment on seafloor microbial communities and functions after 26 years. *Sci. Adv.* 6, eaaz5922.
- Vopel, K., Thistle, D., Rosenberg, R., 2003. Effect of the brittle star *Amphiura filiformis* (Amphiuridae, Echinodermata) on oxygen flux into the sediment. *Limnol. Oceanogr.* 48, 2034–2045.
- Vuillemin, A., Wankel, S.D., Coskun, Ö.K., Magritsch, T., Vargas, S., Estes, E.R., et al., 2019. Archaea dominate oxic subsurface communities over multimillion-year time scales. *Sci. Adv.* 5, eaaw4108.
- Wallmann, K., Pinero, E., Burwicz, E., Haeckel, M., Hensen, C., Dale, A., Ruepke, L., 2012. The global inventory of methane hydrate in marine sediments: a theoretical approach. *Energies* 5, 2449–2498.
- Webb, A.P., Eyre, B.D., 2004. The effect of natural populations of the burrowing thalassinid shrimp *Typaea australiensis* on sediment irrigation and benthic metabolism, nutrient fluxes and denitrification. *Mar. Ecol. Prog. Ser.* 268, 205–220.
- Wei, C.-L., Rowe, G.T., Escobar-Briones, E., Boetius, A., Soltwedel, T., Caley, M.J., Soliman, Y., Huetmann, F., Qu, F., Yu, Z., Pitterer, R., Haedrich, R.L., et al., 2010. Global patterns and predictions of seafloor biomass using random forests. *PLoS One* 5, e15323.

- Wenzhöfer, F., Glud, R.N., 2002. Benthic carbon mineralization in the Atlantic: a synthesis based on in situ data from the last decade. *Deep-Sea Res. I* 49, 1255–1279.
- Wenzhöfer, F., Glud, R.N., 2004. Small-scale spatial and temporal variability in coastal benthic O₂ dynamics: effects of fauna activity. *Limnol. Oceanogr.* 49, 1471–1481.
- Wenzhöfer, F., Holby, O., Kohls, O., 2001. Deep penetrating benthic oxygen profiles measured in situ by oxygen optodes. *Deep-Sea Res. I* 48, 1741–1755.
- Wenzhöfer, F., Lemburg, J., Hofbauer, M., Lehmenhecker, S., Färber, P., 2016a. TRAMPER - An autonomous crawler for long-term benthic oxygen flux studies in remote deep sea ecosystems. *OCEANS 2016 MTS/IEEE Monterey*, 1–6.
- Wenzhöfer, F., Oguri, K., Middelboe, M., Turnewisch, R., Toyofuku, T., Kitazato, H., Glud, R.N., 2016b. Benthic carbon mineralization in hadal trenches: assessment by in situ O₂ microprofile measurements. *Deep-Sea Res. I* 116, 279–286.
- Westberry, T.K., Behrenfeld, M.J., 2014. Oceanic net primary production. In: Hanes, J. (Ed.), *Biophysical Applications of Satellite Remote Sensing*. Springer Remote Sensing/Photogrammetry. Springer, Berlin.
- Wiedmann, I., Ershova, E., Bluhm, B.A., Nöthig, E.-M., Gradinger, R.R., Kosobokova, K., Boetius, A., 2020. What feeds the benthos in the Arctic basins? Assembling a carbon budget for the deep Arctic Ocean. *Front. Mar. Sci.* 7, 224.
- Williams, P.L.LeB., del Giorgio, P.A., 2004. Respiration in aquatic ecosystems: history and background. In: *Respiration in Aquatic Ecosystems*. Oxford University Press, pp. 1–17.
- Witte, U., Pfannkuche, O., 2000. High rates of benthic carbon remineralisation in the abyssal Arabian Sea. *Deep-Sea Res. II* 47, 2785–2804.
- Witte, U., Wenzhofer, F., Sommer, S., Boetius, A., Heinz, P., Aberle, N., Sand, M., Cremer, A., Abraham, W.-R., Jørgensen, B.B., Pfannkuche, O., 2003. In situ experimental evidence of the fate of a phytodetritus pulse at the abyssal sea floor. *Nature* 424, 763–766.
- Woulds, C., Bouillon, S., Cowie, G.L., Drake, E., Middelburg, J.J., Witte, U., 2016. Patterns of carbon processing at the seafloor: the role of faunal and microbial communities in moderating carbon flows. *Biogeoscience* 13, 4343–4357.
- Xie, F., Tao, Z., Zhou, X., Lv, T., Wang, J., 2019. Spatial and temporal variations of particulate organic carbon sinking flux in global ocean from 2003 to 2018. *Remote Sens.* 11, 2941.
- Xu, Y.P., Zehua, J., Xiao, W., Fang, J., Wang, Y., Luo, M., Wenzhöfer, F., Rowden, A.A., Glud, R.N., 2020. Glycerol dialkyl glycerol tetraethers in surface sediments from three Pacific hadal trenches: distribution, source and environmental implications. *Org. Geochem.* 147, 104079.
- Xu, Y., Li, X., Luo, M., Xiao, W., Fang, J., Rashid, H., Peng, Y., Li, W., Wenzhöfer, F., Rowden, A.A., Glud, R.N., 2021. Distribution, source and burial of sedimentary organic carbon in Kermadec and Atacama Trenches. *J. Geophys. Res. Biogeosci.* <https://doi.org/10.1029/2020JG006189>.
- Zhu, Q.Z., Aller, R.C., Fan, Y.Z., 2006. A new ratiometric, planar fluorosensor for measuring high resolution, two dimensional pCO₂ distribution in marine sediments. *Mar. Chem.* 101, 40–53.